MIT Open Access Articles

Wetting phenomena in membrane distillation: Mechanisms, reversal, and prevention

Massachusetts Institute of Technology

Wetting phenomena in membrane distillation:

Mechanisms, reversal, and prevention

Mohammad Rezaei [a],*, David M. Warsinger [b,c], John H. Lienhard V [c], Mikel C. Duke [d], Takeshi Matsuura [e], Wolfgang M. Samhaber [a]

[a] Institute of Process Engineering, Johannes Kepler University Linz, Altenberger Strasse 69, 4040 Linz, Austria

[b] Department of Chemical and Environmental Engineering, Yale University, New Haven, Connecticut 06520-8286, the USA

[c] Rohsenow Kendall Heat Transfer Laboratory, Department of Mechanical Engineering, Massachusetts Institute of Technology, 77 Massachusetts Avenue, Cambridge MA 02139-4307, USA

[d] Institute for Sustainability and Innovation, College of Engineering and Science, Victoria University, Melbourne, Victoria 8001, Australia

[e] Department of Chemical and Biological Engineering, University of Ottawa, Ottawa, Ontario K1N 6N5, Canada

*Corresponding Author: Tel: +4373224689747, Email: mohammad.rezaei@jku.at

Abstract

Membrane distillation (MD) is a rapidly emerging water treatment technology; however, membrane pore wetting is a primary barrier to widespread industrial use of MD. The primary causes of membrane wetting are exceedance of liquid entry pressure and membrane fouling. Developments in membrane design and the use of pretreatment have provided significant advancement toward wetting prevention in membrane distillation, but further progress is needed. In this study, a broad review is carried out on wetting incidence in membrane distillation processes. Based on this perspective, the study describes the wetting mechanisms, wetting causes, and wetting detection methods, as well as hydrophobicity measurements of MD membranes. This review discusses current understanding and areas for future investigation on the influence of operating conditions, MD configuration, and membrane non-wettability characteristics on wetting phenomena. Additionally, the review highlights mathematical wetting models and several approaches to wetting control, such as membrane fabrication and modification, as well as techniques for membrane restoration in MD. The literature shows that inorganic scaling and organic fouling are the main causes of membrane wetting. The regeneration of wetting MD membranes is found to be challenging and the obtained results are usually not favorable. Several pretreatment processes are found to inhibit membrane wetting by removing the wetting agents from the feed solution. Various advanced membrane designs are considered to bring membrane surface non-wettability to the states of superhydrophobicity and superomniphobicity; however, these methods commonly demand complex fabrication processes or high-specialized equipment. Recharging air in the feed to maintain protective air layers on the membrane surface has proven to be very effective to prevent wetting, but such techniques are immature and in need of significant research on design,

Keywords: Membrane distillation; Membrane wetting; Hydrophobicity; Pretreatment; Membrane modification; Review

Contents

1. Introduction

Membrane distillation (MD) is a thermally driven membrane separation process, which utilizes a microporous hydrophobic membrane that allows vapor to pass through it but not liquid. MD's driving force for the mass transfer is the transmembrane vapor pressure difference, which is induced by the transmembrane temperature difference or by reduction of vapor pressure on the permeate side by vacuum or dry gas (Carrero-Parreño et al., 2017; Lee et al., 2015). The volatile components present in the feed solution evaporate at the entrances of pores, and therefore the mass transfer through the membrane only takes place in the vapor phase (Kishor G Nayar et al., 2015; Politano et al., 2016; Swaminathan et al., 2016b).

MD offers several advantages and some potential applications based on the following benefits. MD operates at lower temperatures than the boiling point of the solvent, and therefore it can deal with temperature-sensitive solutions (e.g., in the food or pharmaceutical industries (El-Abbassi et al., 2013)). Since the vapor pressure is not highly dependent on the salt concentration, MD can be used in combination with reverse osmosis (RO) for the treatment of highly saline water (Warsinger et al., 2018).

Although MD is potentially attractive for some applications, it still suffers from a few drawbacks and has gained little acceptance industrially. These disadvantages include high-energy consumption compared to alternative membrane processes, and wetting phenomenon. The energy needs for MD can be provided if it integrates with renewable energy or available "waste" heat (David M. Warsinger et al., 2015) or solar thermal (Guillén-Burrieza et al., 2011), and new configurations and operating conditions continue to improve the energy efficiency of MD (Chung et al., 2016; Summers and Lienhard, 2013; J. Swaminathan et al., 2018; Swaminathan et al., 2016a, 2016c; David E.M. Warsinger et al., 2015). However, the incidence of membrane pore wetting due to the loss of membrane hydrophobicity for the feeds containing wetting compounds (e.g., oils, surfactants) is still challenging its industrial potential (Banat and Simandl, 1994; El-Bourawi et al., 2006; Qtaishat and Banat, 2013).

102 Penetration of feed solution into the membrane pores occurs if solutions with organic or/and inorganic

103 compounds adsorb/deposit to the membrane surface or if the transmembrane hydrostatic pressure surpasses

104 the liquid entry pressure. Pore wetting leads to either permeate flux reduction or permeate quality

105 deterioration depending on the type of pore wetting. The former is the result of partial pore wetting, and the

106 latter is as the consequence of full wetting.

107 A literature search for "membrane distillation" revealed more than 2180 records (through July 2017, in

108 Scopus), with an escalating growth in the number of publications during the past decade (**Fig. 1**). In 1963,

109 the first patent on MD was filed by Bodell (Bodell, 1963); however, the unavailability of adequate

110 membranes for MD led to a lack of interest in MD for some time. Subsequent to the fabrication of porous

111 polytetrafluoroethylene (PTFE) membranes by W. L. Gore and Associates, during the 1980s MD regained

112 the attention of researchers. Nevertheless, research addressing wetting incidence and control wetting in MD

113 remained minimal until recently. The entire number of published papers on MD is more than eleven times

114 greater than that of MD articles exploring the wetting phenomena (2180 articles for MD and 171 for wetting

115 in MD.
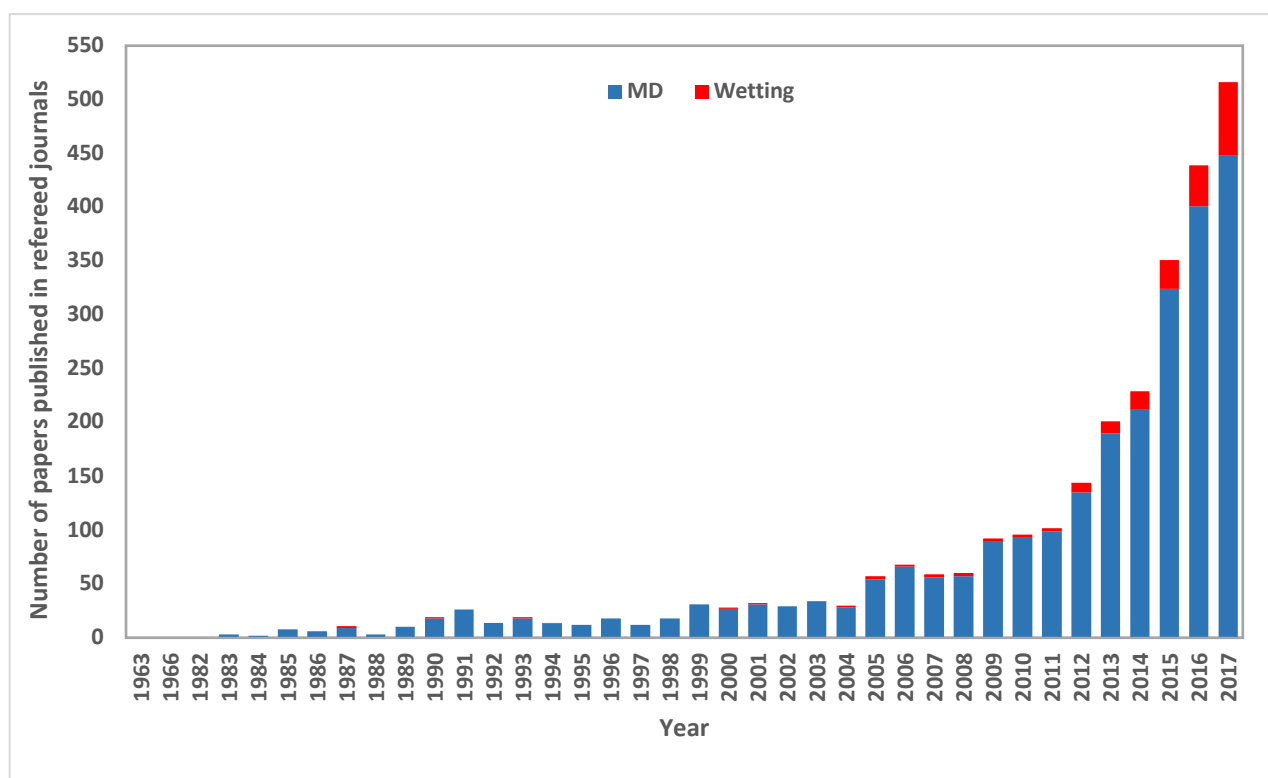
116

117 Fig. 1: The growth of research activity on MD and wetting phenomena, 1963-2016 (data from Scopus).

118 Today, wetting incidence in MD has gained more attention and more publications on MD investigate these

119 phenomena, moving the field toward practical implementation. To the best of authors' knowledge, no

120 comprehensive literature review has focused on the wetting phenomena in MD. This article provides an

121 extensive literature review on the subject. The aim of this paper is to analyze the key wetting conditions,

122 wetting types, harmful effects, and prevention techniques and to lay the groundwork for future

123 technological advances.

124 **2. Parameters for wetting**

125 2.1. Liquid entry pressure

126 The primary metric for measuring membrane wettability is liquid entry pressure (LEP). The LEP of a

127 solution (sometimes incorrectly called "wetting pressure") is the pressure (Pa) that must be applied to the

128 solution before it goes through a dry membrane pore (Smolders and Franken, 1989). The maximum

129 capillary pressure for a hydrophobic membrane depends on liquid surface tension, surface free energy and

130 maximum pore size of the membrane. Based on the Young-Laplace equation (Young, 1807), LEP is defined

131 as:

$$LEP = \frac{-B\gamma_l \cos\theta}{r_{max}} > P_f - P_p = \Delta P_{interface} \qquad (1)$$

132 where P_f and P_p are the hydraulic pressure on the feed and permeate side, B is a pore geometry coefficient

133 (Table 1), γ_l is the liquid surface tension, θ is the contact angle (CA) measured on the liquid side, where

134 the liquid-vapor interface meets the membrane surface and r_{max} is the maximum pore size of the membrane

135 (David M. Warsinger et al., 2016). This simple model is visualized in Fig. 2a and 2b. The θ for a water

136 droplet on different surfaces is shown in Table 2.

137 Many membranes and process conditions can impact the LEP through the variables in Eq. (1), including

138 operating temperature, solution composition, surface roughness, surface porosity, pore shape (i.e., pore

139 radius and fiber radius (Ali et al., 2012; Guillen-Burrieza et al., 2015). For instance, Barbe et al. (Barbe et

140 al., 2000) studied the effect of contact with a membrane with water and a CaCl$_2$ solution for 72 h on

141   membrane surface morphology. They found that the intrusion of water meniscus into large pores led to

142   increase in the porosity, pore area, pore length and pore equivalent diameter, as well as pore spread factor

143   of the membrane. As a result, the LEP of the membrane decreased.

144   Table 1: Pore geometry coefficient for different membrane pores

Type of membrane pore	Pore geometry coefficient	Reference
cylindrical pores	1.0	(David M. Warsinger et al., 2016)
elliptical or irregularly shaped pores	less than 1.0	(David M. Warsinger et al., 2016)
stretched membranes (e.g., PTFE) with small curvature radius	0.4-0.6	(Saffarini et al., 2013)

145   Table 2: Water contact angle (WCA) for different surfaces

Surface	WCA	Reference
Teflon	108° - 115°	(Alkhudhiri et al., 2012)
polyvinylidene difluoride (PVDF)	107°	
polypropylene (PP)	93.5°±0.2°	(Gryta, 2005)
ceramic membrane grafted with fluoroalkylsilanes	177°	(Khemakhem and Amar, 2011)
ceramic zirconia and titania membranes	160°	(Cerneaux et al., 2009)

146   Moreover, the utility of Eq. (1) for calculating LEP is limited because the CA and surface tension of feed

147   may not be known for the system of interest. Therefore, Eq. (1) can be only used to interpret the

148   experimental data (Lawson and Lloyd, 1997). Because membranes do not have cylindrical pores, the Purcell

149   model was developed to describe the location of the pinning point of the liquid in the pores, using more

150   realistic geometry (see Fig. 2d and e) than cylindrical assumed in Equation (1). The equation for LEP based

151   on the Purcell model (Purcell, 1950) is

$$LEP = \frac{-2\gamma_l \cos(\theta + \alpha)}{r(1 + R/r(1 - \cos(\alpha)))} \tag{2}$$

152   where R is the fiber radius and α is the angle below horizontal at which the liquid meniscus pins prior to

153   breakthrough (Fig. 2). The value of α is calculated using the following equation:

$$\sin(\theta + \alpha) = \frac{\sin\theta}{1 + r/R} \tag{3}$$
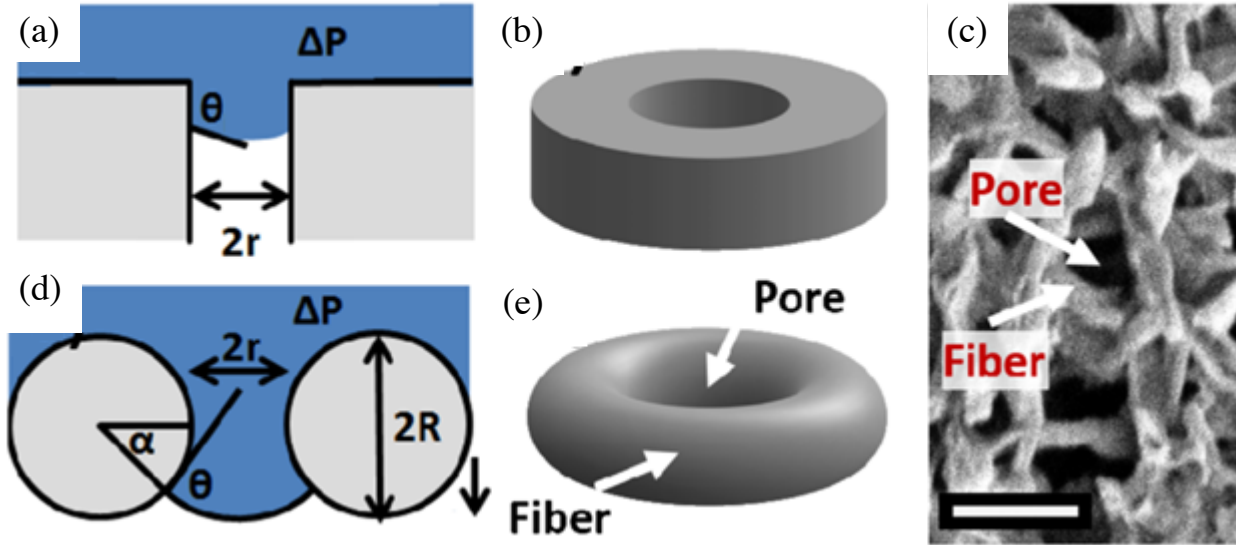
154

155   Fig. 2: (a) and (b) cylindrical pore (Young-Laplace model, Eq. (1)). (c) scanning electron microscopy

156   (SEM) image of the nylon membrane (scale bar is 1 mm). (d) and (e) toroidal pore. Purcell model, Eq. (2)

157   (Servi et al., 2016).

158   Unlike the Young-Laplace model, which predicts the LEP to be less than zero for all values of CA less than

159   90°, the Purcell model predicts positive values of LEP for all values of CA. However, this result is also in

160   contradiction to the fact that many membranes wet at very low values of CA. Therefore, Servi et al. (Servi

161   et al., 2016) developed a new model to predict the LEP for all values of CA considering the interactions

162   between the liquid and the pores below the initially wetted surface by incorporating a "floor" below each

163   pore into the model. This floor describes those fibers that may enable the liquid to penetrate further into the

164   membrane. Therefore, LEP can be determined as the pressure at which the liquid separates from the pore

165   or intercepts the floor, whichever takes place at the lower pressure. To calculate LEP using this new model,

166   Eq. (2) is used along with Eq. (3) and the following equation

$$\frac{r + R\big(1 - \cos(\alpha)\big)}{-\cos(\theta + \alpha)} (1 - \sin(\alpha + \theta)) = R(1 - \sin(\alpha)) + h \tag{4}$$

167 where h is defined as the floor height (nm) describing the fibers that may attract the liquid to enter further

168 into the membrane (Fig. 3). The modified model could explain the observed LEP performance over CAs

169 ranging from 63° to 129°.
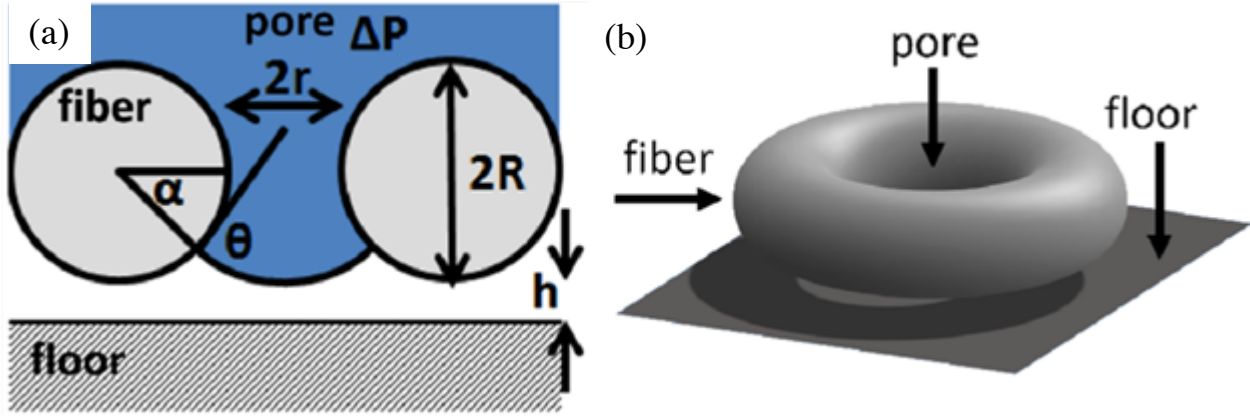
170

171 Fig. 3: The pore configuration for the Servi model, Eq. (4), from (a) the side; and (b) in three dimensions.

172 h is the length between the bottom of the fibers and the floor. h can be positive or negative (Servi et al.,

173 2016).

174 2.2. Membrane surface free energy

175 Surface free energy of a membrane (γ_m) is defined as the energy difference between the bulk and surface

176 of a membrane. It can be estimated by measuring the receding CA (θ_r) and advancing CA (θ_a) of two liquid

177 on the membrane surface using the two following equations (Owens and Wendt, 1969)

$$\left(1 + \frac{\cos\theta_a + \cos\theta_r}{2}\right)\gamma_l = 2(\gamma_m^d \gamma_l^d)^{0.5} + (\gamma_m^{nd} \gamma_l^{nd})^{0.5} \tag{5}$$

$$\gamma_m = \gamma_m^d + \gamma_m^{nd} \tag{6}$$

178 where the superscripts d and nd correspond to the dispersive and nondispersive contributions to the total

179 surface energy, respectively.

180   2.3. Surface wettability

181   The surface wettability is highly dependent on the free energy of the surface and its CA. In its simplest

182   form, the wettability of a liquid droplet on a flat, smooth surface is commonly determined by Young's

183   equation (Young, 1805):

$$\cos\theta = \frac{\gamma_{sv} - \gamma_{sl}}{\gamma_{lv}} \tag{7}$$

184   where θ is the CA in the Young's model, $\gamma_{lv}, \gamma_{sv}, \gamma_{sl}$ are the interfacial tensions liquid/vapor, solid/vapor,

185   and solid/ liquid, respectively.

186   However, in reality, smooth surfaces are rare and some roughness is contained; therefore, the Wenzel's

187   theory (Wenzel, 1936) was proposed where the roughness of the surface was considered for wettability

188   determination.

$$\cos\theta_w = \frac{r(\gamma_{sv} - \gamma_{sl})}{\gamma_{lv}} \tag{8}$$

189   where θ_w is the apparent CA in the Wenzel mode and r is the surface roughness factor as the ratio of the

190   actual solid/liquid contact area to its vertical projection. Based on Wenzel's theory, the liquid enters the

191   grooves of micro-nano composite structure, and therefore this leads to higher CA on a rough surface than

192   CA on a true flat surface (Fig. 4).

193   In Cassie's theory (Cassie and Baxter, 1944), the area fraction of solid and gas phase as a result of surface

194   roughness contributes to the determination of wettability

$$\cos\theta_c = f_s \cos\theta_s + f_v \cos\theta_v = f_s(\cos\theta + 1) - 1 \tag{9}$$

195   where θ_c represents the apparent CA in the Cassie mode, taking into account that $f_s + f_v = 1$, $\theta_s = \theta$, and

196     $\theta_v = 180°$. The Wenzel state and the Cassie state can be coexisting and transition between them can also

197   occur (Lu et al., 2009). Change of the hydrophobicity toward superhydrophobicity is induced by air pockets,

198   so-called "pillars" (Fig. 4c), between liquid and the surface generated by hydrophobic forces (Dumée et al.,

199   2013; David E.M. Warsinger et al., 2015), therefore increasing the CA greater than 150° (Cao et al., 2009),

200   reducing sliding angle ($SA_{water} < 10°$) (Tijing et al., 2014a) and the surface free energy. Superhydrophobic

201   membranes made based on combined micro, and nanoscale roughness behave in Cassie-Baxter state and

202   water droplet is easy to roll off.
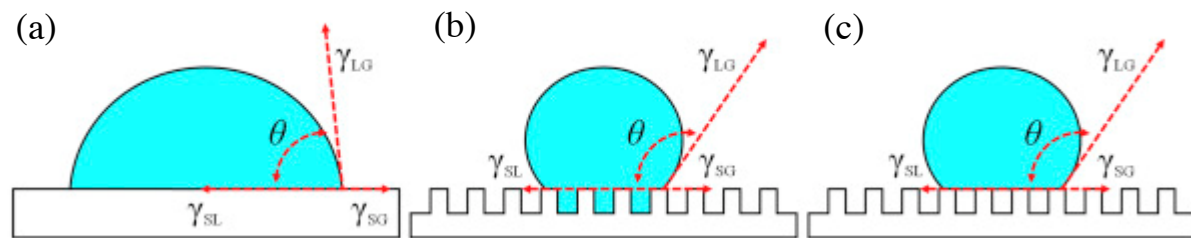
204   Fig. 4: Schematic representation of:(a) the Young model, Eq. (7); (b) the Wenzel model, Eq. 8; and (c) the

205   Cassie-Baxter model, Eq. (9). The last of these best describes unwetted MD membranes (An et al., 2017).

206   **3.   Wetting mechanisms**

207   Membrane pore wetting involves a complex of physical and chemical interactions (Alklaibi and Lior, 2005).

208   The non-wetting liquid facing a hydrophobic membrane forming a fixed interface at the membrane pores

209   was initially considered as one of the first principles of MD process by C. Gostoli et al. in 1987 [3]. They

210   proposed that, based on capillary action, the non-wetting of a liquid is the result of its high surface tension

211   forming a convex meniscus that impedes the liquid from entering the membrane pore. Therefore, the liquid

212   feed in contact with membrane bulges in the pore until the pressure difference arising from the surface

213   tension of the curved interface balances the pressure drop caused by the partial pressures of vapors and air

214   across the membrane. The pressure caused by surface tension is called capillary pressure. When this

215   pressure balance is overwhelmed, the liquid begins penetrating the pores. Once wetting takes place, the

216   membrane starts to lose its hydrophobicity locally, leading to continuous water bridging.

217   Membrane wetting can be distinguished into four degrees (**Fig. 5**): non-wetted, surface-wetted, partially-

218   wetted, and fully-wetted (Gryta, 2007a). Surface wetting shifts the interface of liquid/vapor inward of the

219   membrane cross-section. Permeate flux may then decline gradually as a result of the associated increase in

220   temperature polarization which lowers the temperature of the evaporating interface in the pore (Gryta,

221   2016a; Gryta et al., 1997). Although surface wetting even to a significant depth, e.g. 100–200 µm, still

222   provides a liquid/vapor interface for separation, scaling as a result of solvent evaporation can take place

223 inside the pores in the vicinity of the meniscus (Gryta, 2007a). Moreover, crystal growth inside the pores

224 accelerates scale formation rate by inhibiting diffusive transport of solutes and solvent between wetted

225 pores and the feed bulk, raising solute concentrations locally. Conversely, under certain conditions, the

226 intrusion of liquid into the pore has been observed to cause a temporary flux increase as a result of the

227 shorter vapor diffusion path through the part of the pore that remains dry (Gilron et al., 2013). As feed

228 solution penetrates deeper into the membrane pores, partial wetting can take place. In this case, the MD

229 process can be continued if the majority of pores are dry. However, partial wetting under certain conditions

230 can reduce the permeate flux due to a reduction of the active surface area for mass transport associated with

231 partial wetting (blue solid line in Fig. 5) (Karakulski and Gryta, 2005) or it can cause an increase in the

232 permeate flux due to wetting of some pores (i.e. vapor transport is overtaken by liquid transport) followed

233 by a rapid decrease due to steady blockage of pores by the foulants depending on the experimental setup

234 (blue dash line in Fig. 5) (Dow et al., 2017). The partial wetting also leads to deterioration of permeate

235 quality. Interestingly, all the hydrophobic membranes used in MD, such as PP, PTFE, and PVDF, have

236 shown partial wettability during a long-term use (Gryta, 2005). In the case of full wetting, the MD process

237 no longer acts as a barrier, resulting in a viscous flow of liquid water through membrane pores,

238 incapacitating the MD process (Rezaei et al., 2017a; Rezaei and Samhaber, 2016b). Fig. 5 shows

239 qualitatively the permeate flux and rejection rate for an MD process based on the degree of wetting.
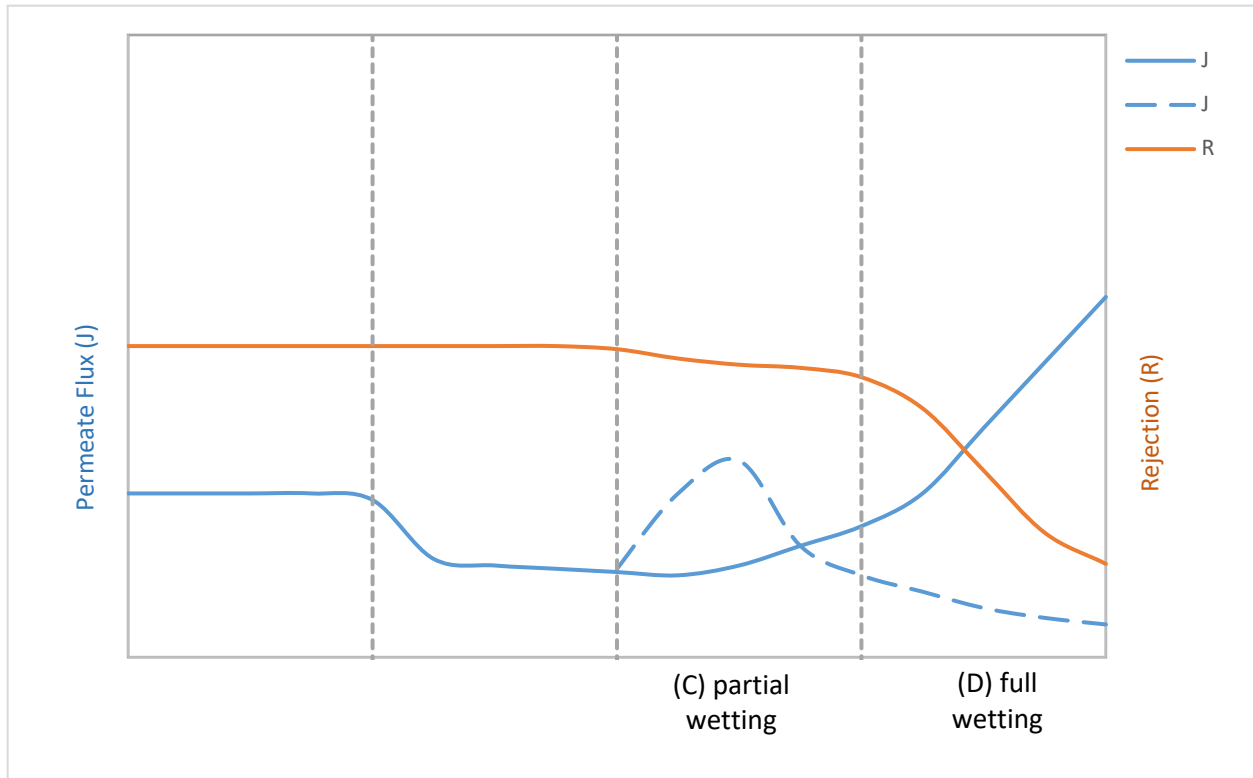
Fig. 5: Wetting degrees: (A) non-wetted; (B) surface-wetted; (C) partially-wetted; and (D) completely-wetted.

4. Wetting detection

Wetting is typically detected by evaluating the permeate quality. When membrane wetting occurs, the electrolyte solutes dissolved in the liquid feed penetrate into membrane pores, which leads to a significant increase of permeate electrical conductivity. This permeate quality change is frequently measured by permeate conductivity readings (Warsinger et al., 2017a). However as electrical conductivity increase also happens when volatile components such as ammonia and carbon dioxide pass through an intact membrane, wetting is detected occasionally by in-situ visual observation of the membrane (wetted membranes transition from opaque to transparent) (Dow et al., 2017), transmembrane pressure changes and membrane autopsy. Recently, Ahmed et al. (Ahmed et al., 2017) applied an electrically conductive layer to a direct contact membrane distillation (DCMD) combined with an electrochemical system to detect wetting (Fig. 6). The membrane acted as an electrode wherein the current through the system enabled Na+ and Cl− ions

254 to complete the cell. A constant voltage of +1V was applied during the MD process, and a quick increase

255 in current was noticed at the moment where wetting occurred.
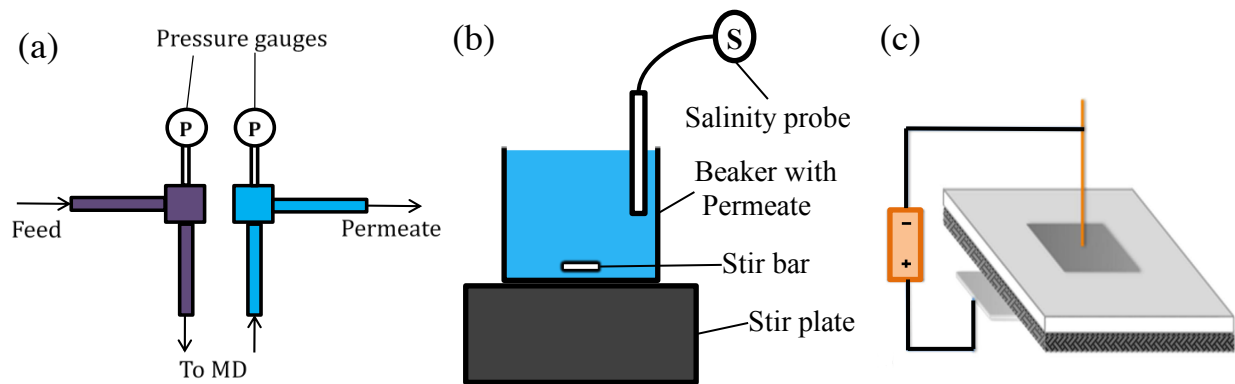
256

257 Fig. 6: Wetting detection mechanisms. a) measuring pressure changes across the membrane, reduced by

258 leaks, b) measuring permeate conductivity, or c) electrochemical cell, where black is the electrically

259 conductive carbon cloth layer, and white is the active electrospun PVDF-HFP (Ahmed et al., 2017).

5. Causes of wetting

261 The numerous causes of wetting in MD are detailed in Table 3. The primary cause of the wetting of MD

262 membranes is fouling, meaning material deposition on the membrane surface and in membrane pores

263 (Camacho et al., 2013; Gryta, 2007a; Hausmann et al., 2011; Tijing et al., 2015) . Other causes of wetting

264 include surfactants which reduce the surface tension of the feed (Rezaei et al., 2017a), capillary

265 condensation, and membrane damage (Ge et al., 2014; Lee et al., 2018). Different types of fouling in MD

266 are distinguished by the deposited materials and include organic fouling (C. Liu et al., 2017; Mokhtar et al.,

267 2016; Nguyen et al., 2017; Wu et al., 2016; Zarebska et al., 2014) such as biological fouling (or biofouling)

268 (Wu et al., 2017; Zodrow et al., 2014) or fouling of organic compounds (Chew et al., 2014; Tan et al.,

269 2016), and particulate or colloidal fouling (Ding et al., 2010; He et al., 2008; Qin et al., 2016; Zarebska et

270 al., 2015), as well as scaling deposition (inorganic fouling). The deposits can reduce LEP as they are often

271 hydrophilic, may damage the membrane (Guillen-Burrieza et al., 2013), and also clog the pores, which

272 leads to a decline of permeate flux and permeate quality due to membrane wetting. Past studies have

273 reviewed these foulants (D. M. Warsinger et al., 2015).

274   Table 3: Pore wetting causes and mechanisms in MD

Cause	Mechanism	Reason
Transmembrane pressure	Higher than LEP	Pressure spikes, operating with low surface tension fluids or large pore size membrane
Capillary condensation	Loss of temperature gradient	Temporary shutdowns or variable operating temperatures: these reduce the saturation pressure for vapor, causing condensation
Scale deposition (inorganic fouling)	Reducing the hydrophobicity of membrane	Deposition on surface and crystallization inside membrane pores
Organic fouling	- Reducing the hydrophobicity of membrane - Lowering the surface tension	- Forming attractive forces between hydrophobic materials within an aqueous system - Increasing the affinity of solution and membrane
Surfactants	Reducing the liquid entry pressure of the feed into the pores	The liquid entry pressure is linearly proportional to surface tension.
Membrane degradation during long-term operation	Formation of hydrophilic groups on membrane surface	Oxidative chemical or mechanical degradation

275   Besides the fouling, pore wetting can also occur when the hydraulic transmembrane pressure exceeds the

276   LEP. Chemical and mechanical degradation of the membrane are also considered to accelerate the

277   membrane wetting during long-term MD process. Gryta et al. (Gryta et al., 2009) reported that hydrophilic

278   groups on the membrane surface (e.g. hydroxyl (OH), carbonyl (C=O) and unsaturated (C=C) groups)

279   formed by chemical oxidative degradation of membranes could reduce the CA from 90° to 61.4°. The

following section discusses the MD wetting caused by inorganic and organic compounds more in detail (El-Bourawi et al., 2006). Weakly hydrophobic membranes are also known to gradually wet over time.

5.1. Inorganic fouling

Crystal growth of inorganic compounds (usually primarily consisting of calcium carbonate, calcium sulfate, and halite) on the surface of the membrane can reduce membrane hydrophobicity and eventually cause water logging due to partial wetting (Banat and Simandl, 1994; Bouchrit et al., 2015; Dah Y. Cheng and Wiersma, 1983; Gilron et al., 2013; M. Gryta, 2002; McGaughey et al., 2017; K.G. Nayar et al., 2015). This phenomenon has only been observed for the treatment of saturated solutions (Cho et al., 2016; Feng et al., 2016; Naidu et al., 2017; Sakai et al., 1988; Sanmartino et al., 2016) and not for diluted solutions (Li and Sirkar, 2004; Mericq et al., 2010; Song et al., 2007).

Extreme temperature and concentration polarization within the feed boundary layer can also result in the growth of minerals or salt crystals on the membrane surface and subsequently membrane scaling and wetting (Martínez-Díez and Vázquez-González, 1999; Meng et al., 2015b; Ruiz Salmón et al., 2017; R.W. Schofield et al., 1990; Warsinger et al., 2017b). However, Gryta (M. Gryta, 2002) observed that only NaCl salt deposits with a higher depth of 10 μm from the pore inlet for a membrane with a wall thickness of 400 μm could cause the pore wetting (Fig. 7).
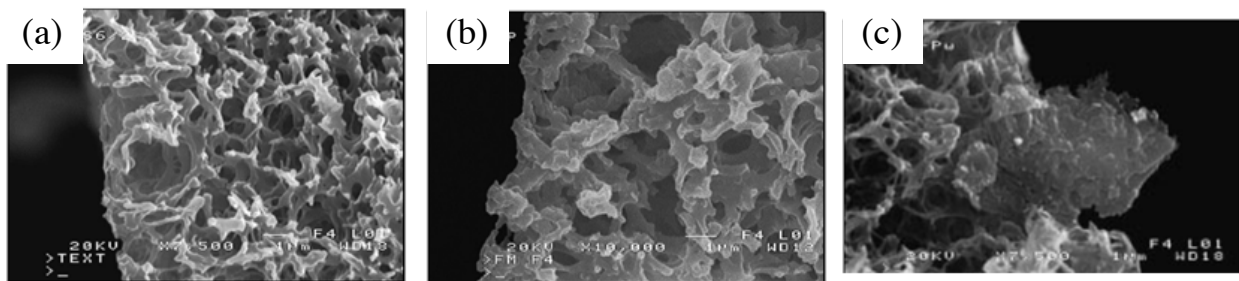
Fig. 7: MD scaling of NaCl crystals: shown here are SEM micrographs of a cross-section of Accurel PP S6/2 membrane demonstrating the pores on the feed side (inside the membrane capillary). a) Pristine membrane, b) after 138 h of MD integrated with salt crystallization, c) membrane with salt crystals inside the membrane pore (M. Gryta, 2002).

301   Importantly, MD membranes benefit from their hydrophobic surfaces, which have low surface energy and

302   thus reduce crystal nucleation (David M. Warsinger et al., 2016).

303   **5.2. Organic fouling**

304   Organic compounds are particularly problematic for MD. When organic compounds are present in the feed

305   solution, the surface tension of the solution decreases, and below a critical surface tension (i.e., surface free

306   energy of the membrane), due to the high affinity of hydrophobic species such as oils to the hydrophobic

307   membrane surface, wetting of the membrane may occur. In this respect, the chemical nature of the foulant

308   (not the thickness) dictates the rate of wetting. For example, a thin layer of an amphiphilic fouling can

309   reduce the CA of the membrane and result in wetting (Goh et al., 2013; Matheswaran and Kwon, 2007;

310   Warsinger, 2015). Notably, while MD membranes are prone to wetting by organic compounds, they have

311   been shown to experience less flux decline than RO or FO membranes undergoing biofouling (Jang et al.,

312   2016).

313   Among different fouling types, growth of microorganisms can be significantly limited in MD due to high

314   operating temperatures and feed salinity (e.g., in clean water production and desalination) (Marek Gryta,

315   2002a; Krivorot et al., 2011; D. M. Warsinger et al., 2015). However, organic foulants can contribute more

316   to the wetting of hydrophobic membranes in MD (Naidu et al., 2015). Among organic foulants, surface-

317   active compounds cause a major challenge in the technical implementation of MD (Soni et al., 2008). When

318   a surfactant reaches a membrane surface, the hydrophobic membrane surface adsorbs the hydrophobic

319   moiety while the hydrophilic part of the surfactant stays in the water phase (Chew et al., 2017a). Therefore,

320   the hydrophobic surface is converted to a hydrophilic surface, resulting in a decreased CA and increased

321   incidence of membrane wetting.

322   Notably, due to the hydrophobicity of MD membranes, solutes with lower surface tension can also cause

323   wetting. For example, alcohols can cause membrane fouling and consequently pore wetting in MD due to

324   the decrease of the surface tension of alcohol solutions, but their concentration plays an important role in

325   the wetting occurrence. Table 4 summarizes the upper alcohol concentrations allowable in water for

326   different membrane materials to avoid wetting.

327   Table 4: The upper alcohol concentrations in water for MD to avoid wetting

Alcohol	Maximum allowable alcohol concentration in water	Membrane	Reference
butanol	1.0 wt. % at 63°C 2.5 wt. % at 63°C	PP PTFE	(Kujawska et al., 2016)
ethanol	10.2 wt.%	PVDF	(Banat and Simandl, 1999)
ethanol	7 wt.% at 55°C	PTFE	(Shirazi et al., 2015)
ethanol	34 wt.%	PVDF with a mean pore size of 0.45 μm	(Treybal, 1980)

328   **6.   Wetting measurement**

329   Hydrophobicity is determined by the interaction between the liquid and the membrane material. Immediate

330   wetting in MD can be predicted by feed solution surface tension and water CA measurements (Lies Eykens

331   et al., 2017). However, long-term performance tests are required to determine the non-wettability of the

332   membrane with non-immediate wetting characteristics. The following section describes the common

333   hydrophobicity measurements for membranes used in MD.

334   **6.1. CA measurement**

335   The conventional method to assess hydrophobicity of a membrane is CA measurement (Shaw, 1992). In

336   this approach, the CA made by a liquid droplet on a membrane surface is measured by a goniometer, which

337   determines relative wettability of membranes. The CA is obtained as the angle between the surface of the

338   wetted membrane and a line tangent to the curved face of the drop at the point of three-phase contact

339   (Onsekizoglu, 2012). The relative wettability of a membrane surface can be studied by measuring the

340   receding and advancing angles of water on a membrane surface. The advancing water CA is associated with

341   membrane hydrophobicity, and the receding angle is related the degree of molecular reorientation necessary

342   to create a new equilibrium state with the aqueous solution (Khayet and Matsuura, 2004). The benefit of

343   this approach is that the actual measurement is easy to perform (K. Y. Wang et al., 2008). However, CAs

344   can show hysteresis and are influenced by the surface structure (roughness) of the membrane (Adamson

345   and Gast, 1997).

346   For CA determination, Neumann et al. (Kwok and Neumann, 1999) established an equation of state using

347   Young-Laplace equation to relate the three interfacial tensions, which can predict the surface energy of a

348   homogeneous dense polymer from surface tension and CA measurements for pure liquids

$$\cos \theta = -1 + 2\sqrt{\gamma_{SV}/\gamma_{LV}} \exp[-\beta(\gamma_{SV} - \gamma_{LV})^2] \tag{10}$$

349   where β is a parameter independent of the solid and the liquid. However, this model can just be applied for

350   high values of surface tensions capable of generating obtuse CAs, thus implicitly excluding the critical zone

351   where wetting occurs (Chibowski and Terpilowski, 2008). Courel et al. (Courel et al., 2001) modified Eq.

352   (10) by introducing surface porosity of the membrane to improve the fitting quality of the model

$$\cos \theta^* = y^2 \cos \theta - (1 - y)^2 - 2y(1 - y)\sqrt{\frac{\gamma_{SV}}{\gamma_{LV}} - \cos \theta} \tag{11}$$

353   where θ^* is the CA of a rough and hairy surface, $1 - y$ is the surface porosity.

6.2. LEP measurement

355   The LEP depends on the interfacial tension of the feed, the CA of the membrane and the size, and structure

356   of the membrane pores (Eq. (1)-(5)) (Franken et al., 1987; Rezaei and Samhaber, 2015, 2014). The LEP of

357   a membrane can be measured by two approaches: static and dynamic method. The static LEP determination

358   proposed by Smolder et al. is a variation of the bubble point method (ASTM International, 2014)

359   (thoroughly described elsewhere (Smolders and Franken, 1989)). However, dynamic LEP measurement

360   can be performed using a typical MD configuration (e.g., vacuum membrane distillation (VMD)). Similar

361   to CA measurements, static LEP measurements have been considered to exhibit hysteresis (Bilad et al.,

362   2015; Durham and Nguyen, 1994; Racz et al., 2015; Sarti et al., 1985). Moreover, this method has been

363   abandoned because membrane compaction occurs during the test, which leads to higher LEP measurements

364   (Durham and Nguyen, 1994). Notably, a recent study showed that this measurement could be improved by

365 measuring the rate of depressurization after stepwise pressure increase, rather than taking the maximum

366 pressure value achieved (Warsinger et al., 2017a).

367 **6.3. Penetrating drop concentration method**

368 To determine the critical solute concentration in the penetrating drop method (Franken et al., 1987), a

369 droplet with the particular concentration of organic material, which is on the verge of penetration into the

370 membrane, is considered as the penetrating drop and the corresponding surface tension is the surface tension

371 of penetrating droplet. The surface tension at which microporous membranes are wetted under process

372 conditions can be calculated by the following equation:

$$\gamma_L = \gamma_L^P + \frac{\Delta P \, r_{max}}{2B} \tag{12}$$

373 where γ_L^P is the surface tension of penetrating liquid measured from penetrating drop method, ΔP is the

374 applied pressure difference and B is a dimensionless geometrical factor. However, this approach can be

375 used for membranes with a surface tension greater than 23 mN/m (Durham and Nguyen, 1994) as the liquid

376 with lower surface tensions wet the membrane instantaneously.

377 **6.4. Sticking bubble technique**

378 In this method, a piece of membrane is placed horizontally at the bottom of the beaker containing a liquid

379 with defined surface tension (Keurentjes et al., 1989). The air bubbles are brought into contact with the top

380 surface by a flat-ended needle. Hydrophobicity is expressed in terms of the surface tension of liquid at

381 which an air bubble has a 50% chance of detaching from the membrane surface ($\gamma_L = \gamma_d$). In the case where

382 radius of bubble (R) is equal to radius of curvature at the top of the bubble (b), the following expression

383 provides the CA of a spherical and deformed air bubble (Fig. 8):

$$\gamma_d = \frac{\Delta\rho g R^2 (\frac{2}{3} + \cos\theta_2 - \frac{1}{3}\cos^3\theta_2)}{2\sin^2\theta_2} \tag{13}$$

$$\sin\theta_1 = \frac{\Delta\rho g R^2 (\frac{2}{3} + \cos\theta_2 - \frac{1}{3}\cos^3\theta_2)}{2\,\gamma_d\sin\theta_2} + \sin\theta_2 \tag{14}$$
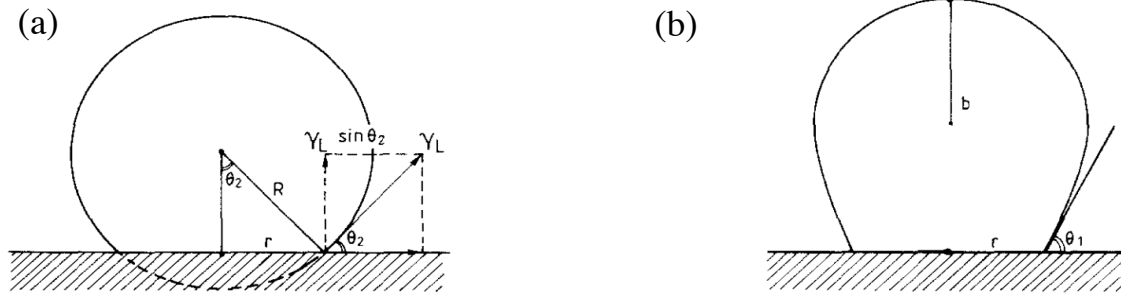
Fig. 8: The air bubble-liquid-membrane system for spherical (a) and deformed air bubbles (b).

6.5. Penetration temperature method

Penetration temperature method was developed for membranes with a surface tension less than 23 mN/m (Durham and Nguyen, 1994). In this approach, either propan-1-ol (*n*-propanol) or propan-2-ol (isopropanol) is placed into a test tube (10 ml at 15° C) with the membrane and thermometer. The test tube is sealed with Parafilm® and placed in a 35° C water bath. The test tube is gradually heated until bubbles appeared on the membrane, then the test tube is lightly tapped, and then the temperature increased at 1° C intervals. The penetration temperature measurement (PT° C) was recorded, when the membrane was almost transparent. The surface tension of the membrane was evaluated using following relationships:

$$\gamma_s = \text{PT° C} \times -0.0777 + 25.253 \qquad \textit{for Propan-1-ol} \qquad (15)$$

$$\gamma_s = \text{PT° C} \times -0.0777 + 22.85 \qquad \textit{for Propan-2-ol} \qquad (16)$$

7. Membrane restoration

Wetted membranes must be entirely dried and cleaned before subsequent usage (Tomaszewska, 2000), which leads to process downtime and potential membrane degradation (Guillen-Burrieza et al., 2013). On one hand, membrane regeneration in the MD process is challenging, and because in many cases fouling is associated with the membrane wettability (Marek Gryta, 2002b), the acquired results are not favorable. On the other hand, reducing the hydrostatic pressure below the LEP will not guarantee the restoration of membrane pores back to unwetted condition. This phenomenon is explained by Lawson et al. (Lawson and Lloyd, 1997) and illustrated in Fig. 9. As $\Delta P_{interface}$ is increased to LEP no liquid wets the membrane pores until LEP is reached (step 1). From this point on the liquid starts to penetrate into and flow through

403   the bigger pores as the pressure increases (step 2). Once all the pores become filled with the liquid, the flux

404   is governed by the Darcy's law ($J = K\Delta P$). Decreasing the pressure results in a linear decrease of flux (step

405   3). In order to restore the membrane to the initial conditions, the membrane needs to be dried. However,

406   solutes in the feed can be left inside the pores of the membrane after the evaporation of the solvent. In this

407   case, the membrane needs to be initially chemically cleaned and then dried in an oven.
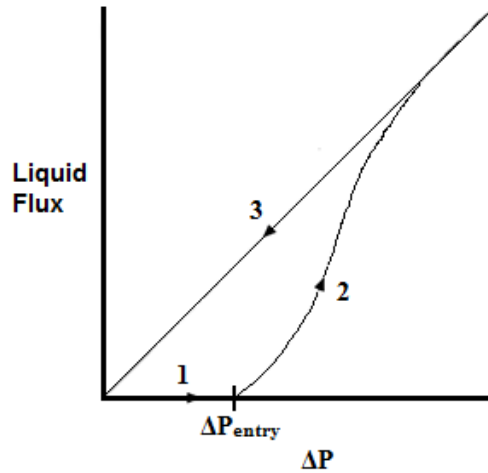
408

409   Fig. 9: Liquid flux versus transmembrane pressure difference (Lawson and Lloyd, 1997) (LEP = ΔP_{entry})

410   Periodic removal of fouling layer can also limit the gradual reduction of permeate flux in MD. Moreover,

411   stabilizing a thinner scaling layer on membrane surface by shortening the interval between the cleaning

412   operation is reported to reduce the risk of partial wetting due to the restriction of the degree of oversaturation

413   inside the wetted pores (Fig. **10**a and b) (Gryta, 2015). However, the dissolution of deposits can facilitate

414   wetting as a result of internal scaling (Fig. **10**c) (Chen et al., 2014a; Gryta, 2017, 2008).

415
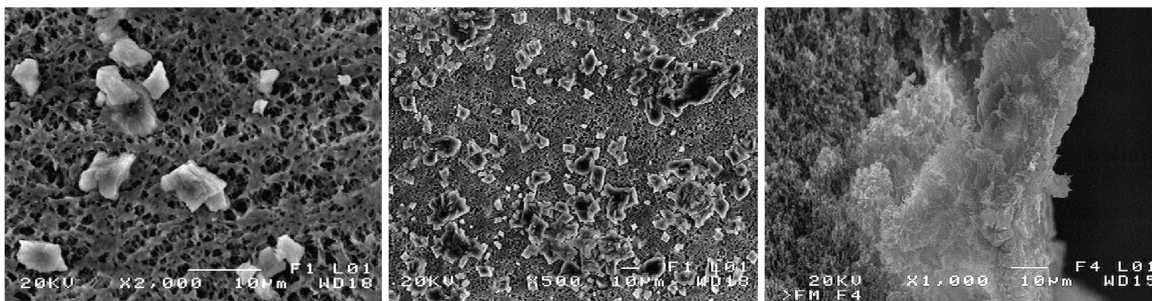
Fig. 10: SEM image of the membrane surface with deposit formed after (a) 1 h of MD process duration (b) 5 h of MD process duration. Feed: tap water (c) SEM image of capillary membrane cross-section. The crystallite formed inside the membrane pores (Gryta, 2015).

7.1. Rinsing and drying

Regeneration of membranes wetted by chemical membrane degradation via rinsing and drying has proved to be ineffective because of the presence of the hydrophilic groups on membrane surface (Gryta et al., 2009). He et al. (He et al., 2008) reported that the effective regeneration of wetted membrane could not be achieved by the process of rinsing the membrane with distilled water, and drying in the oven. This was due to deposition of salt crystals inside the pores and consequently, an irreversible structural change induced by the liquid intrusion inside the pores. Another attempt was also performed to remove the iron dioxide precipitates from the surface and pores of PP membrane with concentrated HCl solutions (Gryta, 2007b). The results showed that the complete removal of iron oxides from the capillary membrane (also including that precipitated into the pores) by rinsing caused wetting of some membrane pores leading to a reduction of permeate flux by 21%. In this case, the acid solution filled the pores adjacent to the pores filled by the deposit, which resulted in an increase of the area of the wetted membrane.

7.2. Backwashing

Another approach for membrane cleaning is backwashing. For instance, air backwashing of the scaled membrane can help to remove crystals and scales. However, when applied to a dried membrane, the effectiveness of this method is limited only for removal of deposits on at the membrane pore mouth (Choi et al., 2017). Backwashing with air is best when a wetted membrane still contains liquid: air pressures exceeding the liquid entry pressure can force wetting liquid out, keeping the solutes from precipitating. (D. M. Warsinger et al., 2016; Warsinger et al., 2017a). Shin et al. (Shin et al., 2016, 2015) explored the dewetting efficiency of high-temperature air on a wetted PVDF membrane. They found that the optimal condition for the air temperature and exposure time ranged from 60-70 °C and 8-12.5 min, respectively. UV irradiation has also been reported to partially clean the PVDF/TiO$_2$ superhydrophobic membranes fouled by gallic acid (Hamzah and Leo, 2017). Their results showed that the gallic acid foulants were

442   decomposed under the irradiation of UV light due to photocatalytic activity of TiO_2 nanoparticles blended

443   in the membrane.

444   Recently, Warsinger et al. (Warsinger et al., 2017a) studied the effectiveness of pressurized air backwashing

445   (PAB) relative to the membrane dryout to reverse membrane wetting in MD. They found out that PAB

446   restored the LEP to 75% of the pristine membrane for lower salinity feeds by removing the saline solution

447   from the membrane without separating water and salts by vaporization. Notably, this method did not involve

448   a dryout step or evaporation (the air was cool), and thus provided dewetting in ~10 seconds of treatment.

449   However, there remains a possibility that air backwashing can cause partial tears in the membrane structure

450   (Fig. **11**).
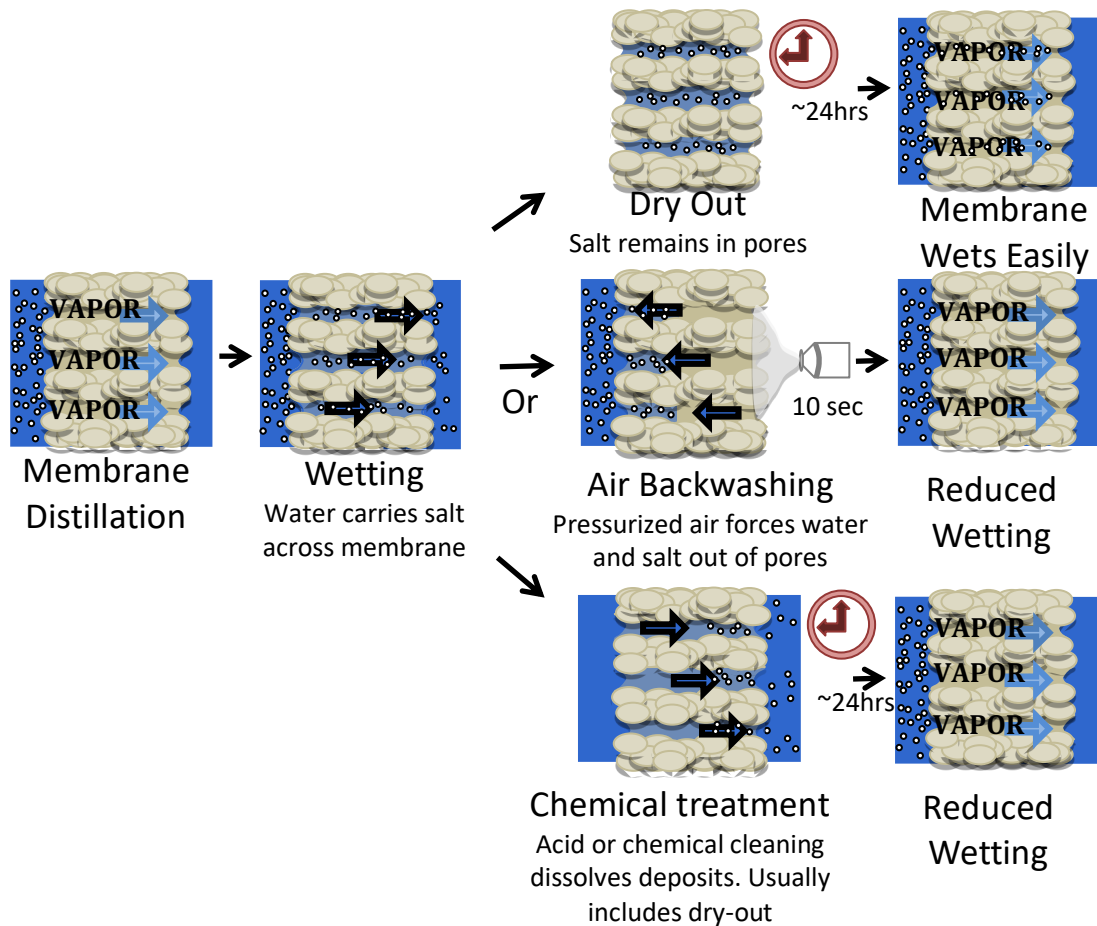
451

452   Fig. 11: Methods for wetting reversal, adapted from (Warsinger et al., 2017a).

8. Mathematical modeling of wetting

One of the main drawbacks in describing the wetting phenomenon in MD is the lack of mathematical models (Babalou et al., 2015). Membrane wetting behavior is complex to simulate, as it is mainly influenced by the microstructural characterization of the membrane itself (Dong et al., 2017). Peña et al. (Peña et al., 1993) proposed a MD model, which evaluates the decrease of permeate flux and steady-state pressure difference due to the progressive membrane pore wetting by the following equation:

$$J = non\ isothermal\ flux - hydraulic\ flux = (1 - \alpha_i)B'\Delta T_b - \alpha_i A\Delta P_i \tag{17}$$

$$J_i = \frac{B'\Delta T_b\ A\Delta P_i^{st}}{B'\Delta T_b + A\Delta P_i^{st}} \tag{18}$$

$$\alpha_i = \frac{B'\Delta T_b}{B'\Delta T_b + A\Delta P_i^{st}} \tag{19}$$

where J is the net volume flux, at the arbitrary time of t_i, J_i is each of the measured fluxes (non-isothermal or hydraulic), B' is a measured or apparent non-isothermal phenomenological coefficient, ΔT_b is the temperature difference in the bulk phases, A is a permeability coefficient, ΔP_i^{st} is the steady-state measured pressure difference when the cold chamber is sealed, and α_i is the percentage of liquid-filled pores. Coefficients A and B' can be calculated based on a two-parameter non-linear regression method from the experimental pairs J_i and ΔP_i^{st} for a given value of ΔT_b. Following the model proposed by Peña, García-Payo et al. (García-Payo et al., 2000) proposed the following equations to calculate the LEP taking into account the axial irregularity of pores:

$$LEP = -\frac{2\gamma_L}{r_{max}}\frac{\cos(\arcsin(\xi))}{[1 + \frac{2R}{r}sin^2\left(\frac{\theta_A}{2} - \frac{\arcsin(\xi)}{2}\right)]} \tag{20}$$

where r is the mean pore radius, θ_A is the advancing CA, R is the mean curvature radius of pore wall elementand $\xi = \frac{\frac{R}{r}\sin\theta_A}{1 + \frac{R}{r}}$ (Fig. **12**).
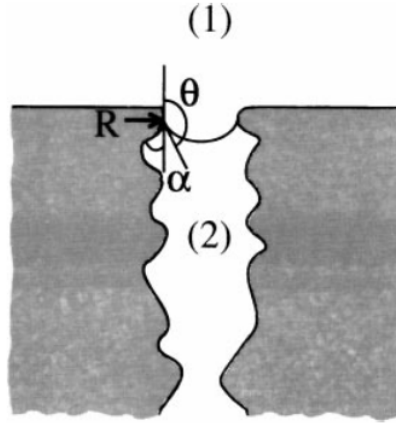
469

470   Fig. 12: Interface in an irregular pore of the hydrophobic membrane. (1) Liquid phase and (2) gas phase.

471   When the geometry of the pore is axially irregular, a structure angle, α, may be defined as the angle

472   between a pore wall element and the normal to the membrane surface in the axial direction (García-Payo

473   et al., 2000).

474   For polar or hydrogen bonding liquids on non-polar solids with low surface energy, the LEP can be

475   calculated based on van der Waals dispersion components of the work of adhesion of a fluid to a solid

476   surface (García-Payo et al., 2000):

$$LEP = \frac{2}{r_{max}}\left(\gamma_L - 2\sqrt{\gamma_S^d \gamma_L^d}\right) = \frac{2}{r_{max}}(\gamma_L - \gamma_L^w) \qquad (21)$$

477   where γ_S^d, γ_L^d are the dispersion components of surface tension of the solid and the liquid and γ_L^w is the

478   wetting surface tension (i.e., LEP=0).

479   **9. Membrane non-wetting characteristics**

480   The main prerequisite to be satisfied by the membranes during MD operation is that solutions on both sides

481   of the membrane do not wet the pores of the hydrophobic membrane (Zydney, 1995). The question of how

482   to characterize the wettability of a MD membrane is a critical one, although few structural studies can be

483   found in the literature.

484   The selection of membrane material and properties can assist to prevent membrane wetting. In MD, intrinsic

485   hydrophobic microporous polymeric membranes such as PVDF, PP, polytetrafluoroethylene (PTFE) and

486   polyethylene (PE) are used. However, these membranes are prone to wetting if LEP is exceeded.

487 As the first prerequisite for a proper membrane operation under fluctuating pressures and temperatures in

488 the plant, the LEP of the membrane is recommended to be higher than 2.5 bar regardless of the MD

489 configuration (Eykens et al., 2016; Schneider et al., 1988a). A more hydrophobic membrane can decrease

490 the chances of reduction of the permeate flux due to partial wetting. PVDF is a less hydrophobic polymer

491 relative to other polymeric MD membranes. PVDF has a surface free energy of 30.3 mN/m while PE, PP,

492 and PTFE membranes have surface free energies of 20-25 mN/m, 30 mN/m, and 9-20 mN/m, respectively

493 (Ashoor et al., 2016; Bonyadi and Chung, 2007; Cheng et al., 2010). Therefore, PVDF membranes might

494 be more prone to the wetting. However, PVDF membranes have been wildly used due to easy

495 processability.

496 Moreover, the intrinsic CA of nonporous PVDF material is less than 90°. However, it can be enhanced by

497 increasing the surface roughness (Kang and Cao, 2014). Compared to the hydrophobicity of the membranes,

498 the surface roughness is more crucial than low surface energy. The reason is that when two surfaces with

499 different hydrophobicity are roughened, both can become superhydrophobic (Tijing et al., 2014a).

500 Wetting concentration (i.e., the lowest concentration of a solution that wets the membrane spontaneously

501 (García-Payo et al., 2000)) is always considerably higher for PTFE membranes than the wetting

502 concentration for PVDF membranes under identical experimental conditions (An et al., 2016a; Courel et

503 al., 2000; García-Payo et al., 2000). However, the utilization of PTFE in large-scale industrial applications

504 is restricted due to its various disadvantages, such as a high fabrication cost and environmental impacts

505 (Gryta, 2016b).

506 PP has a relatively high surface energy (29 mN/m) and the smallest CA among other polymers used in MD.

507 These traits have been found to result in partial wetting after few weeks of operation in an MD process

508 (Gryta, 2005).

509 Using membranes with a small pore size (maximum micropore radius of less than 0.6 µm and LEP more

510 than 100 kPa (L. Eykens et al., 2017; Rao et al., 2014; Thomas et al., 2014)) and high tortuosity (i.e., 50-

511 80%) as well as the sponge-like structure can ensure that process pressure and temperature fluctuations do

512 not lead to membrane wetting (Kezia et al., 2015; Schneider et al., 1988b). Higher membrane porosities

513 than 80% are usually accompanied by large pore sizes which are not suitable as they intensify the danger

514 of membrane pore wetting (Banat and Simandl, 1998). The use of a nonporous membrane in MD similar

515 to pervaporation has been proposed since the dense structure of the membrane inhibits wetting

516 (Purwasasmita et al., 2015).

517 The thickness of the membrane also plays a major role in wettability of the membrane. A decrease in

518 membrane wall thickness significantly improves the permeate flux. However, it increases the risk of

519 membrane wetting.

520 **10. Effect of operating conditions on wetting**

521 The operating conditions for MD can be controlled such that membrane wetting is prevented. For instance,

522 pressure spikes or absence of temperature gradient can result in wetting of some pores and consequent

523 deterioration in the quality of distillate (Peng et al., 2017; Walton et al., 2004). Membrane temperature

524 decline due to membrane dry-out as the result of temporary shutdowns can precipitate dissolved substances

525 from the feed on the membrane surface and pores, accelerating membrane wetting (capillary condensation

526 (Atchariyawut et al., 2006; Meng et al., 2015b)). Therefore, for instance, in the case of intermittent

527 operation, the proper shutdown protocols are needed when storing used MD modules for the extended

528 periods of time (Guillen-Burrieza et al., 2014).

529 On the contrary, the surface tension of solutions decreases with an increase in temperature, making the

530 wetting a greater challenge at higher temperatures (Nayar et al., 2014). For pure water, the value of surface

531 tension varies between 72-64 mN/m for temperatures between 25-70°C. Increasing feed temperature can

532 also increase the scaling and membrane wetting due to oversaturation in the boundary layer for the saturated

533 brine solutions (Edwie and Chung, 2013; Ge et al., 2014; Shirazi et al., 2014). The sustainability of a DCMD

534 process for a hypersaline solution at a higher temperature difference of 40 °C was compromised due to

535 membrane wetting (Hickenbottom and Cath, 2014).

536 Lowering the applied pressure in the feed and the permeate through adjusting the feed and permeate flow

537 rates reduces the pressure difference across the membrane, hence reducing the tendency for the membrane

538 wetting due to operating below LEP (Luo and Lior, 2017; R W Schofield et al., 1990). Moreover, permeate

539 quality deterioration can be avoided if the permeate pressure is kept higher than the feed pressure.

540 Therefore, the feed cannot directly flow through the wet pores to the permeate side. In this case, MD process

541 may be continued; however, after a wetting incident, the permeate flux decreases due to the reduction of

542 active pores. In DCMD, a slightly higher pressure on the permeate side than the feed side has been used to

543 reduce the risk of wetting (Zakrzewska-Trznadel et al., 1999).

544 Although high cross-flow velocity minimizes the boundary layer resistances and leads to higher permeate

545 flux, it increases the pressure difference across the membrane (e.g., 10-20 kPa) and enhances the risk of

546 pore wetting. Thus, the recirculation rate should be high enough to reduce the polarization effect, and

547 sufficiently low to operate below LEP (Lawal and Khalifa, 2015; Naidu et al., 2014; Srisurichan et al.,

548 2006; Y. Zhang et al., 2015). In this case, the feed flow rate must be varied with due precautions as the

549 transmembrane hydrostatic pressure which needs to be always lower than LEP is a function of the second

550 power of the feed velocity.

551 Recently, Guillen-Burrieza et al. (Guillen-Burrieza et al., 2016) conducted DCMD experiments to

552 understand the effect of operational parameters on the wetting phenomenon and concluded that when

553 parameters are adjusted in a way that increases permeate flux, both the wetting time and rate are reduced.

554 Notably, feed and permeate temperatures are more associated with the wetting time (e.g., high ΔT increases

555 the wetting time), while feed and permeate flow rates are more influencing the wetting rate (the lower one

556 decreases the wetting rate).

557 Additionally, it is important to note that numerous operating factors that increase fouling also may increase

558 wetting. These factors imply the need for avoidance of stagnation zones from spacers or piping that give

559 time for crystal nucleation, avoidance of high-energy surfaces (e.g. metals) which may induce nucleation,

560 and implementation of proper pretreatment for fouling particles (Warsinger et al., 2017b).

561 **11. Effect of MD configurations on wetting**

562 As the feed conditions can vary independently of configuration, in most cases the configuration impacts

563 wetting little. Particular attention must be noted in VMD to avoid membrane wetting because in this

564 configuration vacuum is applied to the permeate side and therefore $\Delta P_{interface}$ is usually higher in VMD

565   than in the other MD systems (Hassan et al., 2015; Lawson and Lloyd, 1997; Mohammadi and Akbarabadi,

566   2005). Therefore, the VMD has been used just for removal of volatile organic compounds from dilute

567   aqueous solution and, unlike other membrane processes such as pervaporation, not for separation of

568   organic/organic or organic/water mixtures. Notably, process conditions influenced by configuration choice

569   can have an impact on wetting, such as temperature differences at the membrane surface (which impacts

570   foulants and also surface tension), and concentration polarization caused by greater flux. In a study

571   conducted by Meng et al. (Meng et al., 2015a), membranes in submerged VMD (with no agitation) were

572   wetted quickly within the first 8 h of inland desalination operation, whereas membranes in cross-flow VMD

573   maintained rather low permeate conductivity for 50 h.

574   **12. Approaches to control wetting**

575   Different approaches to control wetting in MD have been proposed by several researchers. Most of the

576   emphasis has been on advancement in membrane fabrication in such a way to ensure a low affinity between

577   the liquid and the polymeric material. This has been mainly done through modifying the membrane surface

578   geometrical structure and surface chemistry. Several studies also investigated the integration of filtration

579   processes with MD as pretreatment steps. The following section reviews these approaches in more detail.

580   **12.1. Pretreatment/Hybrid MD processes**

581   Wetting of the hydrophobic membrane can be avoided by the use of a robust pretreatment of the feed liquid.

582   Many of these processes effectively removed membrane wetting agents before they reached the membrane.

583   However, one should note that the capital and operating costs of the process will increase due to the addition

584   of a pretreatment step.

585   Several methods are proposed to be integrated with MD for different applications (Table 5). Integration of

586   filtration processes with MD can remove most contaminants and foulants from the feed solution, thus

587   mitigating the wetting problem. In the case of protein as a fouling agent, either the feed solution can be

588   boiled followed by filtration to reduce the precipitation of proteins on the membrane surface (Gryta, 2008),

589   or ultrasonic waves can be introduced to mitigate protein fouling (i.e., the deposition of bovine serum

590   albumin aggregates) and consequently wetting incidence (Hou et al., 2017). Nanofiltration can also be used

591   to remove less soluble compounds including divalent salts (Roy et al., 2017): this has been integrated into

592   membrane distillation (Kumar et al., 2017). Ultrasonic treatment in a hybrid process with MD can also

593   mitigate membrane $CaSO_4$ scaling and thus reducing the risk of membrane wetting (Hou et al., 2015).

594   Additionally, coagulation pretreatment to form bigger crystals than the membrane pores can considerably

595   minimize the risk of scale formation inside the membrane pores. Accelerated precipitation softening

596   including pH adjustment with sodium hydroxide along with calcite seeding, followed by microfiltration to

597   avoid clogging by the seeds was integrated before DCMD to desalinate a primary RO concentrate (Qu et

598   al., 2009). Membrane distillation bioreactors (MDBR) couple thermophilic bioprocess, which results in

599   the biological removal of high concentrations of organics and nutrients. This pretreatment expands the

600   application of MD to the reclamation of industrial wastewater containing a low volatile solute content.

601   Another way to reduce scaling incidence in MD is chemical conditioning of the feed using antiscalants

602   (e.g., polyacrylic acid). The use of antiscalant could prolong the induction period for the nucleation of

603   gypsum and calcite, respectively; and slow down the precipitation rate of crystals (He et al., 2009; Peng et

604   al., 2015; P. Zhang et al., 2015). However, high dosing of antiscalant can also increase the risk of membrane

605   wetting because of organic nature of antiscalants. Most recently, Dow et al. (Dow et al., 2017) demonstrated

606   that the MD testing on a textile mill effluent that was first treated by flocculation and anaerobic/aerobic

607   digestions eliminated the wetting issue.

608   Table 5: Pretreatment process applied for MD to control wetting occurrence

Pretreatment	Process	Application	Impact	Results	Ref.
Physical	Ultrafiltration	concentration of grape juice	protein removal	max ~7% increase in juice surface tension	(Bailey et al., 2000)
	Microfiltration	ammonia stripping from pig manure	protein removal	2-4 times increase in ammonia mass	(Zarebska et al., 2015)

			transfer coefficient	32
Forward osmosis	wastewater reuse	ammonium, COD, arsenic removal	>99% removal efficiency of the volatile contaminants	(Husnain et al., 2015)
	real domestic wastewater treatment	removal of most high molecular weight contaminants	>90% removal efficiency of the organic matters, calcium salts, magnesium salts, sodium salts, silicates	(Li et al., 2018)
Integreatd crystallization	shale gas produced water treatment	reducing scalant loading of multivalent ions, such as barium and calcium	increasing the total water recovery from 20% to 62.5%	(Kim et al., 2016)
Multi-stage flash distillation	desalination of rejected brine	reducing concentration of different organic and inorganic contaminants	4-12% less reduction in permeate flux	(Kayvani Fard et al., 2016)

	Activated carbon	seawater and concentrated brine treatment	remove particulates and organic contaminants	21% and 23% removal of the antiscalant and antifoam agent	(Minier-Matar et al., 2014)
	Foam fractionation	concentrating textile mill effluent	capturing surface-active materials	increase of concentration factor from 27 to 34-fold	(Dow et al., 2017)
Chemical	Coagulation	desalination of recirculating cooling water	elimination of total organic carbon, total phosphorus substances	23% increase in permeate flux	(J. Wang et al., 2008)
	Chemical conditioning	treatment of RO brine	removing calcium hardness and sulfate ions	increase of final rejection factor form 58.6% to 97.9%	(Sanmartino et al., 2017)
Biological	Integrated bioreactors	reclamation of industrial wastewater	biological removal of organics and nutrients	delaying wetting by 1.7–3.6 times	(Goh et al., 2013)
	Biological treatments	textile wastewater treatment	digesting surfactants	reduction of TOC from 100 to 26 mg/L	(Dow et al., 2017)

Other	Microwave-assisted photo-catalysis	treating the coal gasification wastewater	preventing organic fouling by photodegrade the organic matters	increase of normalized permeate flux from 79.8% to 98.5%	(J. Wang et al., 2016)

12.2. Advances in membrane fabrication

Preventing and controlling membrane wetting via appropriate membrane design is of significant interest. Nevertheless, at present, most of the developed membranes still undergo some level of wetting. The current MD membrane design process relies heavily on commercial MF membrane fabrication methods, i.e., conventional thermal or dry/wet phase inversion techniques (Tijing et al., 2014a). These manufacturing methods lead to a non-homogeneous pore size distribution, which increases the risk of wetting for larger pores.

The primary goal of advancement in membrane fabrication is to obtain a surface with special non-wettability (Z. Wang et al., 2016a). These surfaces are categorized to superhydrophobic surfaces repellent to water, superoleophobic surfaces repellent to oil and omniphobic surfaces repellent to both water and oil. However, these methods commonly demand complex fabrication processes or high-specialized equipment, making them unacceptable inefficient production (Yang et al., 2016). Finally, the durability and long-term stability of these membranes are also questionable and require systematic research especially against high salinity feeds and different organic foulants (El-Bourawi et al., 2006; Yang et al., 2014; Zhang et al., 2005, 2013a).

Based on the goal of excellent liquid repellency, different strategies are developed to fabricate membranes with special non-wettability. Some of the methods developed to change not only the surface of the membrane but also the membrane matrix characteristics, while others are based on the physical and chemical modifications of surface morphology and microstructure of the fabricated membrane. The main disadvantages of the surface modification techniques are to change the membrane surface wettability

629 without affecting the bulk wetting properties. Superhydrophobic surface coating of the hydrophobic

630 membranes increases the surface roughness and consequently the CA, θ as the contact angle in Eq. (1), but

631 it can have less effect in increasing the LEP. The reason is that CA is a surface property only, while the

632 LEP is affected not only by surface wettability of the membrane but also by the wettability inside of the

633 pores. For example, according to Eq. (4), LEP is affected not only by the surface property but also

634 "h", the floor height describing the interactions between the liquid and the pores below the initially

635 wetted surface (Fig. 3). (Franco et al., 2008; Liao et al., 2013; Prince et al., 2013; Yan et al., 2017). As

636 by surface coating in case of membrane surface wetting, fewer resistances exist inside the pores, and the

637 liquid penetrates more easily throughout the membrane thickness (Jin et al., 2008). Therefore, both surface

638 and bulk modifications are necessary to create the membrane in a designed way, and this cannot be

639 accomplished solely by the structuring of the surface or only by chemical functionalization (D.Y. Cheng

640 and Wiersma, 1983; Kujawa et al., 2017). Table 6 summarizes the applied methods for advancement in

641 membrane non-wettability to increase the membrane hydrophobicity or providing anti-sticking/self-

642 cleaning surfaces.

643 Table 6: Methods applied in MD for wetting prevention

Approach	Method	Inference	Reference
Membrane fabrication	incorporation of hydrophilic nonporous layers	to inhibit a transport of amphipathic molecules, however, includes more resistance than a porous hydrophobic coating	ethylene glycol (Chong et al., 2016; Majidi Salehi et al., 2016) polyvinyl alcohol (Z.-Q. Q. Dong et al., 2015; Mansouri and Fane, 1999; N.M. Mokhtar et al., 2014; Ray et al., 2017) polyethylene glycol (Feng and Jiang, 2006; Zuo and Wang, 2013) alginate (Xu et al., 2004)

			alginic acid-silica (Xu et al., 2005b)
			alginate-carrageenan (Xu et al., 2005a)
			chitosan (Chanachai et al., 2010)
	Loading of perfluorinated polymers	to increase membrane hydrophobicity by reducing surface free energy	(Chen et al., 2015; Edwie et al., 2012; Figoli et al., 2016; Guo et al., 2015; Kujawa et al., 2016; Lalia et al., 2013; Prince et al., 2014b; Tong et al., 2016; Xu et al., 2017; Y. Zhang et al., 2017; Zhao et al., 2017)
	loading of functionalized hydrophobic nanoparticles/nanofibers	to maximize membrane hydrophobicity by increasing the membrane CA and minimize the surface pores size	(Baghbanzadeh et al., 2015; Boo et al., 2016; Z.-Q. Dong et al., 2015; Dong et al., 2014; Efome et al., 2016; Fan et al., 2017; González-Benito et al., 2017; Hammami et al., 2016; Hamzah and Leo, 2017; Lalia et al., 2014; E.-J. Lee et al., 2017; Li et al., 2014a, 2014b, X. Li et al., 2016, 2015; T. Liu et al., 2016; K.-J. Lu et al., 2017; X. Lu et al., 2017, 2016; Ma et al., 2009; Moradi et al., 2015; Qing et al., 2017; Rezaei and Samhaber,

			2016b, 2016c; Su et al., 2017; Tijing et al., 2014b; Z. Wang et al., 2016b; Yan et al., 2017; W. Zhang et al., 2017; Zhong et al., 2017)
	loading of carbon-based micro- and nanomaterials	to enhance the membrane surface roughness	carbon nanotubes (CNTs) (Fan et al., 2016; J.-G. Lee et al., 2017; Y. Li et al., 2015; Mapunda et al., 2017; Okiel et al., 2015; Silva et al., 2015; Tijing et al., 2016; Woo et al., 2016a, 2016b) graphene (An et al., 2017; Moradi et al., 2015; Y. Wang et al., 2017; Woo et al., 2016a)
Membrane modification	Physical modification	to increase membrane surface roughness	plasma treatment (Chul Woo et al., 2017; Dumée et al., 2016; Fane et al., 2012; Li and Sirkar, 2005; L. Liu et al., 2016; Sirkar and Qin, 2001; Tian et al., 2015; Xu et al., 2015; Yang et al., 2014, 2015; X. Yang et al., 2011) layer-by-layer assembly (Arafat et al., 2015; N. M. Mokhtar et al., 2014; Prince et al., 2014b; Rezaei and Samhaber, 2016a; Tijing et al., 2014b; Woo et al., 2015; W. F.

			Yang et al., 2011; Zhu et al., 2015; Zuo et al., 2017) template replication (Peng et al., 2013) phase separation (Thomas et al., 2014; Xiao et al., 2015) electrospinning (An et al., 2016b; Huang et al., 2017) double re-entrant cavities (Domingues et al., 2017) thermal treatment (Shaulsky et al., 2017; Wang et al., 2014; Yao et al., 2017)
	Chemical modification	to reduce surface free energy	incorporation of surface-modifying molecules or low surface tension functional groups (Chua et al., 2015; Huang et al., 2016; Kujawa and Kujawski, 2016; Kujawski et al., 2016; Kyoungjin An et al., 2017; E.-J. J. Lee et al., 2016; K. J. Lu et al., 2016; Prince et al., 2012; Y. Wang et al., 2017; Wang and Lin, 2017; Xiaoxing et al., 2011; Yin et al., 2017; Zhang et al., 2013b; Zuo and Chung, 2016)

644   Some of these techniques have disadvantages. Generally, adding layers to a membrane surface reduces

645   permeability. Ideal MD membranes are highly porous with low conductivity, so denser regions may impair

646   system-level performance (Swaminathan et al., 2018). Added cost in fabrication is also another concern,

647   especially in steps that require long durations or expensive precursors. Importantly, many of the most

648   hydrophobic compounds ideal for MD membrane anti-wetting have environmental toxicity concerns (e.g.

649   fluoropolymers). Some processes (e.g., plasma coating) may damage some substrates, and so should be

650   chosen carefully. Finally, while increasing surface roughness can increase hydrophobicity, surface

651   roughness can have complex interactions with certain foulants, with increased adherence in some situations.

652   The following part of this section reviews some of the new aspects of advancement in membrane fabrication

653   methods for higher wetting resistance in MD.

654   **12.2.1. Membrane surface modifications**

655   As mentioned, the surface chemistry and geometrical structures determine the wetting property of

656   membrane. Surface chemistry adjusts the surface tension at the microscopic level, but geometrical structure

657   controls how these forces act upon the liquid (McHale et al., 2004). Thus, varying one of these two

658   parameters can regulate the surface non-wettability. The functionalization with low surface energy

659   materials particularly fluorosilanes (Fig. 13) can decrease the surface free energy. Alternatively, generating

660   a hierarchical nanostructure surface morphology with multi-level surface roughness can tune the surface

661   wettability (Razmjou et al., 2012). Moreover, increasing the surface roughness via nano-coating not only

662   contributes in engineering the hierarchical structure but also provides sites (OH functional groups) for the

663   hydrolyzed silane coupling agent to be anchored forming a robust uniform water-repellent film (Meng et

664   al., 2014a).
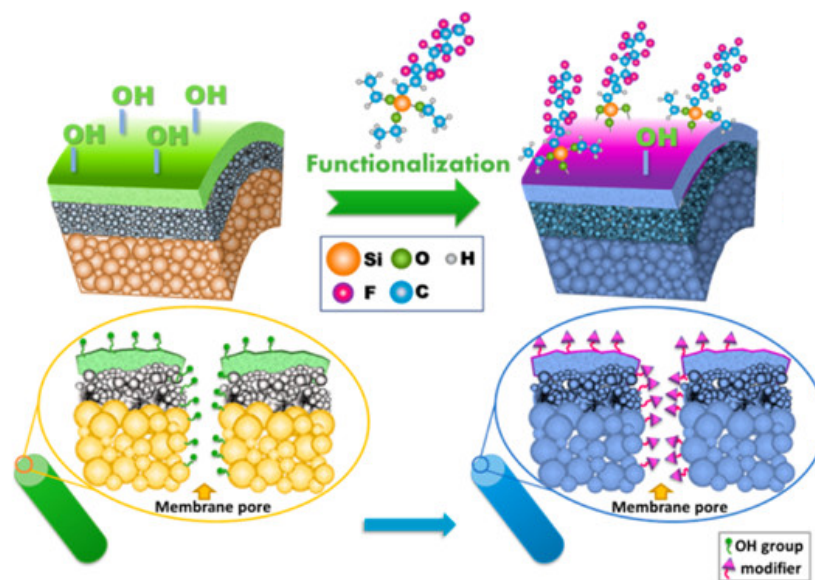
Fig. 13: The scheme of membranes functionalization by perfluoroalkylsilanes molecules (Kujawa et al., 2017).

Although the achievement of superhydrophobic membranes with these strategies is successful, most of the superhydrophobic surfaces are prone to wetting by organic solutions, and very few attempts are made to fabricate omniphobic membranes that provide enhanced repellency to different liquids such as oils and alcohols. Omniphobic membranes with a re-entrant structure provide a local kinetic barrier for shifting from the meta-stable Cassie-Baxter state to the completely wetting Wenzel state for low surface tension liquids. However, the main difficulties in fabricating stable omniphobic membranes for MD applications are the control of faultless and tedious surface topography and complicated fabrication procedures which are too expensive to be implemented in the large scales (Wei et al., 2016). On the other hand, applications of these membranes for the treatment of oily wastewater with all main components and the interaction between these elements via simulations tools are not deeply studied (Han et al., 2017). Until now, only a few reports studied the omniphobicity for non-polar liquids by developing specially designed patterns such as overhang structures, re-entrant curvatures, silicone nanofilaments and candle soots or by using inherently textured substrates (Brown and Bhushan, 2016; Darmanin and Guittard, 2013; Grynyov et al., 2016; Joly and Biben, 2009; Kota et al., 2013; Kota and Tuteja, 2012; L. Li et al., 2016; Song et al., 2013; Tuteja et al., 2007, 2008). Among these works, Lin et al. (Lin et al., 2014) developed the omniphobic microporous membrane

683   for MD that repels both water and low surface tension liquids by coating a hydrophilic glass fiber membrane

684   with silica nanoparticles, followed by subsequent surface fluorination and polymer coating (Fig. **14**). The

685   9 h course of DCMD experiments for the feed solution containing 1.0 M NaCl and 0.4 mM SDS at 60 °C

686   no wetting occurred for the omniphobic membrane, while for the PTFE membrane wetting became

687   progressively more severe as water flux increased more than fivefold and salt rejection dropped to 40% at

688   0.4 mM SDS. However, it is worth noting that the fluorinated chemicals are potentially dangerous and they

689   are regarded as persistent and global contaminants. New non-chemical methods such as pretreatment

690   methods or other physical water treatment techniques to prevent wetting are required to be evaluated. In

691   another study, Lee et al. (J. Lee et al., 2016) fabricated omniphobic nanofiber membranes by preparing

692   positively charged nanofiber mats and grafting negatively charged silica nanoparticles and fluoroalkylsilane

693   to achieve multi-level re-entrant structures. Their fabricated membrane showed wetting resistance to

694   various liquids, including ethanol with a surface tension of 22.1 mN/m and exhibited a stable desalination

695   performance for eight-hour operation.
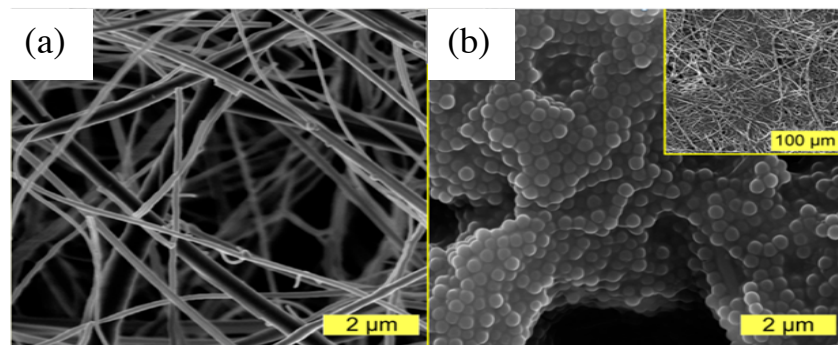
696

697   Fig. 14: SEM images featuring the local morphology of (A) a glass fiber (GF) membrane and (B) an

698   omniphobic membrane after the five-step modification procedure. The inset image in B shows the

699   morphology of a large piece of the omniphobic membrane (Lin et al., 2014).

700   **12.2.2. Membrane bulk modifications**

701   Membrane morphology and crystalline composition have a high impact on the wetting action of a

702   membrane. Formation of finger-like macro-voids in the polymeric membrane matrix due to the type of

703   solvent used in the fabrication process can reduce the LEP and therefore increase the risk of membrane

704   wetting (Fig. **15**). In the wet/dry spinning technique for fabrication of PVDF membranes, faster solvent/

705   nonsolvent exchange rate is responsible for the formation of finger-like structure or even macro-voids

706   (García-Fernández et al., 2014). Blending PVDF and PTFE to form a sponge-like membrane structure is

707   proved to be an effective way to increase membrane hydrophobicity (i.e., CA) (Gryta and Barancewicz,

708   2010). Fabrication of dual-layer membrane comprising finger-like and sponge-like layers can reduce the

709   wetting risk while enhancing the membrane performance in regard to permeability. Wang et al. (Wang et

710   al., 2011) demonstrated that the PVDF dual-layer hollow fiber with a fully finger-like inner layer and an

711   entirely sponge-like outer-layer resulted in 98.6 L m^{-2} h^{-1} permeation flux and LEP of 0.7 bar.
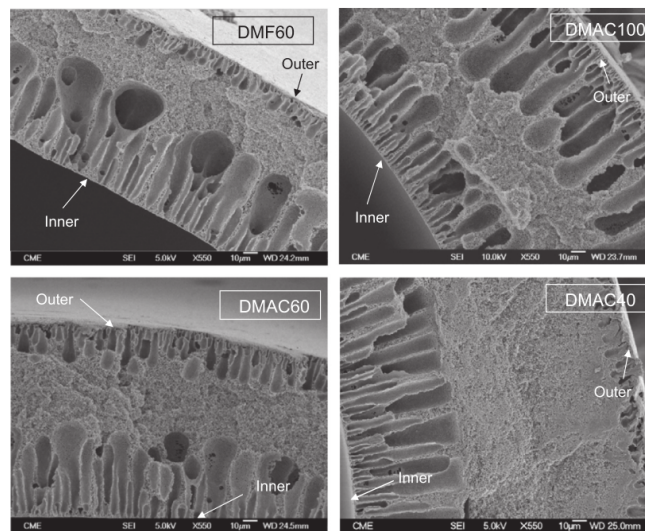
712

713   Fig. 15: SEM images of the cross-section morphology of the PVDF-HFP hollow fiber membranes

714   prepared with different solvents (García-Fernández et al., 2014). All the membranes exhibit a sponge-like

715   structure in the middle layer and a finger-like structure in the internal and external layers of the hollow

716   fiber membranes.

717   A number of theoretical and experimental works have considered the composite hydrophilic/hydrophobic

718   membranes for MD, but few have studied the wetting behavior of these membranes (Bilad et al., 2015;

719   Feng et al., 2017; Gryta and Barancewicz, 2010; Jeong et al., 2014; X. Lu et al., 2016; Meng et al., 2014b;

720   N. M. Mokhtar et al., 2014; Mostafa et al., 2017; Prince et al., 2013; Rezaei and Samhaber, 2016a; Tong et

721   al., 2016; Zhu et al., 2015). Among these works, Peng et al. (Peng et al., 2005) developed a composite

membrane with a hydrophilic layer of polyvinyl alcohol (PVA) blended with polyethylene glycol (PEG) on a hydrophobic PVDF substrate for desalination. The composite membrane showed no wetting incident compared to hydrophobic membranes even after adding 25% ethanol to the brine feed. Later, Edwie et al. (Edwie and Chung, 2012) found out that membrane pore size and morphology beneath the membrane surface is more crucial to mitigate membrane wetting as compared to membrane wall thickness for a supersaturated NaCl feed solution. They fabricated three types of membranes including single-layer PVDF, dual-layer hydrophobic–hydrophobic PVDF and dual-layer hydrophobic–hydrophilic PVDF/polyacrylonitrile (PVDF/PAN) membranes. They found that the single-layer membrane possessing a smaller pore size and a cellular mixed-matrix structure outperformed the dual- layer membranes with a globular morphology with a superior wetting resistance. Triple layer nanofiber/hydrophobic/hydrophilic membranes have also been shown to increase in water CA and LEP. For this type of membranes (Fig. **16**), the intermediate hydrophobic layer increases the LEP of the membrane by narrowing the pore size, while the bottom surface-modifying macromolecules (hydrophilic) layer draws water vapor from the intermediate layer by absorption (Prince et al., 2014a).
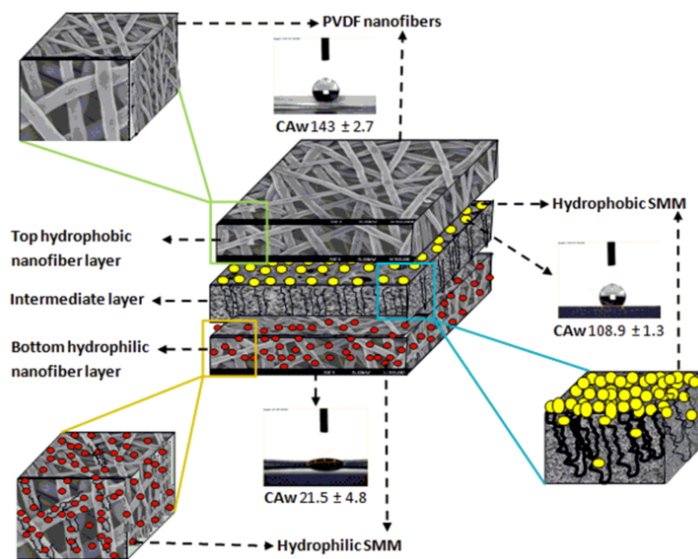
Fig. 16: The configuration of the triple layer membrane (Prince et al., 2014a).

Lin et al. (Lin et al., 2015) proposed a novel approach, hydrogel-covered membrane distillation (HcMD), by attaching an agarose hydrogel layer of a solid content of 6 wt.% with a thickness of 200 μm on the

740   surface of a PTFE membrane to reduce the risk of membrane wetting against various surfactants. The result

741   showed no wetting during 24 h period when the concentration of surfactants was below critical micelle

742   concentration (CMC) due to the repellency of hydrophobic moiety of the surfactant by the hydrogel phase.

743   The agarose hydrogel with high water content acts as a static water layer by adsorbing the hydrophilic

744   moiety and leaving the hydrophobic part outside of the surface, and preventing the surfactant from diffusing

745   further into the hydrogel layer due to Donnan exclusion of ions (Bell, 2016) (Fig. **17a**). This causes the

746   buildup of the surfactant molecules on the interface. Above the CMCs the wetting occurred due to diffusion

747   of the absorbed hydrophilic moiety of micelles into the hydrogel phase, but to a lower extent and at a slower

748   pace compared to bare membranes (Fig. **17b**). Attachment of hydrogel layer also decreased the permeate

749   flux to about 71% of the flux using a bare membrane.
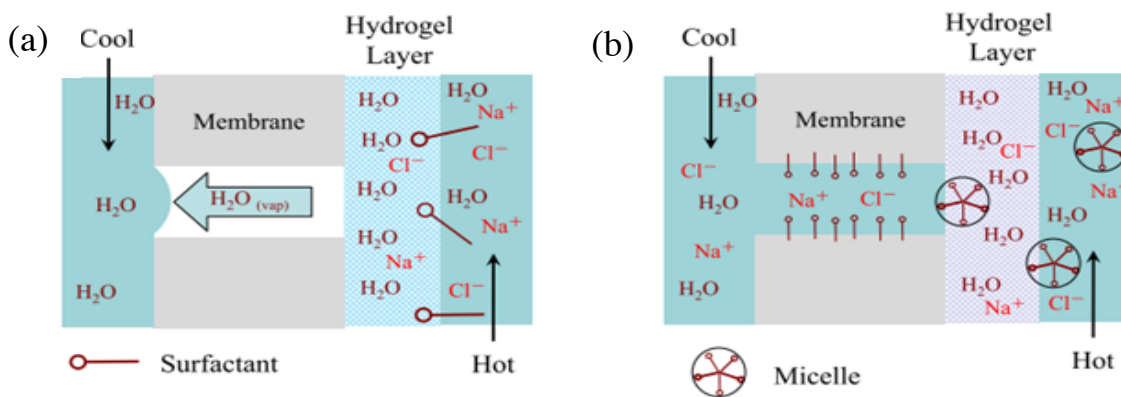
750

751   Fig. 17: The mechanism of hydrogel layer (a) against surfactant wetting (b) for the penetration of micelles

752   through hydrogel layer.

753   **12.3. Flow effects of buoyancy**

754   Certain foulants have significant buoyancy differences from the bulk solution. MD systems can be designed

755   to use this benefit to reduce surface adherence. For instance, in a study by Tan et al. (2017), inclined

756   modules were used, with the membrane below the bulk fluid. The more buoyant oils in the seawater floated

757   to the surface, and thus the inclination angle reduced fouling. This design works for flat plate modules

758   (Warsinger et al., 2014), but the curved modules seen in the spiral wound and hollow fiber systems may be

759 more complex, as there will always be a surface above the foulant unless these modules are vertical (Tan
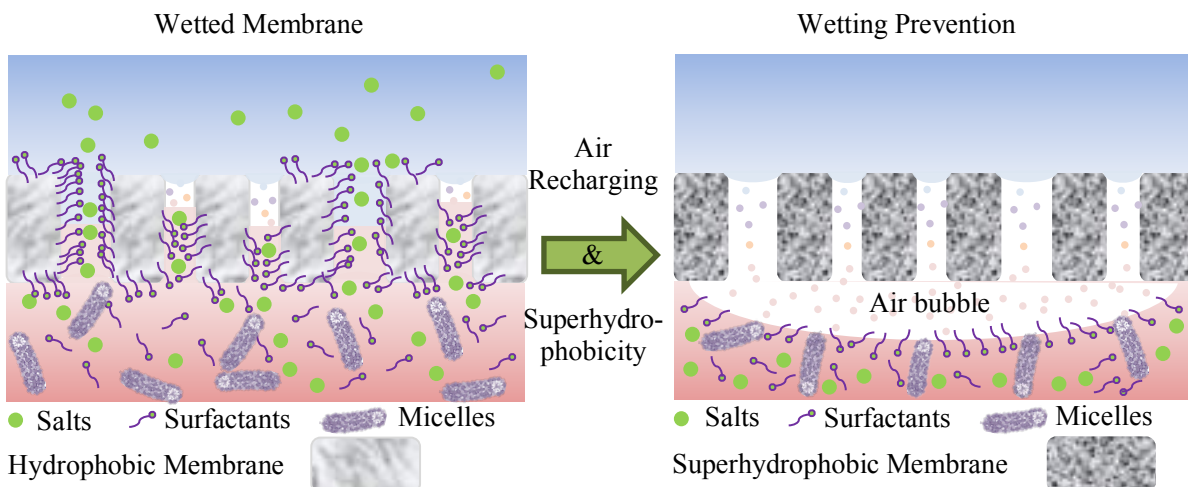760 et al., 2017).

12.4. Operating conditions

762 Flow operating conditions can be chosen to avoid fouling. Such systems can use saturation
763 conditions, biocidal flow conditions, flow rates, and temperatures to minimize fouling. Past studies
764 have developed a framework for operating MD systems at supersaturated salinities of inorganic foulants,
765 by designing module geometry and saturation conditions so that the maximum residence time of potential
766 salt particles is less than the nucleation induction time (Warsinger et al., 2017b). This control of timescales
767 can inhibit inorganic deposition on the membrane, a major cause of wetting. Additionally, numerous studies
768 have shown that temperatures in excess of ~60°C have biocidal effects in desalination systems. Operating
769 conditions for avoiding wetting heavily overlap with conditions for preventing membrane fouling (D. M.
770 Warsinger et al., 2015).

12.5. Membrane surface barrier protection

772 Partial or complete removal of dissolved air from the feed water before MD causes a decrease in partial
773 pressure of air in the membrane due to equilibrium considerations. This is proved to lead to an increase in
774 pressure difference across the liquid/gas interface, thus increasing the tendency for membrane wetting (R
775 W Schofield et al., 1990). The use of gas bubbling has been considered for scaling and fouling control in
776 MD (Chen et al., 2014b, 2013; Ding et al., 2011). These studies have shown bubbling of air in the MD feed
777 could control fouling due to the reduced concentration polarization by increased mixing. Recently, a new
778 approach to control membrane wetting has been studied for MD systems by preventing adsorption
779 equilibrium at the liquid/solid interface through displacing the liquid which partly tends to penetrate the
780 macroporous membrane structure with gas bubbles (D. M. Warsinger et al., 2016; Rezaei et al., 2017b;
781 Rezaei and Samhaber, 2017a, 2017b). Therefore, based on the surface renewal theory (Danckwerts, 1951),
782 the wetting agents do not have enough time to accumulate on the macroporous structures, because the
783 interface is displaced or swept from the system by the gas bubbles. Recently, Rezaei et al. (Rezaei et al.,

784 2017a) examined the effect of recharging air bubbles on the membrane surfaces for the wetting incidence

785 in a DCMD setup when a surfactant (sodium dodecyl sulfate, SDS) exists in a concentrated NaCl aqueous

786 solution. The results showed that the in-situ air bubbles on the surface of the superhydrophobic membrane

787 prevented the incident of wetting (~100% salt rejection) even for high concentrations of the surface-active

788 species (up to 0.8mM SDS) in the feed solution. They concluded that introducing air into the feed side of

789 the membrane displaces the liquid which partly tends to penetrate the macroporous structure with air

790 bubbles and thus enhances the LEP, and also, the simultaneous use of a superhydrophobic membrane

791 increases the solution CA (Fig. **18**). In the other studies (Chen et al., 2014c, 2013; Wu et al., 2015), the air

792 bubbling in MD has also shown to improve the permeate flux due to the reduction of boundary layer effects

793 and enhancement of heat and mass transfer. Therefore, the research on air bubbling in MD should be a

794 future focus and its capability to achieve multiple improvements needs to be further investigated.

795 Fig. 18: Wetting prevention mechanism by maintaining an air layer on the surface of a superhydrophobic

796 membrane (Rezaei et al., 2017a).

797 **13. Conclusions and perspective**

798 Wetting is a key challenge limiting the application of MD into a wider number of industrial applications.

799 In such cases where wetting is a risk, membrane design and prevention methods have been shown to be

800 effective in controlling wetting. Three degrees of wetting have been recognized in MD: surface wetting,

801 partial wetting, and full wetting. Surface wetting is considered to lead to scaling as a result of solvent

802 evaporation inside the membrane pores but does not deteriorate permeate quality. Partial wetting takes place

803 when solutions penetrate deeper into the larger pores leading to reduced permeate quality, while full wetting

804 can incapacitate the process of MD.The literature shows that inorganic scaling and organic fouling are the

805 main causes of membrane wetting, and different prevention methods are discussed. Several pretreatment

806 processes are found to inhibit membrane wetting by removing the wetting agents from the feed solution.

807 Various advanced membrane designs are evaluated to bring the surface non-wettability to the states of

808 superhydrophobicity and superomniphobicity through altering not only the surface chemistry and surface

809 geometrical structure, but also modifying the membrane wall properties. In summary, the following needs

810 are proposed for further assessment of wetting phenomenon in MD.

811 ▪ The possibility ofwetting occurrence for long-term performance and large-scale plant operations

812 of MD needs to be further studied to obtain an entire outlook of the applicability of MD process

813 for the treatment of solutions with low surface tension. When wetting has occurred, the

814 possibility of its prevention should be investigated.

815 ▪ Commercial hydrophobic membranes still suffer wetting due to capillary condensation.

816 Therefore, development of a straight- forward and efficient approach for the fabrication of super-

817 hydrophobic and superoleophobic surface for MD process is highly needed (Chew et al., 2017b;

818 Z. Wang et al., 2017).

819 ▪ Despite the promising prospect of MD with omniphobic mem- branes, additional investigations

820 are required to examine other fabrication techniques and to optimize membrane performance. It

821 is also crucial to assess the omniphobic membrane with a broad spectrum of surface-active agents

822 and with feeds of more complex organic compositions (Liu (H. Liu et al., 2017).

823 ▪ Potentially dangerous additives such as fluorinated chemicals are regarded as the persistent and

824 global contaminants. New non-chemical methods such as pretreatment methods or other physical

825 water treatment techniques to prevent wetting are should be evaluated.

826 ▪ The impact of salinity and different organic foulants on the stability of the membrane with special

827 wettability requires systematic research. Application of MD for the treatment of oily wastewater

828   with all main components should be more deeply studied, and more insight of the interaction

829   between these elements via molecular dynamics simulations would be essential (Han et al.,

830   2017).

831   ▪   Further research is needed on the impact of air backwashing and air layer recharging for

832   preventing fouling and wetting incidence in MD, especially at pilot scale.

833   ▪   Due to lack of an appropriate model, mathematical models describing physics and

834   thermodynamics of wetting phenomena for different wetting stages (i.e., surface, partial and full

835   wetting) in MD need to be developed. To do so, a better mechanistic understanding of wetting

836   as caused by different foulants is required

837   ▪   More studies need to be focused on the design of large-scale MD modules, as regards the impact

838   of module design on wetting and wetting reversal.

839   ▪   Studies on improving membrane lifetime while avoiding wet- ting need to be conducted, and

840   novel membrane material scale- up and testing for wetting should be established.

841 **Funding**

844 **Author Contributions**

845 All authors have given approval to the final version of the manuscript.

846 **Notes**

847 The authors declare no competing financial interest.

848 **Declarations of interest:**

849 None.

850 **Nomenclature**

851 BSA   Bovine serum albumin

852 CA   Contact angle

853 CMC   Critical micelle concentration

854 DCMD   Direct contact membrane distillation

855 GF   Glass fiber

856 HA   Humic acid

857 HcMD   Hydrogel-covered membrane distillation

858 HLB   Hydrophilic-lipophilic balance

859 LEP   Liquid entry pressure

860 LTH   Low temperature hydrothermal

861 MD   Membrane distillation

862 NTIPS   Non-solvent thermally induced phase separation

863 PAB   Pressurized air backwashing

864 PP   Polypropylene

865 RO   Reverse osmosis

866 SEM   Scanning electron microscopy

867 VMD   Vacuum membrane distillation

868 WCA   Water contact angle

869 **References**

870 Adamson, A.W., Gast, A.P., 1997. Physical Chemistry of Surfaces, 6th ed. John Wiley & Sons, Ltd.

871 Ahmed, F.E., Lalia, B.S., Hashaikeh, R., 2017. Membrane-based detection of wetting phenomenon in direct

872   contact membrane distillation. J. Memb. Sci. 535, 89–93.

873   https://doi.org/10.1016/j.memsci.2017.04.035

874 Ali, M.I., Summers, E.K., Arafat, H.A., Lienhard, J.H., 2012. Effects of membrane properties on water

875   production cost in small scale membrane distillation systems. Desalination 306, 60–71.

876   https://doi.org/10.1016/j.desal.2012.07.043

877 Alkhudhiri, A., Darwish, N., Hilal, N., 2012. Membrane distillation: A comprehensive review. Desalination

878   287, 2–18. https://doi.org/10.1016/j.desal.2011.08.027

879 Alklaibi, A.M., Lior, N., 2005. Membrane-distillation desalination: Status and potential. Desalination 171,

880   111–131. https://doi.org/10.1016/j.desal.2004.03.024

881 An, A.K., Guo, J., Jeong, S., Lee, E.-J., Tabatabai, S.A.A., Leiknes, T., 2016a. High flux and antifouling

882   properties of negatively charged membrane for dyeing wastewater treatment by membrane distillation.

883   Water Res. 103, 362–371. https://doi.org/10.1016/j.watres.2016.07.060

884 An, A.K., Guo, J., Lee, E.-J., Jeong, S., Zhao, Y., Wang, Z., Leiknes, T., 2016b. PDMS/PVDF hybrid

885   electrospun membrane with superhydrophobic property and drop impact dynamics for dyeing

886   wastewater treatment using membrane distillation. J. Memb. Sci. 525, 57–67.

887   https://doi.org/10.1016/j.memsci.2016.10.028

888 An, S., Joshi, B.N., Lee, J.-G., Lee, M.W., Kim, Y. Il, Kim, M., Jo, H.S., Yoon, S.S., 2017. A

889   comprehensive review on wettability, desalination, and purification using graphene-based materials

890   at water interfaces. Catal. Today 295, 14–25. https://doi.org/10.1016/j.cattod.2017.04.027

891 Arafat, H., Bilad, M., Marzooqi, F., 2015. New Concept for Dual-Layer Hydrophilic/Hydrophobic

892   Composite Membrane for Membrane Distillation. J. Membr. Sep. Technol. 4, 122–133.

893   https://doi.org/10.6000/1929-6037.2015.04.03.4

894 Ashoor, B.B., Mansour, S., Giwa, A., Dufour, V., Hasan, S.W., 2016. Principles and applications of direct

895   contact membrane distillation (DCMD): A comprehensive review. Desalination 398, 222–246.

896   https://doi.org/10.1016/j.desal.2016.07.043

897 ASTM International, 2014. Standard Test Methods for Pore Size Characteristics of Membrane Filters by

898   Bubble Point and Mean Flow Pore Test. Astm 3, 1–7. https://doi.org/10.1520/F0316-03R11.2

899 Atchariyawut, S., Feng, C., Wang, R., Jiraratananon, R., Liang, D.T., 2006. Effect of membrane structure

900   on mass-transfer in the membrane gas-liquid contacting process using microporous PVDF hollow

901   fibers. J. Memb. Sci. 285, 272–281. https://doi.org/10.1016/j.memsci.2006.08.029

902 Babalou, A.A., Rafia, N., Ghasemzadeh, K., 2015. Pervaporation, Vapour Permeation and Membrane

903 Distillation, Pervaporation, Vapour Permeation and Membrane Distillation.

904 https://doi.org/10.1016/B978-1-78242-246-4.00003-9

905 Baghbanzadeh, M., Rana, D., Lan, C.Q., Matsuura, T., 2015. Effects of hydrophilic silica nanoparticles and

906 backing material in improving the structure and performance of VMD PVDF membranes. Sep. Purif.

907 Technol. 157, 60–71. https://doi.org/10.1016/j.seppur.2015.11.029

908 Bailey, A.F.G., Barbe, A.M., Hogan, P.A., Johnson, R.A., Sheng, J., 2000. The effect of ultrafiltration on

909 the subsequent concentration of grape juice by osmotic distillation. J. Memb. Sci. 164, 195–204.

910 https://doi.org/10.1016/S0376-7388(99)00209-4

911 Banat, F.A., Simandl, J., 1999. Membrane distillation for dilute ethanol. J. Memb. Sci. 163, 333–348.

912 https://doi.org/10.1016/S0376-7388(99)00178-7

913 Banat, F.A., Simandl, J., 1998. Desalination by Membrane Distillation: A Parametric Study. Sep. Sci.

914 Technol. 33, 201–226. https://doi.org/10.1080/01496399808544764

915 Banat, F.A., Simandl, J., 1994. Theoretical and experimental study in membrane distillation. Desalination

916 95, 39–52. https://doi.org/10.1016/0011-9164(94)00005-0

917 Barbe, A.M., Hogan, P.A., Johnson, R.A., 2000. Surface morphology changes during initial usage of

918 hydrophobic, microporous polypropylene membranes. J. Memb. Sci. 172, 149–156.

919 https://doi.org/10.1016/S0376-7388(00)00338-0

920 Bell, C.M., 2016. Comparison of polyelectrolyte coated PVDF membranes in thermopervaporation with

921 porous hydrophobic membranes in membrane distillation using plate-and-frame modules. Chem. Eng.

922 Process. Process Intensif. 104, 58–65. https://doi.org/10.1016/j.cep.2016.02.013

923 Bilad, M.R., Guillen-Burrieza, E., Mavukkandy, M.O., Al Marzooqi, F.A., Arafat, H.A., 2015. Shrinkage,

924 defect and membrane distillation performance of composite PVDF membranes. Desalination 376, 62–

925 72. https://doi.org/10.1016/j.desal.2015.08.015

926 Bodell, B.R., 1963. Silicone rubber vapor diffusion in saline water distillation. United States Pat. Ser.

927 Bonyadi, S., Chung, T.S., 2007. Flux enhancement in membrane distillation by fabrication of dual layer

928 hydrophilic-hydrophobic hollow fiber membranes. J. Memb. Sci. 306, 134–146.

929   https://doi.org/10.1016/j.memsci.2007.08.034

930   Boo, C., Lee, J., Elimelech, M., 2016. Engineering Surface Energy and Nanostructure of Microporous Films

931   for Expanded Membrane Distillation Applications. Environ. Sci. Technol. 50, 8112–8119.

932   https://doi.org/10.1021/acs.est.6b02316

933   Bouchrit, R., Boubakri, A., Hafiane, A., Bouguecha, S.A.T., 2015. Direct contact membrane distillation:

934   Capability to treat hyper-saline solution. Desalination 376, 117–129.

935   https://doi.org/10.1016/j.desal.2015.08.014

936   Brown, P.S., Bhushan, B., 2016. Designing bioinspired superoleophobic surfaces. APL Mater. 4.

937   https://doi.org/10.1063/1.4935126

938   Camacho, L., Dumée, L., Zhang, J., Li, J., Duke, M., Gomez, J., Gray, S., 2013. Advances in Membrane

939   Distillation for Water Desalination and Purification Applications. Water 5, 94–196.

940   https://doi.org/10.3390/w5010094

941   Cao, L., Jones, A.K., Sikka, V.K., Wu, J., Gao, D., 2009. Anti-Icing Superhydrophobic Coatings 25, 12444–

942   12448. https://doi.org/10.1021/la902882b

943   Carrero-Parreño, A., Onishi, V.C., Ruiz-Femenia, R., Salcedo-Díaz, R., Caballero, J.A., Reyes-Labarta,

944   J.A., 2017. Multistage Membrane Distillation for the Treatment of Shale Gas Flowback Water: Multi-

945   Objective Optimization under Uncertainty. Comput. Aided Chem. Eng. 40, 571–576.

946   https://doi.org/10.1016/B978-0-444-63965-3.50097-0

947   Cassie, A.B.D., Baxter, S., 1944. Wettability of porous surfaces. Trans. Faraday Soc. 40, 546.

948   https://doi.org/10.1039/tf9444000546

949   Cerneaux, S., Struzyńska, I., Kujawski, W.M., Persin, M., Larbot, A., 2009. Comparison of various

950   membrane distillation methods for desalination using hydrophobic ceramic membranes. J. Memb. Sci.

951   337, 55–60. https://doi.org/10.1016/j.memsci.2009.03.025

952   Chanachai, A., Meksup, K., Jiraratananon, R., 2010. Coating of hydrophobic hollow fiber PVDF membrane

953   with chitosan for protection against wetting and flavor loss in osmotic distillation process. Sep. Purif.

954   Technol. 72, 217–224. https://doi.org/10.1016/j.seppur.2010.02.014

955 Chen, G., Lu, Y., Krantz, W.B., Wang, R., Fane, A.G., 2014a. Optimization of operating conditions for a
956 continuous membrane distillation crystallization process with zero salty water discharge. J. Memb.
957 Sci. 450, 1–11. https://doi.org/10.1016/j.memsci.2013.08.034

958 Chen, G., Yang, X., Lu, Y., Wang, R., Fane, A.G., 2014b. Heat transfer intensification and scaling
959 mitigation in bubbling-enhanced membrane distillation for brine concentration. J. Memb. Sci. 470,
960 60–69. https://doi.org/10.1016/j.memsci.2014.07.017

961 Chen, G., Yang, X., Lu, Y., Wang, R., Fane, A.G., 2014c. Heat transfer intensification and scaling
962 mitigation in bubbling-enhanced membrane distillation for brine concentration. J. Memb. Sci. 470,
963 60–69. https://doi.org/10.1016/j.memsci.2014.07.017

964 Chen, G., Yang, X., Wang, R., Fane, A.G., 2013. Performance enhancement and scaling control with gas
965 bubbling in direct contact membrane distillation. Desalination 308, 47–55.
966 https://doi.org/10.1016/j.desal.2012.07.018

967 Chen, K., Xiao, C., Huang, Q., Liu, H., Liu, H., Wu, Y., Liu, Z., 2015. Study on vacuum membrane
968 distillation (VMD) using FEP hollow fiber membrane. Desalination 375, 24–32.
969 https://doi.org/10.1016/j.desal.2015.07.021

970 Cheng, D.Y., Wiersma, S.J., 1983. Apparatus and method for thermal membrane distillation. US Parent
971 No. 4,419, 187.

972 Cheng, D.Y., Wiersma, S.J., 1983. Composite membrane for membrane distillation system. US4316772.

973 Cheng, T.-W., Han, C.-J., Hwang, K.-J., Ho, C.-D., Cooper, W.J., 2010. Influence of Feed Composition on
974 Distillate Flux and Membrane Fouling in Direct Contact Membrane Distillation. Sep. Sci. Technol.
975 45, 967–974. https://doi.org/10.1080/01496391003666908

976 Chew, J.W., Krantz, W.B., Fane, A.G., 2014. Effect of a macromolecular- or bio-fouling layer on
977 membrane distillation. J. Memb. Sci. 456, 66–76. https://doi.org/10.1016/j.memsci.2014.01.025

978 Chew, N.G.P., Zhao, S., Loh, C.H., Permogorov, N., Wang, R., 2017a. Surfactant effects on water recovery
979 from produced water via direct-contact membrane distillation. J. Memb. Sci. 528, 126–134.
980 https://doi.org/10.1016/j.memsci.2017.01.024

981 Chew, N.G.P., Zhao, S., Malde, C., Wang, R., 2017b. Superoleophobic surface modification for robust

982   membrane distillation performance. J. Memb. Sci. 541, 162–173.

983   https://doi.org/10.1016/j.memsci.2017.06.089

984 Chibowski, E., Terpilowski, K., 2008. Surface free energy of sulfur-Revisited. I. Yellow and orange

985   samples solidified against glass surface. J. Colloid Interface Sci. 319, 505–513.

986   https://doi.org/10.1016/j.jcis.2007.10.059

987 Cho, D.-W., Song, H., Yoon, K., Kim, S., Han, J., Cho, J., 2016. Treatment of Simulated Coalbed Methane

988   Produced Water Using Direct Contact Membrane Distillation. Water 8, 194.

989   https://doi.org/10.3390/w8050194

990 Choi, Y., Naidu, G., Jeong, S., Vigneswaran, S., Lee, S., Wang, R., Fane, A.G., 2017. Experimental

991   comparison of submerged membrane distillation configurations for concentrated brine treatment.

992   Desalination 420, 54–62. https://doi.org/10.1016/j.desal.2017.06.024

993 Chong, K.C., Lai, S.O., Thiam, H.S., Lee, S.S., Lau, W.J., Mokhtar, N.M., 2016. Reactive Blue Dye

994   Removal by Membrane Distillation using PVDF Membrane. Indian J. Sci. Technol. 9, 1–5.

995   https://doi.org/10.17485/ijst/2016/v9iS1/110379

996 Chua, Y.T., Ji, G., Birkett, G., Lin, C.X.C., Kleitz, F., Smart, S., 2015. Nanoporous organosilica membrane

997   for water desalination: Theoretical study on the water transport. J. Memb. Sci. 482, 56–66.

998   https://doi.org/10.1016/j.memsci.2015.01.060

999 Chul Woo, Y., Chen, Y., Tijing, L.D., Phuntsho, S., He, T., Choi, J.-S., Kim, S.-H., Kyong Shon, H., 2017.

1000   CF4 plasma-modified omniphobic electrospun nanofiber membrane for produced water brine

1001   treatment by membrane distillation. J. Memb. Sci. 529, 234–242.

1002   https://doi.org/10.1016/j.memsci.2017.01.063

1003 Chung, H.W., Swaminathan, J., Warsinger, D.M., Lienhard, J.H., 2016. Multistage vacuum membrane

1004   distillation (MSVMD) systems for high salinity applications. J. Memb. Sci. 497, 128–141.

1005   https://doi.org/10.1016/j.memsci.2015.09.009

1006 Courel, M., Dornier, M., Rios, G.M., Reynes, M., 2000. Modelling of water transport in osmotic distillation

1007   using asymmetric membrane. J. Memb. Sci. 173, 107–122. https://doi.org/10.1016/S0376-

1008   7388(00)00348-3

1009 Courel, M., Tronel-Peyroz, E., Rios, G.M., Dornier, M., Reynes, M., 2001. The problem of membrane

1010   characterization for the process of osmotic distillation. Desalination 140, 15–25.

1011   https://doi.org/10.1016/S0011-9164(01)00351-4

1012 D. M. Warsinger, Swaminathan, A. Servi, J., V, J.H.L., 2016. Maintenance of gas layers for fouling

1013   prevention on submerged surfaces. 15/157,663.

1014 Danckwerts, P. V., 1951. Significance of Liquid-Film Coefficients in Gas Absorption. Ind. Eng. Chem. 43,

1015   1460–1467. https://doi.org/10.1021/ie50498a055

1016 Darmanin, T., Guittard, F., 2013. Superoleophobic surfaces with short fluorinated chains? Soft Matter 9,

1017   5982. https://doi.org/10.1039/c3sm50643f

1018 Ding, Z., Liu, L., Liu, Z., Ma, R., 2011. The use of intermittent gas bubbling to control membrane fouling

1019   in concentrating TCM extract by membrane distillation. J. Memb. Sci. 372, 172–181.

1020   https://doi.org/10.1016/j.memsci.2011.01.063

1021 Ding, Z., Liu, L., Liu, Z., Ma, R., 2010. Fouling resistance in concentrating TCM extract by direct contact

1022   membrane distillation. J. Memb. Sci. 362, 317–325. https://doi.org/10.1016/j.memsci.2010.06.040

1023 Domingues, E., Arunachalam, S., Mishra, H., 2017. Doubly Reentrant Cavities Prevent Catastrophic

1024   Wetting Transitions on Intrinsically Wetting Surfaces. ACS Appl. Mater. Interfaces acsami.7b03526.

1025   https://doi.org/10.1021/acsami.7b03526

1026 Dong, G., Kim, J.F., Kim, J.H., Drioli, E., Lee, Y.M., 2017. Open-source predictive simulators for scale-

1027   up of direct contact membrane distillation modules for seawater desalination. Desalination 402, 72–

1028   87. https://doi.org/10.1016/j.desal.2016.08.025

1029 Dong, Z.-Q., Ma, X.-H., Xu, Z.-L., Gu, Z.-Y., 2015. Superhydrophobic modification of PVDF/SiO2

1030   electrospun nanofiber membranes for vacuum membrane distillation. RSC Adv. 5, 67962–67970.

1031   https://doi.org/10.1039/C5RA10575G

1032 Dong, Z.-Q.Q., Wang, B.-J.J., Ma, X.H., Wei, Y.-M.M., Xu, Z.-L.L., 2015. FAS Grafted Electrospun

Poly(vinyl alcohol) Nanofiber Membranes with Robust Superhydrophobicity for Membrane Distillation. ACS Appl. Mater. Interfaces 7, 22652–22659. https://doi.org/10.1021/acsami.5b07454

Dong, Z.Q., Ma, X. hua, Xu, Z.L., You, W.T., Li, F. bing, 2014. Superhydrophobic PVDF-PTFE electrospun nanofibrous membranes for desalination by vacuum membrane distillation. Desalination 347, 175–183. https://doi.org/10.1016/j.desal.2014.05.015

Dow, N., Villalobos García, J., Naidoo, L., Milne, N., Zhang, J., Gray, S., Duke, M., 2017. Demonstration of membrane distillation on textile waste water: assessment of long term performance, membrane cleaning and waste heat integration. Environ. Sci. Water Res. Technol. https://doi.org/10.1039/C6EW00290K

Dumée, L.F., Alglave, H., Chaffraix, T., Lin, B., Magniez, K., Schütz, J., 2016. Morphology-properties relationship of gas plasma treated hydrophobic meso-porous membranes and their improved performance for desalination by membrane distillation. Appl. Surf. Sci. 363, 273–285. https://doi.org/10.1016/j.apsusc.2015.12.034

Dumée, L.F., Gray, S., Duke, M., Sears, K., Schütz, J., Finn, N., 2013. The role of membrane surface energy on direct contact membrane distillation performance. Desalination 323, 22–30. https://doi.org/10.1016/j.desal.2012.07.012

Durham, R.J., Nguyen, M.H., 1994. Hydrophobic membrane evaluation and cleaning for osmotic distillation of tomato puree. J. Memb. Sci. 87, 181–189. https://doi.org/10.1016/0376-7388(93)E0142-7

Edwie, F., Chung, T.S., 2013. Development of simultaneous membrane distillation-crystallization (SMDC) technology for treatment of saturated brine. Chem. Eng. Sci. 98, 160–172. https://doi.org/10.1016/j.ces.2013.05.008

Edwie, F., Chung, T.S., 2012. Development of hollow fiber membranes for water and salt recovery from highly concentrated brine via direct contact membrane distillation and crystallization. J. Memb. Sci. 421–422, 111–123. https://doi.org/10.1016/j.memsci.2012.07.001

Edwie, F., Teoh, M.M., Chung, T.-S., 2012. Effects of additives on dual-layer hydrophobic–hydrophilic

PVDF hollow fiber membranes for membrane distillation and continuous performance. Chem. Eng. Sci. 68, 567–578. https://doi.org/10.1016/j.ces.2011.10.024

Efome, J.E., Rana, D., Matsuura, T., Lan, C.Q., 2016. Enhanced performance of PVDF nanocomposite membrane by nanofiber coating: A membrane for sustainable desalination through MD. Water Res. 89, 39–49. https://doi.org/10.1016/j.watres.2015.11.040

El-Abbassi, A., Hafidi, A., Khayet, M., García-Payo, M.C., 2013. Integrated direct contact membrane distillation for olive mill wastewater treatment. Desalination 323, 31–38. https://doi.org/10.1016/j.desal.2012.06.014

El-Bourawi, M.S., Ding, Z., Ma, R., Khayet, M., 2006. A framework for better understanding membrane distillation separation process. J. Memb. Sci. 285, 4–29. https://doi.org/10.1016/j.memsci.2006.08.002

Eykens, L., De Sitter, K., Dotremont, C., De Schepper, W., Pinoy, L., Van Der Bruggen, B., 2017. Wetting Resistance of Commercial Membrane Distillation Membranes in Waste Streams Containing Surfactants and Oil. Appl. Sci. 7, 118. https://doi.org/10.3390/app7020118

Eykens, L., De Sitter, K., Dotremont, C., Pinoy, L., Van der Bruggen, B., 2017. Membrane synthesis for membrane distillation: A review. Sep. Purif. Technol. https://doi.org/10.1016/j.seppur.2017.03.035

Eykens, L., De Sitter, K., Dotremont, C., Pinoy, L., Van Der Bruggen, B., 2016. How to Optimize the Membrane Properties for Membrane Distillation: A Review. Ind. Eng. Chem. Res. 55, 9333–9343. https://doi.org/10.1021/acs.iecr.6b02226

Fan, X., Liu, Y., Quan, X., Zhao, H., Chen, S., Yi, G., Du, L., 2016. High desalination permeability, wetting and fouling resistance on superhydrophobic carbon nanotube hollow fiber membrane under self-powered electrochemical assistance. J. Memb. Sci. 514, 501–509. https://doi.org/10.1016/j.memsci.2016.05.003

Fan, Y., Chen, S., Zhao, H., Liu, Y., 2017. Distillation membrane constructed by TiO2 nanofiber followed by fluorination for excellent water desalination performance. Desalination 405, 51–58. https://doi.org/10.1016/j.desal.2016.11.028

1085   Fane, A.G., Wang, R., Tang, C.Y., Yang, X., 2012. Membrane distillation and forward osmosis: advances

1086   in membranes, modules, and applications. IDA J. 4, 22–26.

1087   Feng, B.X., Jiang, L., 2006. Design and Creation of Superwetting / Antiwetting Surfaces 3063–3078.

1088   https://doi.org/10.1002/adma.200501961

1089   Feng, X., Jiang, L.Y., Matsuura, T., Wu, P., 2017. Fabrication of hydrophobic/hydrophilic composite

1090   hollow fibers for DCMD: Influence of dope formulation and external coagulant. Desalination 401,

1091   53–63. https://doi.org/10.1016/j.desal.2016.07.026

1092   Feng, X., Jiang, L.Y., Song, Y., 2016. Titanium white sulfuric acid concentration by direct contact

1093   membrane distillation. Chem. Eng. J. 285, 101–111. https://doi.org/10.1016/j.cej.2015.09.064

1094   Figoli, A., Ursino, C., Galiano, F., Di Nicolò, E., Carnevale, M.C., Criscuoli, A., 2016. Innovative

1095   hydrophobic coating of perfluoropolyether (PFPE) on commercial hydrophilic membranes for DCMD

1096   application. J. Memb. Sci. https://doi.org/10.1016/j.memsci.2016.08.066

1097   Franco, J.A., Kentish, S.E., Perera, J.M., Stevens, G.W., 2008. Fabrication of a superhydrophobic

1098   polypropylene membrane by deposition of a porous crystalline polypropylene coating. J. Memb. Sci.

1099   318, 107–113. https://doi.org/10.1016/j.memsci.2008.02.032

1100   Franken, A.C.M., Nolten, J.A.M., Mulder, M.H.V., Bargeman, D., Smolders, C.A., 1987. Wetting criteria

1101   for   the   applicability   of   membrane   distillation.   J.   Memb.   Sci.   33,   315–328.

1102   https://doi.org/10.1016/S0376-7388(00)80288-4

1103   García-Fernández, L., García-Payo, M.C., Khayet, M., 2014. Effects of mixed solvents on the structural

1104   morphology and membrane distillation performance of PVDF-HFP hollow fiber membranes. J.

1105   Memb. Sci. 468, 324–338. https://doi.org/10.1016/j.memsci.2014.06.014

1106   García-Payo, M.C., Izquierdo-Gil, M.A., Fernández-Pineda, C., 2000. Wetting Study of Hydrophobic

1107   Membranes via Liquid Entry Pressure Measurements with Aqueous Alcohol Solutions. J. Colloid

1108   Interface Sci. 230, 420–431. https://doi.org/10.1006/jcis.2000.7106

1109   Ge, J., Peng, Y., Li, Z., Chen, P., Wang, S., 2014. Membrane fouling and wetting in a DCMD process for

1110   RO brine concentration. Desalination 344, 97–107. https://doi.org/10.1016/j.desal.2014.03.017

1111   Gilron, J., Ladizansky, Y., Korin, E., 2013. Silica fouling in direct contact membrane distillation. Ind. Eng.

1112   Chem. Res. 52, 10521–10529. https://doi.org/10.1021/ie400265b

1113   Goh, S., Zhang, J., Liu, Y., Fane, A.G., 2013. Fouling and wetting in membrane distillation (MD) and MD-

1114   bioreactor   (MDBR)   for   wastewater   reclamation.   Desalination   323,   39–47.

1115   https://doi.org/10.1016/j.desal.2012.12.001

1116   González-Benito, J., Teno, J., González-Gaitano, G., Xu, S., Chiang, M.Y., 2017. PVDF/TiO2

1117   nanocomposites prepared by solution blow spinning: Surface properties and their relation with

1118   S. Mutans adhesion. Polym. Test. 58, 21–30. https://doi.org/10.1016/j.polymertesting.2016.12.005

1119   Grynyov, R., Bormashenko, E., Whyman, G., Bormashenko, Y., Musin, A., Pogreb, R., Starostin, A.,

1120   Valtsifer, V., Strelnikov, V., Schechter, A., Kolagatla, S., 2016. Superoleophobic Surfaces Obtained

1121   via   Hierarchical   Metallic   Meshes.   Langmuir   32,   4134–4140.

1122   https://doi.org/10.1021/acs.langmuir.6b00248

1123   Gryta, M., 2017. The application of polypropylene membranes for production of fresh water from brines

1124   by membrane distillation. Chem. Pap. 71, 775–784. https://doi.org/10.1007/s11696-016-0059-6

1125   Gryta, M., 2016a. The Application of Membrane Distillation for Broth Separation in Membrane

1126   Bioreactors. J. Membr. Sci. Res. 2, 193–200.

1127   Gryta, M., 2016b. The study of performance of polyethylene chlorinetrifluoroethylene membranes used for

1128   brine   desalination   by   membrane   distillation.   Desalination   398,   52–63.

1129   https://doi.org/10.1016/j.desal.2016.07.021

1130   Gryta, M., 2015. Water desalination using membrane distillation with acidic stabilization of scaling layer

1131   thickness. Desalination 365, 160–166. https://doi.org/10.1016/j.desal.2015.02.031

1132   Gryta, M., 2008. Fouling in direct contact membrane distillation process. J. Memb. Sci. 325, 383–394.

1133   https://doi.org/10.1016/j.memsci.2008.08.001

1134   Gryta, M., 2007a. Influence of polypropylene membrane surface porosity on the performance of membrane

1135   distillation process. J. Memb. Sci. 287, 67–78. https://doi.org/10.1016/j.memsci.2006.10.011

1136   Gryta, M., 2007b. Effect of iron oxides scaling on the MD process performance. Desalination 216, 88–102.

1137 https://doi.org/10.1016/j.desal.2007.01.002

1138 Gryta, M., 2005. Long-term performance of membrane distillation process. J. Memb. Sci. 265, 153–159.

1139 https://doi.org/10.1016/j.memsci.2005.04.049

1140 Gryta, M., 2002. Direct contact membrane distillation with crystallization applied to NaCl solutions. Chem.

1141 Pap. 56, 14–19.

1142 Gryta, M., 2002a. The assessment of microorganism growth in the membrane distillation system.

1143 Desalination 142, 79–88. https://doi.org/10.1016/S0011-9164(01)00427-1

1144 Gryta, M., 2002b. Concentration of NaCl solution by membrane distillation integrated with crystallization.

1145 Sep. Sci. Technol. 37, 3535–3558. https://doi.org/10.1081/SS-120014442

1146 Gryta, M., Barancewicz, M., 2010. Influence of morphology of PVDF capillary membranes on the

1147 performance of direct contact membrane distillation. J. Memb. Sci. 358, 158–167.

1148 https://doi.org/10.1016/j.memsci.2010.04.044

1149 Gryta, M., Grzechulska-Damszel, J., Markowska, A., Karakulski, K., 2009. The influence of polypropylene

1150 degradation on the membrane wettability during membrane distillation. J. Memb. Sci. 326, 493–502.

1151 https://doi.org/10.1016/j.memsci.2008.10.022

1152 Gryta, M., Tomaszewska, M., Morawski, A.W., 1997. Membrane distillation with laminar flow. Sep. Purif.

1153 Technol. 11, 93–101. https://doi.org/10.1016/S1383-5866(97)00002-6

1154 Guillén-Burrieza, E., Blanco, J., Zaragoza, G., Alarcón, D.-C., Palenzuela, P., Ibarra, M., Gernjak, W.,

1155 2011. Experimental analysis of an air gap membrane distillation solar desalination pilot system. J.

1156 Memb. Sci. 379, 386–396. https://doi.org/10.1016/j.memsci.2011.06.009

1157 Guillen-Burrieza, E., Mavukkandy, M.O., Bilad, M.R., Arafat, H.A., 2016. Understanding wetting

1158 phenomena in membrane distillation and how operational parameters can affect it. J. Memb. Sci. 515,

1159 163–174. https://doi.org/10.1016/j.memsci.2016.05.051

1160 Guillen-Burrieza, E., Ruiz-Aguirre, A., Zaragoza, G., Arafat, H.A., 2014. Membrane fouling and cleaning

1161 in long term plant-scale membrane distillation operations. J. Memb. Sci. 468, 360–372.

1162 https://doi.org/10.1016/j.memsci.2014.05.064

1163   Guillen-Burrieza, E., Servi, A., Lalia, B.S., Arafat, H.A., 2015. Membrane structure and surface

1164   morphology impact on the wetting of MD membranes. J. Memb. Sci. 483, 94–103.

1165   https://doi.org/10.1016/j.memsci.2015.02.024

1166   Guillen-Burrieza, E., Thomas, R., Mansoor, B., Johnson, D., Hilal, N., Arafat, H., 2013. Effect of dry-out

1167   on the fouling of PVDF and PTFE membranes under conditions simulating intermittent seawater

1168   membrane distillation (SWMD). J. Memb. Sci. 438, 126–139.

1169   https://doi.org/10.1016/j.memsci.2013.03.014

1170   Guo, F., Servi, A., Liu, A., Gleason, K.K., Rutledge, G.C., 2015. Desalination by Membrane Distillation

1171   using Electrospun Polyamide Fiber Membranes with Surface Fluorination by Chemical Vapor

1172   Deposition. ACS Appl. Mater. Interfaces 7, 8225–8232. https://doi.org/10.1021/acsami.5b01197

1173   Hammami, M.A., Croissant, J., Francis, L., Alsaiari, S.K., Anjum, D.H., Ghaffour, N., Khashab, N.M.,

1174   2016. Engineering Hydrophobic Organosilica Doped Nanofibers for Enhanced and Fouling Resistant

1175   Membrane Distillation. ACS Appl. Mater. Interfaces acsami.6b11167.

1176   https://doi.org/10.1021/acsami.6b11167

1177   Hamzah, N., Leo, C.P., 2017. Membrane distillation of saline with phenolic compound using

1178   superhydrophobic PVDF membrane incorporated with TiO2 nanoparticles: Separation, fouling and

1179   self-cleaning evaluation. Desalination 418, 79–88. https://doi.org/10.1016/j.desal.2017.05.029

1180   Han, L., Tan, Y.Z., Netke, T., Fane, A.G., Chew, J.W., 2017. Understanding oily wastewater treatment via

1181   membrane distillation. J. Memb. Sci. 539, 284–294. https://doi.org/10.1016/j.memsci.2017.06.012

1182   Hassan, M.I., Brimmo, A.T., Swaminathan, J., Lienhard, J.H., Arafat, H.A., 2015. A new vacuum

1183   membrane distillation system using an aspirator: concept modeling and optimization. Desalin. Water

1184   Treat. 57, 12915–12928. https://doi.org/10.1080/19443994.2015.1060902

1185   Hausmann, A., Sanciolo, P., Vasiljevic, T., Ponnampalam, E., Quispe-Chavez, N., Weeks, M., Duke, M.,

1186   2011. Direct contact membrane distillation of dairy process streams. Membranes (Basel). 1, 48–58.

1187   https://doi.org/10.3390/membranes1010048

1188   He, F., Gilron, J., Lee, H., Song, L., Sirkar, K.K., 2008. Potential for scaling by sparingly soluble salts in

1189   crossflow DCMD. J. Memb. Sci. 311, 68–80. https://doi.org/10.1016/j.memsci.2007.11.056

1190   He, F., Sirkar, K.K., Gilron, J., 2009. Effects of antiscalants to mitigate membrane scaling by direct contact

1191   membrane distillation. J. Memb. Sci. 345, 53–58. https://doi.org/10.1016/j.memsci.2009.08.021

1192   Hickenbottom, K.L., Cath, T.Y., 2014. Sustainable operation of membrane distillation for enhancement of

1193   mineral recovery from hypersaline solutions. J. Memb. Sci. 454, 426–435.

1194   https://doi.org/10.1016/j.memsci.2013.12.043

1195   Hou, D., Lin, D., Zhao, C., Wang, J., Fu, C., 2017. Control of protein (BSA) fouling by ultrasonic irradiation

1196   during membrane distillation process. Sep. Purif. Technol. 175, 287–297.

1197   https://doi.org/10.1016/j.seppur.2016.11.047

1198   Hou, D., Wang, Z., Li, G., Fan, H., Wang, J., Huang, H., 2015. Ultrasonic assisted direct contact membrane

1199   distillation hybrid process for membrane scaling mitigation. Desalination 375, 33–39.

1200   https://doi.org/10.1016/j.desal.2015.07.018

1201   Huang, C.-Y., Ko, C.-C., Chen, L.-H., Huang, C.-T., Tung, K.-L., Liao, Y.-C., 2016. A simple coating

1202   method to prepare superhydrophobic layers on ceramic alumina for vacuum membrane distillation.

1203   Sep. Purif. Technol. https://doi.org/10.1016/j.seppur.2016.12.037

1204   Huang, Y.-X., Wang, Z., Hou, D., Lin, S., 2017. Coaxially Electrospun Super-amphiphobic Silica-based

1205   Membrane for Anti-surfactant-wetting Membrane Distillation. J. Memb. Sci.

1206   https://doi.org/10.1016/j.memsci.2017.02.044

1207   Husnain, T., Liu, Y., Riffat, R., Mi, B., 2015. Integration of forward osmosis and membrane distillation for

1208   sustainable wastewater reuse. Sep. Purif. Technol. 156, 424–431.

1209   https://doi.org/10.1016/j.seppur.2015.10.031

1210   Jang, Y., Cho, H., Shin, Y., Choi, Y., Lee, S., Koo, J., 2016. Comparison of fouling propensity and physical

1211   cleaning effect in forward osmosis, reverse osmosis, and membrane distillation. Desalin. Water Treat.

1212   57, 24532–24541. https://doi.org/10.1080/19443994.2016.1152650

1213   Jeong, S., Lee, S., Chon, H.T., Lee, S., 2014. Structural analysis and modeling of the commercial high

1214   performance composite flat sheet membranes for membrane distillation application. Desalination 349,

1215 115–125. https://doi.org/10.1016/j.desal.2014.05.027

1216 Jin, Z., Yang, D.L., Zhang, S.H., Jian, X.G., 2008. Hydrophobic modification of poly(phthalazinone ether

1217 sulfone ketone) hollow fiber membrane for vacuum membrane distillation. Chinese Chem. Lett. 19,

1218 367–370. https://doi.org/10.1016/j.cclet.2007.12.029

1219 Joly, L., Biben, T., 2009. Wetting and friction on superoleophobic surfaces. Soft Matter.

1220 https://doi.org/10.1039/b821214g

1221 Kang, G., Cao, Y., 2014. Application and modification of poly(vinylidene fluoride) (PVDF) membranes –

1222 A review. J. Memb. Sci. 463, 145–165. https://doi.org/10.1016/j.memsci.2014.03.055

1223 Karakulski, K., Gryta, M., 2005. Water demineralisation by NF/MD integrated processes. Desalination 177,

1224 109–119. https://doi.org/10.1016/j.desal.2004.11.018

1225 Kayvani Fard, A., Rhadfi, T., Khraisheh, M., Atieh, M.A., Khraisheh, M., Hilal, N., 2016. Reducing flux

1226 decline and fouling of direct contact membrane distillation by utilizing thermal brine from MSF

1227 desalination plant. Desalination 379, 172–181. https://doi.org/10.1016/j.desal.2015.11.004

1228 Keurentjes, J.T.F., Harbrecht, J.G., Brinkman, D., Hanemaaijer, J.H., Cohen Stuart, M.A., van't Riet, K.,

1229 1989. Hydrophobicity measurements of microfiltration and ultrafiltration membranes. J. Memb. Sci.

1230 47, 333–344. https://doi.org/10.1016/S0376-7388(00)83084-7

1231 Kezia, K., Lee, J., Weeks, M., Kentish, S., 2015. Direct contact membrane distillation for the concentration

1232 of saline dairy effluent. Water Res. 81, 167–177. https://doi.org/10.1016/j.watres.2015.05.042

1233 Khayet, M., Matsuura, T., 2004. Pervaporation and vacuum membrane distillation processes: Modeling and

1234 experiments. AIChE J. 50, 1697–1712. https://doi.org/10.1002/aic.10161

1235 Khemakhem, S., Amar, R. Ben, 2011. Grafting of fluoroalkylsilanes on microfiltration Tunisian clay

1236 membrane. Ceram. Int. 37, 3323–3328. https://doi.org/10.1016/j.ceramint.2011.04.128

1237 Kim, J., Kwon, H., Lee, S.S., Lee, S.S., Hong, S., 2016. Membrane distillation (MD) integrated with

1238 crystallization (MDC) for shale gas produced water (SGPW) treatment. Desalination 403, 4–7.

1239 https://doi.org/10.1016/j.desal.2016.07.045

1240 Kota, A.K., Mabry, J.M., Tuteja, A., 2013. Superoleophobic surfaces: design criteria and recent studies.

Surf. Innov. 1, 71–83. https://doi.org/10.1680/si.12.00017

Kota, A.K., Tuteja, A., 2012. Superoleophobic surfaces. ACS Symp. Ser. 1106, 171–185. https://doi.org/10.1021/bk-2012-1106.ch011

Krivorot, M., Kushmaro, A., Oren, Y., Gilron, J., 2011. Factors affecting biofilm formation and biofouling in membrane distillation of seawater. J. Memb. Sci. 376, 15–24. https://doi.org/10.1016/j.memsci.2011.01.061

Kujawa, J., Al-Gharabli, S., Kujawski, W., Knozowska, K., 2017. Molecular Grafting of Fluorinated and Nonfluorinated Alkylsiloxanes on Various Ceramic Membrane Surfaces for the Removal of Volatile Organic Compounds Applying Vacuum Membrane Distillation. ACS Appl. Mater. Interfaces 9, 6571–6590. https://doi.org/10.1021/acsami.6b14835

Kujawa, J., Cerneaux, S., Kujawski, W., Bryjak, M., Kujawski, J., 2016. How To Functionalize Ceramics by Perfluoroalkylsilanes for Membrane Separation Process? Properties and Application of Hydrophobized Ceramic Membranes. ACS Appl. Mater. Interfaces 8, 7564–77. https://doi.org/10.1021/acsami.6b00140

Kujawa, J., Kujawski, W., 2016. Functionalization of Ceramic Metal Oxide Powders and Ceramic Membranes by Perfluroalkylsilanes and Alkylsilanes Possessing Different Reactive Groups – Physicochemical and Tribological Properties. ACS Appl. Mater. Interfaces acsami.5b11975. https://doi.org/10.1021/acsami.5b11975

Kujawska, A., Kujawski, J.K., Bryjak, M., Cichosz, M., Kujawski, W., 2016. Removal of volatile organic compounds from aqueous solutions applying thermally driven membrane processes. 2. Air gap membrane distillation. J. Memb. Sci. 499, 245–256. https://doi.org/10.1016/j.memsci.2015.10.047

Kujawski, W., Kujawa, J., Wierzbowska, E., Cerneaux, S., Bryjak, M., Kujawski, J., 2016. Influence of hydrophobization conditions and ceramic membranes pore size on their properties in vacuum membrane distillation of water-organic solvent mixtures. J. Memb. Sci. 499, 442–451. https://doi.org/10.1016/j.memsci.2015.10.067

Kumar, R., Ghosh, A.K., Pal, P., 2017. Fermentative energy conversion: Renewable carbon source to

1267   biofuels (ethanol) using Saccharomyces cerevisiae and downstream purification through solar driven

1268   membrane distillation and nanofiltration. Energy Convers. Manag. 150, 545–557.

1269   https://doi.org/10.1016/j.enconman.2017.08.054

1270   Kwok, D.Y., Neumann, a. W., 1999. Contact angle measurement and contact angle interpretation,

1271   Advances in Colloid and Interface Science. https://doi.org/10.1016/S0001-8686(98)00087-6

1272   Kyoungjin An, A., Lee, E.-J., Guo, J., Jeong, S., Lee, J.-G., Ghaffour, N., 2017. Enhanced vapor transport

1273   in membrane distillation via functionalized carbon nanotubes anchored into electrospun nanofibres.

1274   Sci. Rep. 7, 41562. https://doi.org/10.1038/srep41562

1275   Lalia, B.S., Guillen-Burrieza, E., Arafat, H.A., Hashaikeh, R., 2013. Fabrication and characterization of

1276   polyvinylidenefluoride-co-hexafluoropropylene (PVDF-HFP) electrospun membranes for direct

1277   contact membrane distillation. J. Memb. Sci. 428, 104–115.

1278   https://doi.org/10.1016/j.memsci.2012.10.061

1279   Lalia, B.S., Guillen, E., Arafat, H.A., Hashaikeh, R., 2014. Nanocrystalline cellulose reinforced PVDF-

1280   HFP membranes for membrane distillation application. Desalination 332, 134–141.

1281   https://doi.org/10.1016/j.desal.2013.10.030

1282   Lawal, D.U., Khalifa, A.E., 2015. Experimental investigation of an air gap membrane distillation unit with

1283   double-sided cooling channel. Desalin. Water Treat. 1–15.

1284   https://doi.org/10.1080/19443994.2015.1042065

1285   Lawson, K.W., Lloyd, D.R., 1997. Membrane distillation. J. Memb. Sci. 124, 1–25.

1286   https://doi.org/10.1016/S0376-7388(96)00236-0

1287   Lee, E.-J., An, A.K., Hadi, P., Lee, S., Woo, Y.C., Shon, H.K., 2017. Advanced multi-nozzle electrospun

1288   functionalized titanium dioxide/polyvinylidene fluoride-co-hexafluoropropylene (TiO 2 /PVDF-HFP)

1289   composite membranes for direct contact membrane distillation. J. Memb. Sci. 524, 712–720.

1290   https://doi.org/10.1016/j.memsci.2016.11.069

1291   Lee, E.-J.J., An, A.K., He, T., Woo, Y.C., Shon, H.K., 2016. Electrospun nanofiber membranes

1292   incorporating fluorosilane-coated TiO2 nanocomposite for direct contact membrane distillation. J.

Memb. Sci. 520, 145–154. https://doi.org/10.1016/j.memsci.2016.07.019

Lee, J.-G., Lee, E.-J., Jeong, S., Guo, J., An, A.K., Guo, H., Kim, J., Leiknes, T., Ghaffour, N., 2017. Theoretical modeling and experimental validation of transport and separation properties of carbon nanotube electrospun membrane distillation. J. Memb. Sci. 526, 395–408. https://doi.org/10.1016/j.memsci.2016.12.045

Lee, J., Boo, C., Ryu, W.-H., Taylor, A.D., Elimelech, M., 2016. Development of Omniphobic Desalination Membranes Using a Charged Electrospun Nanofiber Scaffold. ACS Appl. Mater. Interfaces 8, 11154–61. https://doi.org/10.1021/acsami.6b02419

Lee, J.G., Jang, Y., Fortunato, L., Jeong, S., Lee, S., Leiknes, T.O., Ghaffour, N., 2018. An advanced online monitoring approach to study the scaling behavior in direct contact membrane distillation. J. Memb. Sci. 546, 50–60. https://doi.org/10.1016/j.memsci.2017.10.009

Lee, J.G., Kim, Y.D., Kim, W.S., Francis, L., Amy, G., Ghaffour, N., 2015. Performance modeling of direct contact membrane distillation (DCMD) seawater desalination process using a commercial composite membrane. J. Memb. Sci. 478, 85–95. https://doi.org/10.1016/j.memsci.2014.12.053

Li, B., Sirkar, K.K., 2005. Novel membrane and device for vacuum membrane distillation-based desalination process. J. Memb. Sci. 257, 60–75. https://doi.org/10.1016/j.memsci.2004.08.040

Li, B., Sirkar, K.K., 2004. Novel Membrane and Device for Direct Contact Membrane Distillation-Based Desalination Process. Ind. Eng. Chem. Res. 43, 5300–5309. https://doi.org/10.1021/ie030871s

Li, J., Hou, D., Li, K., Zhang, Y., Wang, J., Zhang, X., 2018. Domestic wastewater treatment by forward osmosis-membrane distillation (FO-MD) integrated system. Water Sci. Technol. wst2018031. https://doi.org/10.2166/wst.2018.031

Li, L., Li, B., Dong, J., Zhang, J., 2016. Roles of silanes and silicones in forming superhydrophobic and superoleophobic materials. J. Mater. Chem. A 4, 13677–13725. https://doi.org/10.1039/C6TA05441B

Li, X., Deng, L., Yu, X., Wang, M., Wang, X., García-Payo, C., Khayet, M., 2016. A Novel Profiled Core-Shell Nanofibrous Membrane for Wastewater Treatment by Direct Contact Membrane Distillation. J. Mater. Chem. A. https://doi.org/10.1039/C6TA05492G

1319   Li, X., Wang, C., Yang, Y., Wang, X., Zhu, M., Hsiao, B.S., 2014a. Dual-Biomimetic Superhydrophobic

1320   Electrospun Polystyrene Nanofibrous Membranes for Membrane Distillation. ACS Appl. Mater.

1321   Interfaces 6, 2423–2430. https://doi.org//10.1021/am4048128

1322   Li, X., Wang, C., Yang, Y., Wang, X., Zhu, M., Hsiao, B.S., 2014b. Dual-Biomimetic Superhydrophobic

1323   Electrospun Polystyrene Nanofibrous Membranes for Membrane Distillation. ACS Appl. Mater.

1324   Interfaces 6, 2423–2430. https://doi.org/10.1021/am4048128

1325   Li, X., Yu, X., Cheng, C., Deng, L., Wang, M., Wang, X., 2015. Electrospun Superhydrophobic

1326   Organic/Inorganic Composite Nanofibrous Membranes for Membrane Distillation. ACS Appl. Mater.

1327   Interfaces 7, 21919–21930. https://doi.org/10.1021/acsami.5b06509

1328   Li, Y., Zhu, Z., Yu, J., Ding, B., 2015. Carbon Nanotubes Enhanced Fluorinated Polyurethane Macroporous

1329   Membranes for Waterproof and Breathable Application. ACS Appl. Mater. Interfaces 7, 13538–

1330   13546. https://doi.org/10.1021/acsami.5b02848

1331   Liao, Y., Wang, R., Fane, A.G., 2013. Engineering superhydrophobic surface on poly(vinylidene fluoride)

1332   nanofiber membranes for direct contact membrane distillation. J. Memb. Sci. 440, 77–87.

1333   https://doi.org/10.1016/j.memsci.2013.04.006

1334   Lin, P.-J., Yang, M.-C., Li, Y.-L., Chen, J.-H., 2015. Prevention of surfactant wetting with agarose hydrogel

1335   layer for direct contact membrane distillation used in dyeing wastewater treatment. J. Memb. Sci. 475,

1336   511–520. https://doi.org/10.1016/j.memsci.2014.11.001

1337   Lin, S., Nejati, S., Boo, C., Hu, Y., Osuji, C.O., Elimelech, M., 2014. Omniphobic Membrane for Robust

1338   Membrane Distillation. Environ. Sci. Technol. Lett. 1, 443–447. https://doi.org/10.1021/ez500267p

1339   Liu, C., Chen, L., Zhu, L., 2017. Fouling behavior of lysozyme on different membrane surfaces during the

1340   MD operation: An especial interest in the interaction energy evaluation. Water Res. 119, 33–46.

1341   https://doi.org/10.1016/j.watres.2017.04.041

1342   Liu, H., Huang, Q., Wang, Y., Xiao, C., 2017. PTFE conductive membrane for EVMD process and the

1343   application of electro-catalysis. Sep. Purif. Technol. https://doi.org/10.1016/j.seppur.2017.06.067

1344   Liu, L., Shen, F., Chen, X., Luo, J., Su, Y., Wu, H., Wan, Y., 2016. A novel plasma-induced surface

1345   hydrophobization strategy for membrane distillation: Etching, dipping and grafting. J. Memb. Sci.

1346   499, 544–554. https://doi.org/10.1016/j.memsci.2015.11.003

1347   Liu, T., Li, X., Wang, D., Huang, Q., Liu, Z., Li, N., Xiao, C., 2016. Superhydrophobicity and regeneration

1348   of PVDF/SiO2 composite films. Appl. Surf. Sci. https://doi.org/10.1016/j.apsusc.2016.11.184

1349   Lu, J., Yu, Y., Zhou, J., Song, L., Hu, X., Larbot, A., 2009. FAS grafted superhydrophobic ceramic

1350   membrane. Appl. Surf. Sci. 255, 9092–9099. https://doi.org/10.1016/j.apsusc.2009.06.112

1351   Lu, K.-J., Zuo, J., Chung, T.-S., 2017. Novel PVDF membranes comprising n-butylamine functionalized

1352   graphene oxide for direct contact membrane distillation. J. Memb. Sci. 539, 34–42.

1353   https://doi.org/10.1016/j.memsci.2017.05.064

1354   Lu, K.J., Zuo, J., Chung, T.S., 2016. Tri-bore PVDF hollow fibers with a super-hydrophobic coating for

1355   membrane distillation. J. Memb. Sci. 514, 165–175. https://doi.org/10.1016/j.memsci.2016.04.058

1356   Lu, X., Peng, Y., Ge, L., Lin, R., Zhu, Z., Liu, S., 2016. Amphiphobic PVDF composite membranes for

1357   anti-fouling direct contact membrane distillation. J. Memb. Sci. 505, 61–69.

1358   https://doi.org/10.1016/j.memsci.2015.12.042

1359   Lu, X., Peng, Y., Qiu, H., Liu, X., Ge, L., 2017. Anti-fouling membranes by manipulating surface

1360   wettability and their anti-fouling mechanism. Desalination 413, 127–135.

1361   https://doi.org/10.1016/j.desal.2017.02.022

1362   Luo, A., Lior, N., 2017. Study of advancement to higher temperature membrane distillation. Desalination

1363   419, 88–100. https://doi.org/10.1016/j.desal.2017.05.020

1364   Ma, Z., Hong, Y., Ma, L., Su, M., 2009. Superhydrophobic Membranes with Ordered Arrays of Nanospiked

1365   Microchannels for Water Desalination. Langmuir 25, 5446–5450. https://doi.org/10.1021/la900494u

1366   Majidi Salehi, S., Di Profio, G., Fontananova, E., Nicoletta, F.P., Curcio, E., De Filpo, G., 2016. Membrane

1367   distillation by novel hydrogel composite membranes. J. Memb. Sci. 504, 220–229.

1368   https://doi.org/10.1016/j.memsci.2015.12.062

1369   Mansouri, J., Fane, A.G., 1999. Osmotic distillation of oily feeds. J. Memb. Sci. 153, 103–120.

1370   https://doi.org/10.1016/S0376-7388(98)00252-X

1371   Mapunda, E.C., Mamba, B.B., Msagati, T.A.M., 2017. Carbon nanotube embedded PVDF membranes:

1372   Effect of solvent composition on the structural morphology for membrane distillation. Phys. Chem.

1373   Earth, Parts A/B/C 1–8. https://doi.org/10.1016/j.pce.2017.01.003

1374   Martínez-Díez, L., Vázquez-González, M.., 1999. Temperature and concentration polarization in

1375   membrane distillation of aqueous salt solutions. J. Memb. Sci. 156, 265–273.

1376   https://doi.org/10.1016/S0376-7388(98)00349-4

1377   Matheswaran, M., Kwon, T., 2007. Factors affecting flux and water separation performance in air gap

1378   membrane distillation. J. Ind. Eng. Chem. 13, 965–970.

1379   McGaughey, A.L., Gustafson, R.D., Childress, A.E., 2017. Effect of long-term operation on membrane

1380   surface characteristics and performance in membrane distillation. J. Memb. Sci. 543, 143–150.

1381   https://doi.org/10.1016/j.memsci.2017.08.040

1382   McHale, G., Shirtcliffe, N.J., Newton, M.I., 2004. Super-hydrophobic and super-wetting surfaces:

1383   Analytical potential? Analyst 129, 284. https://doi.org/10.1039/b400567h

1384   Meng, S., Hsu, Y.C., Ye, Y., Chen, V., 2015a. Submerged membrane distillation for inland desalination

1385   applications. Desalination 361, 72–80. https://doi.org/10.1016/j.desal.2015.01.038

1386   Meng, S., Mansouri, J., Ye, Y., Chen, V., 2014a. Effect of templating agents on the properties and

1387   membrane distillation performance of TiO2-coated PVDF membranes. J. Memb. Sci. 450, 48–59.

1388   https://doi.org/10.1016/j.memsci.2013.08.036

1389   Meng, S., Ye, Y., Mansouri, J., Chen, V., 2015b. Crystallization behavior of salts during membrane

1390   distillation with hydrophobic and superhydrophobic capillary membranes. J. Memb. Sci. 473, 165–

1391   176. https://doi.org/10.1016/j.memsci.2014.09.024

1392   Meng, S., Ye, Y., Mansouri, J., Chen, V., 2014b. Fouling and crystallisation behaviour of superhydrophobic

1393   nano-composite PVDF membranes in direct contact membrane distillation. J. Memb. Sci. 463, 102–

1394   112. https://doi.org/10.1016/j.memsci.2014.03.027

1395   Mericq, J.P., Laborie, S., Cabassud, C., 2010. Vacuum membrane distillation of seawater reverse osmosis

1396   brines. Water Res. 44, 5260–5273. https://doi.org/10.1016/j.watres.2010.06.052

1397   Minier-Matar, J., Hussain, A., Janson, A., Benyahia, F., Adham, S., 2014. Field evaluation of membrane

1398   distillation technologies for desalination of highly saline brines. Desalination 351, 101–108.

1399   https://doi.org/10.1016/j.desal.2014.07.027

1400   Mohammadi, T., Akbarabadi, M., 2005. Separation of ethylene glycol solution by vacuum membrane

1401   distillation (VMD). Desalination 181, 35–41. https://doi.org/10.1016/j.desal.2005.01.012

1402   Mokhtar, N.M., Lau, W.J., Ismail, A.F., Kartohardjono, S., Lai, S.O., Teoh, H.C., 2016. The potential of

1403   direct contact membrane distillation for industrial textile wastewater treatment using PVDF-Cloisite

1404   15A   nanocomposite   membrane.   Chem.   Eng.   Res.   Des.   111,   284–293.

1405   https://doi.org/10.1016/j.cherd.2016.05.018

1406   Mokhtar, N.M., Lau, W.J., Ismail, A.F., Ng, B.C., 2014. Physicochemical study of polyvinylidene fluoride–

1407   Cloisite15A® composite membranes for membrane distillation application. RSC Adv. 4, 63367–

1408   63379. https://doi.org/10.1039/C4RA10289D

1409   Mokhtar, N.M., Lau, W.J., Ng, B.C., Ismail, A.F., Veerasamy, D., 2014. Preparation and characterization

1410   of PVDF membranes incorporated with different additives for dyeing solution treatment using

1411   membrane   distillation.   Desalin.   Water   Treat.   56,   1999–2012.

1412   https://doi.org/10.1080/19443994.2014.959063

1413   Moradi, R., Karimi-Sabet, J., Shariaty-Niassar, M., Koochaki, M.A., 2015. Preparation and characterization

1414   of polyvinylidene fluoride/graphene superhydrophobic fibrous films. Polymers (Basel). 7, 1444–

1415   1463. https://doi.org/10.3390/polym7081444

1416   Mostafa, M.G., Zhu, B., Cran, M., Dow, N., Milne, N., Desai, D., Duke, M., 2017. Membrane Distillation

1417   of Meat Industry Effluent with Hydrophilic Polyurethane Coated Polytetrafluoroethylene Membranes.

1418   Membranes (Basel). 7, 55. https://doi.org/10.3390/membranes7040055

1419   Naidu, G., Jeong, S., Choi, Y., Vigneswaran, S., 2017. Membrane distillation for wastewater reverse

1420   osmosis   concentrate   treatment   with   water   reuse   potential.   J.   Memb.   Sci.   524,   565–575.

1421   https://doi.org/10.1016/j.memsci.2016.11.068

1422   Naidu, G., Jeong, S., Vigneswaran, S., 2014. Influence of feed/permeate velocity on scaling development

1423   in a direct contact membrane distillation. Sep. Purif. Technol. 125, 291–300.

1424   https://doi.org/10.1016/j.seppur.2014.01.049

1425 Naidu, G., Jeong, S., Vigneswaran, S., Hwang, T.-M., Choi, Y.-J., Kim, S.-H., 2015. A review on fouling

1426   of membrane distillation. Desalin. Water Treat. 3994, 1–25.

1427   https://doi.org/10.1080/19443994.2015.1040271

1428 Nayar, K.G., Panchanathan, D., McKinley, G.H., Lienhard, J.H., 2014. Surface Tension of Seawater. J.

1429   Phys. Chem. Ref. Data 43, 43103. https://doi.org/10.1063/1.4899037

1430 Nayar, K.G., Swaminathan, J., Warsinger, D.M., Lienhard, J.H., 2015. Performance Limits and

1431   Opportunities for Low Temperature Thermal Desalination, in: Proceedings of the 2015 India Water

1432   Week, 13-17 January. New Delhi.

1433 Nayar, K.G., Swaminathan, J., Warsinger, D.M., McKinley, G.H., Lienhard, J.H., 2015. Effect of scale

1434   deposition on surface tension of seawater and membrane distillation. Proc. Int. Desalin. Assoc. World

1435   Congr. Desalin. Water Reuse, San Diego, CA, USA.

1436 Nguyen, Q., Jeong, S., Lee, S., 2017. Characteristics of membrane foulants at different degrees of SWRO

1437   brine concentration by membrane distillation. Desalination 409, 7–20.

1438   https://doi.org/10.1016/j.desal.2017.01.007

1439 Okiel, K., El-Aassar, A.H.M., Temraz, T., El-Etriby, S., Shawky, H.A., 2015. Performance assessment of

1440   synthesized CNT/polypropylene composite membrane distillation for oil field produced water

1441   desalination. Desalin. Water Treat. 1–13. https://doi.org/10.1080/19443994.2015.1044475

1442 Onsekizoglu, P., 2012. Membrane Distillation: Principle, Advances, Limitations and Future Prospects in

1443   Food Industry, in: Distillation - Advances from Modeling to Applications. InTech.

1444   https://doi.org/10.5772/37625

1445 Owens, D.K., Wendt, R.C., 1969. Estimation of the surface free energy of polymers. J. Appl. Polym. Sci.

1446   13, 1741–1747. https://doi.org/10.1002/app.1969.070130815

1447 Peña, L., de Zárate, J.M.O., Mengual, J.I., 1993. Steady states in membrane distillation: influence of

1448   membrane wetting. J. Chem. Soc., Faraday Trans. 89, 4333–4338.

1449   https://doi.org/10.1039/FT9938904333

1450   Peng, P., Fane, A.G., Li, X., 2005. Desalination by membrane distillation adopting a hydrophilic membrane.

1451   Desalination 173, 45–54. https://doi.org/10.1016/j.desal.2004.06.208

1452   Peng, P., Ke, Q., Zhou, G., Tang, T., 2013. Fabrication of microcavity-array superhydrophobic surfaces

1453   using an improved template method. J. Colloid Interface Sci. 395, 326–328.

1454   https://doi.org/10.1016/j.jcis.2012.12.036

1455   Peng, Y., Ge, J., Li, Z., Wang, S., 2015. Effects of anti-scaling and cleaning chemicals on membrane scale

1456   in direct contact membrane distillation process for RO brine concentrate. Sep. Purif. Technol. 154,

1457   22–26. https://doi.org/10.1016/j.seppur.2015.09.007

1458   Peng, Y., Ge, J., Wang, S., Li, Z., 2017. Occurrence of salt breakthrough and air-vapor pocket in a direct-

1459   contact membrane distillation. Desalination 402, 42–49. https://doi.org/10.1016/j.desal.2016.09.033

1460   Politano, A., Argurio, P., Di Profio, G., Sanna, V., Cupolillo, A., Chakraborty, S., Arafat, H.A., Curcio, E.,

1461   2016. Photothermal Membrane Distillation for Seawater Desalination. Adv. Mater. 1–6.

1462   https://doi.org/10.1002/adma.201603504

1463   Prince, J.A., Anbharasi, V., Shanmugasundaram, T.S., Singh, G., 2013. Preparation and characterization of

1464   novel triple layer hydrophilic–hydrophobic composite membrane for desalination using air gap

1465   membrane distillation. Sep. Purif. Technol. 118, 598–603.

1466   https://doi.org/10.1016/j.seppur.2013.08.006

1467   Prince, J.A., Rana, D., Matsuura, T., Ayyanar, N., Shanmugasundaram, T.S., Singh, G., 2014a. Nanofiber

1468   based triple layer hydro-philic/-phobic membrane - a solution for pore wetting in membrane

1469   distillation. Sci. Rep. 4, 6949. https://doi.org/10.1038/srep06949

1470   Prince, J.A., Rana, D., Singh, G., Matsuura, T., Jun Kai, T., Shanmugasundaram, T.S., 2014b. Effect of

1471   hydrophobic surface modifying macromolecules on differently produced PVDF membranes for direct

1472   contact membrane distillation. Chem. Eng. J. 242, 387–396. https://doi.org/10.1016/j.cej.2013.11.039

1473   Prince, J.A., Singh, G., Rana, D., Matsuura, T., Anbharasi, V., Shanmugasundaram, T.S., 2012. Preparation

1474   and characterization of highly hydrophobic poly(vinylidene fluoride) - Clay nanocomposite nanofiber

1475   membranes (PVDF-clay NNMs) for desalination using direct contact membrane distillation. J. Memb.

1476   Sci. 397–398, 80–86. https://doi.org/10.1016/j.memsci.2012.01.012

1477 Purcell, W.R., 1950. Interpretation of Capillary Pressure Data. J. Pet. Technol. 2, 11–12.

1478   https://doi.org/10.2118/950369-G

1479 Purwasasmita, M., Kurnia, D., Mandias, F.C., Khoiruddin, Wenten, I.G., 2015. Beer dealcoholization using

1480   non-porous   membrane   distillation.   Food   Bioprod.   Process.   94,   180–186.

1481   https://doi.org/10.1016/j.fbp.2015.03.001

1482 Qin, W., Zhang, J., Xie, Z., Ng, D., Ye, Y., Gray, S., Xie, M., 2016. Synergistic effect of combined colloidal

1483   and organic fouling in membrane distillation: measurements and mechanisms. Environ. Sci. Water

1484   Res. Technol. https://doi.org/10.1039/C6EW00156D

1485 Qing, W., Shi, X., Deng, Y., Zhang, W., Wang, J., Tang, C.Y., 2017. Robust superhydrophobic-

1486   superoleophilic polytetrafluoroethylene nanofibrous membrane for oil/water separation. J. Memb. Sci.

1487   540, 354–361. https://doi.org/10.1016/j.memsci.2017.06.060

1488 Qtaishat, M.R., Banat, F., 2013. Desalination by solar powered membrane distillation systems. Desalination

1489   308, 186–197. https://doi.org/10.1016/j.desal.2012.01.021

1490 Qu, D., Wang, J., Wang, L., Hou, D., Luan, Z., Wang, B., 2009. Integration of accelerated precipitation

1491   softening with membrane distillation for high-recovery desalination of primary reverse osmosis

1492   concentrate. Sep. Purif. Technol. 67, 21–25. https://doi.org/10.1016/j.seppur.2009.02.021

1493 Racz, G., Kerker, S., Schmitz, O., Schnabel, B., Kovacs, Z., Vatai, G., Ebrahimi, M., Czermak, P., 2015.

1494   Experimental determination of liquid entry pressure (LEP) in vacuum membrane distillation for oily

1495   wastewaters. Membr. Water Treat. 6, 237–249. https://doi.org/10.12989/mwt.2015.6.3.237

1496 Rao, G., Hiibel, S.R., Childress, A.E., 2014. Simplified flux prediction in direct-contact membrane

1497   distillation   using   a   membrane   structural   parameter.   Desalination   351,   151–162.

1498   https://doi.org/10.1016/j.desal.2014.07.006

1499 Ray, S.S., Chen, S.-S., Nguyen, N.C., Hsu, H.-T., Nguyen, H.T., Chang, C.-T., 2017. Poly(vinyl alcohol)

1500   incorporated with surfactant based electrospun nanofibrous layer onto polypropylene mat for

improved desalination by using membrane distillation. Desalination 414, 18–27. https://doi.org/10.1016/j.desal.2017.03.032

Razmjou, A., Arifin, E., Dong, G., Mansouri, J., Chen, V., 2012. Superhydrophobic modification of TiO2 nanocomposite PVDF membranes for applications in membrane distillation. J. Memb. Sci. 415–416, 850–863. https://doi.org/10.1016/j.memsci.2012.06.004

Rezaei, M, Samhaber, W., 2016a. Wetting study of Dual-Layer Hydrophilic / Hydrophobic Composite Membranes Coated with Nanoparticles for Membrane Distillation, in: DECHEMA.

Rezaei, M., Samhaber, W.M., 2017a. Impact of gas bubbling on wetting control in a submerged membrane distillation, in: 13th Minisymposium Der Verfahrenstechnik in Österreich.

Rezaei, M., Samhaber, W.M., 2017b. Impact of gas recharging on wetting control in membrane distillation for the concentration of highly saline brines, in: 3rd International Conference on Desalination Using Membrane Technology.

Rezaei, M., Samhaber, W.M., 2016b. Wetting Behaviour of Superhydrophobic Membranes Coated with Nanoparticles in Membrane Distillation. Chem. Eng. Trans. 47, 373–378. https://doi.org/10.3303/CET1647063

Rezaei, M., Samhaber, W.M., 2016c. Wetting control of Multiscale-Layer Membranes for Membrane Distillation, in: 12th Minisymposium Der Verfahrenstechnik. Graz, pp. 147–150. https://doi.org/10.3217/978-3-85125-456-3

Rezaei, M., Samhaber, W.M., 2015. Characterization of Macroporous Hydrophobic Membranes Used in Membrane Distillation Process, in: Filtech. p. 141.

Rezaei, M., Samhaber, W.M., 2014. Wetting phenomenon in membrane distillation processes, in: 10th Minisymposium Der Verfahrenstechnik. pp. 56–58.

Rezaei, M., Warsinger, D.M., Lienhard, J.H., Samhaber, W.M., 2017a. Wetting prevention in membrane distillation through superhydrophobicity and recharging an air layer on the membrane surface. J. Memb. Sci. 530, 42–52. https://doi.org/10.1016/j.memsci.2017.02.013

Rezaei, M., Warsinger, D.M., Lienhard, J.H., Samhaber, W.M., 2017b. Wetting prevention in membrane

1527 distillation through superhydrophobicity and recharging an air layer on the membrane surface, Journal

1528 of Membrane Science. Elsevier. https://doi.org/10.1016/j.memsci.2017.02.013

1529 Roy, Y., Warsinger, D.M., Lienhard, J.H., 2017. Effect of temperature on ion transport in nanofiltration

1530 membranes: Diffusion, convection and electromigration. Desalination 420, 241–257.

1531 https://doi.org/10.1016/j.desal.2017.07.020

1532 Ruiz Salmón, I., Janssens, R., Luis, P., 2017. Mass and heat transfer study in osmotic membrane distillation-

1533 crystallization for CO2 valorization as sodium carbonate. Sep. Purif. Technol. 176, 173–183.

1534 https://doi.org/10.1016/j.seppur.2016.12.010

1535 Saffarini, R.B., Mansoor, B., Thomas, R., Arafat, H.A., 2013. Effect of temperature-dependent

1536 microstructure evolution on pore wetting in PTFE membranes under membrane distillation conditions.

1537 J. Memb. Sci. 429, 282–294. https://doi.org/10.1016/j.memsci.2012.11.049

1538 Sakai, K., Koyano, T., Muroi, T., Tamura, M., 1988. Effects of temperature and concentration polarization

1539 on water vapour permeability for blood in membrane distillation. Chem. Eng. J. 38, B33–B39.

1540 https://doi.org/10.1016/0300-9467(88)80081-9

1541 Sanmartino, J.A., Khayet, M., García-Payo, M.C., El-Bakouri, H., Riaza, A., 2017. Treatment of reverse

1542 osmosis brine by direct contact membrane distillation: Chemical pretreatment approach. Desalination

1543 420, 79–90. https://doi.org/10.1016/j.desal.2017.06.030

1544 Sanmartino, J.A., Khayet, M., García-Payo, M.C., El Bakouri, H., Riaza, A., 2016. Desalination and

1545 concentration of saline aqueous solutions up to supersaturation by air gap membrane distillation and

1546 crystallization fouling. Desalination 393, 39–51. https://doi.org/10.1016/j.desal.2016.03.010

1547 Sarti, G.C., Gostoli, C., Matulli, S., 1985. Low energy cost desalination processes using hydrophobic

1548 membranes. Desalination 56, 277–286. https://doi.org/10.1016/0011-9164(85)85031-1

1549 Schneider, K., Hölz, W., Wollbeck, R., Ripperger, S., 1988a. Membranes and modules for transmembrane

1550 distillation. J. Memb. Sci. 39, 25–42. https://doi.org/10.1016/S0376-7388(00)80992-8

1551 Schneider, K., Hölz, W., Wollbeck, R., Ripperger, S., 1988b. Membranes and modules for transmembrane

1552 distillation. J. Memb. Sci. 39, 25–42. https://doi.org/10.1016/S0376-7388(00)80992-8

1553   Schofield, R.W., Fane, A.G., Fell, C.J.D., 1990. Gas and vapour transport through microporous membranes.

1554   II. Membrane distillation. J. Memb. Sci. 53, 173–185.

1555   Schofield, R.W., Fane, A.G., Fell, C.J.D., Macoun, R., 1990. Factors affecting flux in membrane

1556   distillation. Desalination 77, 279–294. https://doi.org/10.1016/0011-9164(90)85030-E

1557   Servi, A.T., Kharraz, J., Klee, D., Notarangelo, K., Eyob, B., Guillen-Burrieza, E., Liu, A., Arafat, H.A.,

1558   Gleason, K.K., 2016. A systematic study of the impact of hydrophobicity on the wetting of MD

1559   membranes. J. Memb. Sci. 520, 850–859. https://doi.org/10.1016/j.memsci.2016.08.021

1560   Shaulsky, E., Nejati, S., Boo, C., Perreault, F., Osuji, C.O., Elimelech, M., 2017. Post-fabrication

1561   modification of electrospun nanofiber mats with polymer coating for membrane distillation

1562   applications. J. Memb. Sci. 530, 158–165. https://doi.org/10.1016/j.memsci.2017.02.025

1563   Shaw, D.J., 1992. Colloid & Surface Chemistry 315. https://doi.org/10.1007/s13398-014-0173-7.2

1564   Shin, Y., Cho, H., Choi, J., Sun Jang, Y., Choi, Y.-J., Sohn, J., Lee, S., Choi, J., 2016. Application of

1565   response surface methodology (RSM) in the optimization of dewetting conditions for flat sheet

1566   membrane distillation (MD) membranes. Desalin. Water Treat. 57, 10020–10030.

1567   https://doi.org/10.1080/19443994.2015.1038114

1568   Shin, Y., Choi, J., Lee, T., Sohn, J., Lee, S., 2015. Optimization of dewetting conditions for hollow fiber

1569   membranes in vacuum membrane distillation. Desalin. Water Treat. 1044266, 1–11.

1570   https://doi.org/10.1080/19443994.2015.1044266

1571   Shirazi, M.M.A., Kargari, A., Tabatabaei, M., 2015. Sweeping Gas Membrane Distillation (SGMD) as an

1572   Alternative for Integration of Bioethanol Processing: Study on a Commercial Membrane and

1573   Operating Parameters. Chem. Eng. Commun. 202, 457–466.

1574   https://doi.org/10.1080/00986445.2013.848805

1575   Shirazi, M.M.A., Kargari, A., Tabatabaei, M., 2014. Evaluation of commercial PTFE membranes in

1576   desalination by direct contact membrane distillation. Chem. Eng. Process. Process Intensif. 76, 16–

1577   25. https://doi.org/10.1016/j.cep.2013.11.010

1578   Silva, T.L.S., Morales-Torres, S., Figueiredo, J.L., Silva, A.M.T., 2015. Multi-walled carbon

nanotube/PVDF blended membranes with sponge- and finger-like pores for direct contact membrane distillation. Desalination 357, 233–245. https://doi.org/10.1016/j.desal.2014.11.025

Sirkar, K.K., Qin, Y., 2001. Novel membrane and device for direct contact membrane distillation based desalination process, DWPR Program Report No. 87.

Smolders, K., Franken, A.C.M., 1989. Terminology for Membrane Distillation. Desalination 72, 249–262. https://doi.org/10.1016/0011-9164(89)80010-4

Song, J., Huang, S., Hu, K., Lu, Y., Liu, X., Xu, W., 2013. Fabrication of Superoleophobic surfaces on Al Substrates. J. Mater. Chem. A 1. https://doi.org/10.1039/c3ta13807k

Song, L., Li, B., Sirkar, K.K., Gilron, J.L., 2007. Direct contact membrane distillation-based desalination: Novel membranes, devices, larger-scale studies, and a model. Ind. Eng. Chem. Res. 46, 2307–2323. https://doi.org/10.1021/ie0609968

Soni, V., Abildskov, J., Jonsson, G., Gani, R., 2008. Modeling and analysis of vacuum membrane distillation for the recovery of volatile aroma compounds from black currant juice. J. Memb. Sci. 320, 442–455. https://doi.org/10.1016/j.memsci.2008.04.025

Srisurichan, S., Jiraratananon, R., Fane, A.G., 2006. Mass transfer mechanisms and transport resistances in direct contact membrane distillation process. J. Memb. Sci. 277, 186–194. https://doi.org/10.1016/j.memsci.2005.10.028

Su, C., Chang, J., Tang, K., Gao, F., Li, Y., Cao, H., 2017. Novel Three-dimensional Superhydrophobic and Strength-enhanced Electrospun Membranes for Long-term Membrane Distillation. Sep. Purif. Technol. 178, 279–287. https://doi.org/10.1016/j.seppur.2017.01.050

Summers, E.K., Lienhard, J.H., 2013. Experimental study of thermal performance in air gap membrane distillation systems, including the direct solar heating of membranes. Desalination 330, 100–111. https://doi.org/10.1016/j.desal.2013.09.023

Swaminathan, J., Chung, H.W., Warsinger, D.M., AlMarzooqi, F.A., Arafat, H.A., Lienhard, J.H., 2016a. Energy efficiency of permeate gap and novel conductive gap membrane distillation. J. Memb. Sci. 502, 171–178. https://doi.org/10.1016/j.memsci.2015.12.017

1605 Swaminathan, J., Chung, H.W., Warsinger, D.M., Lienhard, J.H., 2018. Membrane distillation at high

1606   salinity: evaluating critical system size and optimal membrane thickness. J. Memb. Sci. 211, 715–

1607   734. https://doi.org/10.1016/j.apenergy.2017.11.043

1608 Swaminathan, J., Chung, H.W., Warsinger, D.M., Lienhard, J.H., 2018. Energy efficiency of membrane

1609   distillation up to high salinity: Evaluating critical system size and optimal membrane thickness. Appl.

1610   Energy 211, 715–734. https://doi.org/10.1016/j.apenergy.2017.11.043

1611 Swaminathan, J., Chung, H.W., Warsinger, D.M., Lienhard, J.H., 2016b. Simple method for balancing

1612   direct contact membrane distillation. Desalination 383, 53–59.

1613   https://doi.org/10.1016/j.desal.2016.01.014

1614 Swaminathan, J., Chung, H.W., Warsinger, D.M., Lienhard, J.H., 2016c. Membrane distillation model

1615   based on heat exchanger theory and configuration comparison. Appl. Energy 184, 491–505.

1616   https://doi.org/10.1016/j.apenergy.2016.09.090

1617 Tan, Y.Z., Chew, J.W., Krantz, W.B., 2016. Effect of humic-acid fouling on membrane distillation. J.

1618   Memb. Sci. 504, 263–273. https://doi.org/10.1016/j.memsci.2015.12.051

1619 Tan, Y.Z., Han, L., Chow, W.H., Fane, A.G., Chew, J.W., 2017. Influence of module orientation and

1620   geometry in the membrane distillation of oily seawater. Desalination 423, 111–123.

1621   https://doi.org/10.1016/j.desal.2017.09.019

1622 Thomas, R., Guillen-Burrieza, E., Arafat, H.A., 2014. Pore structure control of PVDF membranes using a

1623   2-stage coagulation bath phase inversion process for application in membrane distillation (MD). J.

1624   Memb. Sci. 452, 470–480. https://doi.org/10.1016/j.memsci.2013.11.036

1625 Tian, M., Yin, Y., Yang, C., Zhao, B., Song, J., Liu, J., Li, X.-M., He, T., 2015. CF4 plasma modified

1626   highly interconnective porous polysulfone membranes for direct contact membrane distillation

1627   (DCMD). Desalination 369, 105–114. https://doi.org/10.1016/j.desal.2015.05.002

1628 Tijing, L.D., Choi, J.S., Lee, S., Kim, S.H., Shon, H.K., 2014a. Recent progress of membrane distillation

1629   using electrospun nanofibrous membrane. J. Memb. Sci. 453, 435–462.

1630   https://doi.org/10.1016/j.memsci.2013.11.022

1631   Tijing, L.D., Woo, Y.C., Choi, J.-S., Lee, S., Kim, S.-H., Shon, H.K., 2015. Fouling and its control in

1632   membrane distillation—A review. J. Memb. Sci. 475, 215–244. https://doi.org/10.1016/j.memsci.2014.09.042

1633   https://doi.org/10.1016/j.memsci.2014.09.042

1634   Tijing, L.D., Woo, Y.C., Johir, M.A.H., Choi, J.S., Shon, H.K., 2014b. A novel dual-layer bicomponent

1635   electrospun nanofibrous membrane for desalination by direct contact membrane distillation. Chem.

1636   Eng. J. 256, 155–159. https://doi.org/10.1016/j.cej.2014.06.076

1637   Tijing, L.D., Woo, Y.C., Shim, W.G., He, T., Choi, J.S., Kim, S.H., Shon, H.K., 2016. Superhydrophobic

1638   nanofiber membrane containing carbon nanotubes for high-performance direct contact membrane

1639   distillation. J. Memb. Sci. 502, 158–170. https://doi.org/10.1016/j.memsci.2015.12.014

1640   Tomaszewska, M., 2000. Membrane distillation-examples of applications in technology and environmental

1641   protection. Polish J. Environ. Stud. 9, 27–36.

1642   Tong, D., Wang, X., Ali, M., Lan, C.Q., Wang, Y., Drioli, E., Wang, Z., Cui, Z., 2016. Preparation of

1643   Hyflon AD60/PVDF composite hollow fiber membranes for vacuum membrane distillation. Sep.

1644   Purif. Technol. 157, 1–8. https://doi.org/10.1016/j.seppur.2015.11.026

1645   Treybal, R.E., 1980. Mass-Transfer Operations, Mc Graw Hill International Book Company.

1646   Tuteja, A., Choi, W., Ma, M., Mabry, J.M., Mazzella, S.A., Rutledge, G.C., McKinley, G.H., Cohen, R.E.,

1647   2007. Designing Superoleophobic Surfaces. Science (80-.). 318, 1618–1622.

1648   https://doi.org/10.1126/science.1148326

1649   Tuteja, a, Choi, W., Mabry, J.M., McKinley, G.H., Cohen, R.E., 2008. Engineering superhydrophobic and

1650   superoleophobic surfaces. Tech. Proc. 2008 NSTI Nanotechnol. Conf. Trade Show, NSTI-Nanotech,

1651   Nanotechnol. 2008 1, 439–442.

1652   Walton, J., Lu, H., Turner, C., Solis, S., Hein, H., 2004. Solar and waste heat desalination by membrane

1653   distillation.

1654   Wang, F., Li, J., Zhu, H., Zhang, H., Tang, H., Chen, J., Guo, Y., 2014. Physical modification of

1655   polytetrafluoroethylene flat membrane by a simple heat setting process and membrane wetting

1656   remission in SGMD for desalination. Desalination 354, 143–152.

1657 https://doi.org/10.1016/j.desal.2014.09.030

1658 Wang, J., Qu, D., Tie, M., Ren, H., Peng, X., Luan, Z., 2008. Effect of coagulation pretreatment on

1659 membrane distillation process for desalination of recirculating cooling water. Sep. Purif. Technol. 64,

1660 108–115. https://doi.org/10.1016/j.seppur.2008.07.022

1661 Wang, J., Sun, X., Yuan, Y., Chen, H., Wang, H., Hou, D., 2016. A novel microwave assisted photo-

1662 catalytic membrane distillation process for treating the organic wastewater containing inorganic ions.

1663 J. Water Process Eng. 9, 1–8. https://doi.org/10.1016/j.jwpe.2015.11.004

1664 Wang, K.Y., Chung, T.S., Gryta, M., 2008. Hydrophobic PVDF hollow fiber membranes with narrow pore

1665 size distribution and ultra-thin skin for the fresh water production through membrane distillation.

1666 Chem. Eng. Sci. 63, 2587–2594. https://doi.org/10.1016/j.ces.2008.02.020

1667 Wang, P., Teoh, M.M., Chung, T.S., 2011. Morphological architecture of dual-layer hollow fiber for

1668 membrane distillation with higher desalination performance. Water Res. 45, 5489–5500.

1669 https://doi.org/10.1016/j.watres.2011.08.012

1670 Wang, Y., Yu, Y., Hu, X., Feng, A., Jiang, F., Song, L., 2017. p -Phenylenediamine strengthened graphene

1671 oxide for the fabrication of superhydrophobic surface. Mater. Des.

1672 https://doi.org/10.1016/j.matdes.2017.04.033

1673 Wang, Z., Elimelech, M., Lin, S., 2016a. Environmental Applications of Interfacial Materials with Special

1674 Wettability. Environ. Sci. Technol. 50, 2132–2150. https://doi.org/10.1021/acs.est.5b04351

1675 Wang, Z., Hou, D., Lin, S., 2016b. Composite Membrane with Underwater-Oleophobic Surface for Anti-

1676 Oil-Fouling Membrane Distillation. Environ. Sci. Technol. 50, 3866–3874.

1677 https://doi.org/10.1021/acs.est.5b05976

1678 Wang, Z., Lin, S., 2017. The impact of low-surface-energy functional groups on oil fouling resistance in

1679 membrane distillation. J. Memb. Sci. 527, 68–77. https://doi.org/10.1016/j.memsci.2016.12.063

1680 Wang, Z., Tang, Y., Li, B., 2017. Excellent wetting resistance and anti-fouling performance of PVDF

1681 membrane modified with superhydrophobic papillae-like surfaces. J. Memb. Sci. 540, 401–410.

1682 https://doi.org/10.1016/j.memsci.2017.06.073

Warsinger, D., Swaminathan, J., Lienhard, J.H., 2014. Effect of Module Inclination Angle on Air Gap Membrane Distillation, in: Proceedings of the 15th International Heat Transfer Conference. Begellhouse, Connecticut, pp. 1–14. https://doi.org/10.1615/IHTC15.mtr.009351

Warsinger, D.E.M., 2015. Thermodynamic Design and Fouling of Membrane Distillation Systems. PhD thesis, Massachusetts Institute of Technology.

Warsinger, D.E.M., Swaminathan, J., Maswadeh, L.A., Lienhard, J.H., 2015. Superhydrophobic condenser surfaces for air gap membrane distillation. J. Memb. Sci. 492, 578–587. https://doi.org/10.1016/j.memsci.2015.05.067

Warsinger, D.M., Mistry, K.H., Nayar, K.G., Chung, H.W., Lienhard, J.H., 2015. Entropy Generation of Desalination Powered by Variable Temperature Waste Heat. Entropy 17, 7530–7566. https://doi.org/10.3390/e17117530

Warsinger, D.M., Servi, A., Connors, G., Gonzalez, J., Swaminathan, J., Chung, H.W., Arafat, H.A., Gleason, K.K., Lienhard, J.H., 2016. A novel air-cleaning method for membrane distillation, in: Proceedings of the AMTA Membrane Technology Conference & Exposition (MTC16). San Antonio, Texas.

Warsinger, D.M., Servi, A., Connors, G.B., Mavukkandy, M.O., Arafat, H.A., Gleason, K.K., Lienhard, J.H., 2017a. Reversing membrane wetting in membrane distillation: comparing dryout to backwashing with pressurized air. Environ. Sci. Water Res. Technol. 3, 930–939. https://doi.org/10.1039/C7EW00085E

Warsinger, D.M., Servi, A., Van Belleghem, S., Gonzalez, J., Swaminathan, J., Kharraz, J., Chung, H.W., Arafat, H.A., Gleason, K.K., Lienhard, J.H., 2016. Combining air recharging and membrane superhydrophobicity for fouling prevention in membrane distillation. J. Memb. Sci. 505, 241–252. https://doi.org/10.1016/j.memsci.2016.01.018

Warsinger, D.M., Swaminathan, J., Guillen-Burrieza, E., Arafat, H.A., Lienhard, J.H., 2015. Scaling and fouling in membrane distillation for desalination applications: A review. Desalination 356, 294–313. https://doi.org/10.1016/j.desal.2014.06.031

Warsinger, D.M., Tow, E.W., Maswadeh, L.A., Connors, G., Swaminathan, J., Lienhard, J.H., 2018. Inorganic fouling mitigation by salinity cycling in batch reverse osmosis. Water Res. https://doi.org/10.1016/j.watres.2018.01.060

Warsinger, D.M., Tow, E.W., Swaminathan, J., Lienhard, J.H., 2017b. Theoretical framework for predicting inorganic fouling in membrane distillation and experimental validation with calcium sulfate. J. Memb. Sci. 528, 381–390. https://doi.org/10.1016/j.memsci.2017.01.031

Wei, C., Tang, Y., Zhang, G., Zhang, Q., Zhan, X., Chen, F., 2016. Facile fabrication of highly omniphobic and self-cleaning surfaces based on water mediated fluorinated nanosilica aggregation. RSC Adv. 6, 74340–74348. https://doi.org/10.1039/C6RA13367C

Wenzel, R.N., 1936. Resistance of Solid Surfaces To Wetting By Water. Ind. Eng. Chem. 28, 988–994. https://doi.org/10.1021/ie50320a024

Woo, Y.C., Kim, Y., Shim, W.-G., Tijing, L.D., Yao, M., Nghiem, L.D., Choi, J.-S., Kim, S.-H., Shon, H.K., 2016a. Graphene/PVDF flat-sheet membrane for the treatment of RO brine from coal seam gas produced water by air gap membrane distillation. J. Memb. Sci. 513, 74–84. https://doi.org/10.1016/j.memsci.2016.04.014

Woo, Y.C., Tijing, L.D., Park, M.J., Yao, M., Choi, J.S., Lee, S., Kim, S.H., An, K.J., Shon, H.K., 2015. Electrospun dual-layer nonwoven membrane for desalination by air gap membrane distillation. Desalination. https://doi.org/10.1016/j.desal.2015.09.009

Woo, Y.C., Tijing, L.D., Shim, W.-G., Choi, J.-S., Kim, S.-H., He, T., Drioli, E., Shon, H.K., 2016b. Water desalination using graphene-enhanced electrospun nanofiber membrane via air gap membrane distillation. J. Memb. Sci. https://doi.org/10.1016/j.memsci.2016.07.049

Wu, C., Li, Z., Zhang, J., Jia, Y., Gao, Q., Lu, X., 2015. Study on the heat and mass transfer in air-bubbling enhanced vacuum membrane distillation. Desalination 373, 16–26. https://doi.org/10.1016/j.desal.2015.07.001

Wu, H., Shen, F., Wang, J., Luo, J., Liu, L., Khan, R., Wan, Y., 2016. Separation and concentration of ionic liquid aqueous solution by vacuum membrane distillation. J. Memb. Sci. 518, 216–228.

1735   https://doi.org/10.1016/j.memsci.2016.07.017

1736 Wu, Y., Kang, Y., Zhang, L., Qu, D., Cheng, X., Feng, L., 2017. Performance and fouling mechanism of

1737   direct contact membrane distillation (DCMD) treating fermentation wastewater with high organic

1738   concentrations. J. Environ. Sci. 1–9. https://doi.org/10.1016/j.jes.2017.01.015

1739 Xiao, T., Wang, P., Yang, X., Cai, X., Lu, J., 2015. Fabrication and characterization of novel asymmetric

1740   polyvinylidene fluoride (PVDF) membranes by the nonsolvent thermally induced phase separation

1741   (NTIPS) method for membrane distillation applications. J. Memb. Sci. 489, 160–174.

1742   https://doi.org/10.1016/j.memsci.2015.03.081

1743 Xiaoxing, S., Wenfang, Y., Qingfu, Z., 2011. Hydrophobic modification of PVDF 687, 658–661.

1744   https://doi.org/10.4028/www.scientific.net/MSF.687.658

1745 Xu, J.B., Bartley, J.P., Johnson, R.A., 2005a. Application of Sodium Alginate- Carrageenan Coatings to

1746   PTFE Membranes for Protection Against Wet- Out by Surface- Active Agents. Sep. Sci. Technol.

1747   40, 1067–1081. https://doi.org/10.1081/SS-200048167

1748 Xu, J.B., Lange, S., Bartley, J.P., Johnson, R.A., 2004. Alginate-coated microporous PTFE membranes for

1749   use in the osmotic distillation of oily feeds. J. Memb. Sci. 240, 81–89.

1750   https://doi.org/10.1016/j.memsci.2004.04.016

1751 Xu, J.B., Spittler, D.A., Bartley, J.P., Johnson, R.A., 2005b. Alginic acid-silica hydrogel coatings for the

1752   protection of osmotic distillation membranes against wet-out by surface-active agents. J. Memb. Sci.

1753   260, 19–25. https://doi.org/10.1016/j.memsci.2005.03.017

1754 Xu, W.T., Zhao, Z.P., Liu, M., Chen, K.C., 2015. Morphological and hydrophobic modifications of PVDF

1755   flat membrane with silane coupling agent grafting via plasma flow for VMD of ethanol-water mixture.

1756   J. Memb. Sci. 491, 110–120. https://doi.org/10.1016/j.memsci.2015.05.024

1757 Xu, Z., Liu, Z., Song, P., Xiao, C., 2017. Fabrication of super-hydrophobic polypropylene hollow fiber

1758   membrane and its application in membrane distillation. Desalination 414, 10–17.

1759   https://doi.org/10.1016/j.desal.2017.03.029

1760 Yan, H., Lu, X., Wu, C., Sun, X., Tang, W., 2017. Fabrication of a super-hydrophobic polyvinylidene

1761   fluoride hollow fiber membrane using a particle coating process. J. Memb. Sci. 533, 130–140.

1762   https://doi.org/10.1016/j.memsci.2017.03.033

1763   Yang, C., Li, X.M., Gilron, J., Kong, D. feng, Yin, Y., Oren, Y., Linder, C., He, T., 2014. CF4 plasma-

1764   modified superhydrophobic PVDF membranes for direct contact membrane distillation. J. Memb. Sci.

1765   456, 155–161. https://doi.org/10.1016/j.memsci.2014.01.013

1766   Yang, C., Tian, M., Xie, Y., Li, X.M., Zhao, B., He, T., Liu, J., 2015. Effective evaporation of CF4 plasma

1767   modified PVDF membranes in direct contact membrane distillation. J. Memb. Sci. 482, 25–32.

1768   https://doi.org/10.1016/j.memsci.2015.01.059

1769   Yang, H.-C.C., Zhong, W., Hou, J., Chen, V., Xu, Z.-K.K., 2016. Janus hollow fiber membrane with a

1770   mussel-inspired coating on the lumen surface for direct contact membrane distillation. J. Memb. Sci.

1771   523, 1–7. https://doi.org/10.1016/j.memsci.2016.09.044

1772   Yang, W.F., Zhang, Z.Q., Gu, Z.Y., Shen, X.X., Zhang, Q.F., 2011. Research on the Superhydrophobic

1773   Modification of Polyvinylidene Fluoride Membrane. Adv. Mater. Res. 197–198, 514–517.

1774   https://doi.org/10.4028/www.scientific.net/AMR.197-198.514

1775   Yang, X., Wang, R., Shi, L., Fane, A.G., Debowski, M., 2011. Performance improvement of PVDF hollow

1776   fiber-based membrane distillation process. J. Memb. Sci. 369, 437–447.

1777   https://doi.org/10.1016/j.memsci.2010.12.020

1778   Yao, M., Woo, Y., Tijing, L., Cesarini, C., Shon, H., 2017. Improving Nanofiber Membrane Characteristics

1779   and Membrane Distillation Performance of Heat-Pressed Membranes via Annealing Post-Treatment.

1780   Appl. Sci. 7, 78. https://doi.org/10.3390/app7010078

1781   Yin, X., Sun, C., Zhang, B., Song, Y., Wang, N., Zhu, L., Zhu, B., 2017. A facile approach to fabricate

1782   superhydrophobic coatings on porous surfaces using cross-linkable fluorinated emulsions. Chem.

1783   Eng. J. https://doi.org/10.1016/j.cej.2017.06.145

1784   Young, T., 1807. A Course of Lectures on Natural Philosophy and the Mechanical Arts. Johnson.

1785   Young, T., 1805. An Essay on the Cohesion of Fluids. Philos. Trans. R. Soc. London 95, 65–87.

1786   https://doi.org/10.1098/rstl.1805.0005

1787 Zakrzewska-Trznadel, G., Harasimowicz, M., Chmielewski, A.G., 1999. Concentration of radioactive
1788   components in liquid low-level radioactive waste by membrane distillation. J. Memb. Sci. 163, 257–
1789   264. https://doi.org/10.1016/S0376-7388(99)00171-4

1790 Zarebska, A., Amor, Á.C., Ciurkot, K., Karring, H., Thygesen, O., Andersen, T.P., Hägg, M.-B.,
1791   Christensen, K.V., Norddahl, B., 2015. Fouling mitigation in membrane distillation processes during
1792   ammonia   stripping   from   pig   manure.   J.   Memb.   Sci.   484,   119–132.
1793   https://doi.org/10.1016/j.memsci.2015.03.010

1794 Zarebska, A., Nieto, D.R., Christensen, K. V., Norddahl, B., 2014. Ammonia recovery from agricultural
1795   wastes by membrane distillation: Fouling characterization and mechanism. Water Res. 56, 1–10.
1796   https://doi.org/10.1016/j.watres.2014.02.037

1797 Zhang, H., Lamb, R., Lewis, J., 2005. Engineering nanoscale roughness on hydrophobic surface -
1798   Preliminary   assessment   of   fouling   behaviour.   Sci.   Technol.   Adv.   Mater.   6,   236–239.
1799   https://doi.org/10.1016/j.stam.2005.03.003

1800 Zhang, J., Song, Z., Li, B., Wang, Q., Wang, S., 2013a. Fabrication and characterization of
1801   superhydrophobic poly (vinylidene fluoride) membrane for direct contact membrane distillation.
1802   Desalination 324, 1–9. https://doi.org/10.1016/j.desal.2013.05.018

1803 Zhang, J., Song, Z., Li, B., Wang, Q., Wang, S., 2013b. Fabrication and characterization of
1804   superhydrophobic poly (vinylidene fluoride) membrane for direct contact membrane distillation.
1805   Desalination 324, 1–9. https://doi.org/10.1016/j.desal.2013.05.018

1806 Zhang, P., Knötig, P., Gray, S., Duke, M., 2015. Scale reduction and cleaning techniques during direct
1807   contact membrane distillation of seawater reverse osmosis brine. Desalination 374, 20–30.
1808   https://doi.org/10.1016/j.desal.2015.07.005

1809 Zhang, W., Li, Y., Liu, J., Li, B., Wang, S., 2017. Fabrication of hierarchical poly (vinylidene fluoride)
1810   micro/nano-composite membrane with anti-fouling property for membrane distillation. J. Memb. Sci.
1811   https://doi.org/10.1016/j.memsci.2017.04.051

1812 Zhang, Y., Peng, Y., Ji, S., Li, Z., Chen, P., 2015. Review of thermal efficiency and heat recycling in

1813   membrane distillation processes. Desalination 367, 223–239.

1814   https://doi.org/10.1016/j.desal.2015.04.013

1815   Zhang, Y., Wang, X., Cui, Z., Drioli, E., Wang, Z., Zhao, S., 2017. Enhancing wetting resistance of

1816   poly(vinylidene fluoride) membranes for vacuum membrane distillation. Desalination 415, 58–66.

1817   https://doi.org/10.1016/j.desal.2017.04.011

1818   Zhao, D., Zuo, J., Lu, K.-J., Chung, T.-S., 2017. Fluorographite modified PVDF membranes for seawater

1819   desalination via direct contact membrane distillation. Desalination 413, 119–126.

1820   https://doi.org/10.1016/j.desal.2017.03.012

1821   Zhong, W., Hou, J., Yang, H.-C., Chen, V., 2017. Superhydrophobic membranes via facile bio-inspired

1822   mineralization for vacuum membrane distillation. J. Memb. Sci.

1823   https://doi.org/10.1016/j.memsci.2017.06.033

1824   Zhu, J., Jiang, L., Matsuura, T., 2015. New insights into fabrication of hydrophobic/hydrophilic composite

1825   hollow fibers for direct contact membrane distillation. Chem. Eng. Sci. 137, 79–90.

1826   https://doi.org/10.1016/j.ces.2015.05.064

1827   Zodrow, K.R., Bar-Zeev, E., Giannetto, M.J., Elimelech, M., 2014. Biofouling and Microbial Communities

1828   in Membrane Distillation and Reverse Osmosis. Environ. Sci. Technol. 48, 13155–13164.

1829   https://doi.org/10.1021/es503051t

1830   Zuo, G., Wang, R., 2013. Novel membrane surface modification to enhance anti-oil fouling property for

1831   membrane distillation application. J. Memb. Sci. 447, 26–35.

1832   https://doi.org/10.1016/j.memsci.2013.06.053

1833   Zuo, J., Chung, T.-S., 2016. Metal–Organic Framework-Functionalized Alumina Membranes for Vacuum

1834   Membrane Distillation. Water 8, 586. https://doi.org/10.3390/w8120586

1835   Zuo, J., Chung, T.-S., O'Brien, G.S., Kosar, W., 2017. Hydrophobic/hydrophilic PVDF/Ultem® dual-layer

1836   hollow fiber membranes with enhanced mechanical properties for vacuum membrane distillation. J.

1837   Memb. Sci. 523, 103–110. https://doi.org/10.1016/j.memsci.2016.09.030

1838   Zydney, A.L., 1995. Membrane handbook. AIChE J. 41, 2343–2344.

1839   https://doi.org/10.1002/aic.690411024

1840

Highlights

• This review offers an extensive literature survey on the wetting phenomenon in MD.

• Describes wetting fundamentals, equations, parameters, and measurement techniques

• Analyzes wetting conditions, effects, prevention, and reversal techniques

• This review lays the groundwork for future technological advances in MD.

Graphical Abstract